NATIONAL ADVISORY COMMITTEE FOR AERONAUTICS

TECHNICAL NOTE 3336

REVIEW OF EXPERIMENTAL INVESTIGATIONS OF LIQUID-METAL HEAT TRANSFER

By Bernard Lubarsky and Samuel J. Kaufman

Lewis Flight Propulsion Laboratory
Cleveland, Ohio

Washington
March 1955

NATIONAL ADVISORY COMMITTEE FOR AERONAUTICS

TECHNICAL NOTE 3336

REVIEW OF EXPERIMENTAL INVESTIGATIONS OF LIQUID-METAL HEAT TRANSFER

By Bernard Lubarsky and Samuel J. Kaufman

SUMMARY

The experimentally obtained results of various investigators of liquid-metal heat-transfer characteristics were examined and found to be not always directly comparable because of differences in experimental apparatus or in methods of calculation. The experimental data were therefore re-evaluated using as consistent assumptions and methods as possible and then compared with each other and with theoretical results.

The re-evaluated data for both local fully developed and average Nusselt numbers in the turbulent flow region were found still to have considerable spread, with the bulk of the data being lower than predicted by existing analysis. An equation based on empirical grounds which best represents most of the fully developed heat-transfer data is

$$Nu = 0.625\ Pe^{0.4}$$

where Nu represents the Nusselt number and Pe, the Peclet number. The theoretical prediction of the heat transfer in the entrance region was found to give lower values, in most cases, than those found in the experimental work.

The theoretical and experimental results for the ratio of local Nusselt number to fully developed Nusselt number were integrated to obtain predictions for the ratio of average Nusselt number to fully developed Nusselt number for a range of Peclet numbers and length-diameter ratios. Most of the experimental data fall between 60 to 80 percent of the predicted values.

The experimental evidence was insufficient to serve as a basis for any conclusion concerning liquid-metal heat transfer in the laminar or transition flow regions.

INTRODUCTION

The use of liquid metals as heat-transfer media is presently of considerable interest. A number of theoretical and experimental investigations to determine the heat-transfer characteristics of liquid metals have been made by various investigators (refs. 1 to 26). In the literature, the results of the experimental investigations often have been compared with each other and with the results of theoretical investigations. During the course of investigations of liquid-metal heat-transfer characteristics at the NACA Lewis laboratory, the work of the various experimental investigators was carefully examined. It was found that different investigations were not always directly comparable because of differences in the experimental apparatus or in the methods of calculation. Some of the differences found were:

(a) Liquid-metal physical properties different from those currently accepted were sometimes used.

(b) At times, center-line temperatures in and out of the test section were measured rather than "mixing-cup" temperatures.

(c) Some of the experiments were conducted with uniform heat input to the wall of the test section, while others more closely approached constant wall temperature.

(d) Some investigators measured the combined heat-transfer coefficient in a tube and concentric annulus; different methods were used to obtain the individual coefficients.

(e) Some investigators measured local fully developed heat-transfer coefficients; others measured average over-all coefficients.

(f) The velocity profiles entering the test section varied; some approached a fully developed turbulent profile, while others were more nearly uniform.

(g) Different length-diameter ratios of test section were used.

The differences in experimental apparatus of items (f) and (g) affect only the average heat-transfer coefficient and not the fully developed coefficient.

Because of the differences in experimental apparatus and methods of calculation listed, the experimental data of references 1 to 26 were reevaluated using consistent assumptions and methods in order to permit a better intercomparison of the experimental results and comparison with the results of theoretical investigations.

SYMBOLS

a	constant
c	specific heat, Btu/(lb)(°F)
D	equivalent or hydraulic diameter, ft
D_i	annulus inner diameter, ft
D_o	annulus outer diameter, ft
f	friction factor
G	weight flow per unit area, lb/(hr)(sq ft)
Gz	Graetz number, PeD/L
h	heat-transfer coefficient, Btu/(hr)(sq ft)(°F)
k	thermal conductivity, Btu/(hr)(sq ft)(°F/ft)
L	length of test section, ft
m	constant, eq. (10)
Nu	Nusselt number, hD/k
n	constant, eq. (10)
Pe	Peclet number, RePr, GDc/k
Pr	Prandtl number, $c\mu/k$
Re	Reynolds number, GD/μ
St	Stanton number, h/cG
t_c	fluid center-line temperature, °F
t_m	fluid bulk temperature, °F ("bulk temperature" as used in this report is synonymous with "mixing-cup temperature" and "mixed mean temperature ")
t_w	wall temperature, °F
x	distance along test section, ft
μ	fluid bulk viscosity, lb/(hr)(ft)

Subscripts and superscripts refer to:

a average

f fully developed

x at station x

' annulus

PROCEDURE

The experimental data of the various references were re-evaluated as consistently as possible, plotted as Nusselt number against Peclet or Graetz number or against both, and the results compared with theoretical predictions. These three steps will be discussed in reverse order because some of the methods used in re-evaluating the data were determined by theoretical considerations.

Theoretical Investigations of Liquid-Metal Heat Transfer

The following discussion gives a brief description of some of the results of theoretical investigations and is not intended to be complete. All the theoretical investigations discussed consider only the turbulent flow region.

Fully developed heat-transfer coefficients. - Heat-transfer coefficients for liquid metals in turbulent flow with fully developed velocity and temperature profiles have been predicted by a number of investigators using somewhat different assumptions.

(a) Uniform heat input to the wall; round tubes: The most frequently analyzed case is that of heat transfer to a round tube with uniform rate of heat input along the length of the tube. This case was investigated by Martinelli (ref. 27) using the "momentum transfer analogy." Lyon (ref. 6) found a simplified equation which approximated Martinelli's more complex relation. This equation, which is recommended by the Liquid-Metals Handbook (ref. 28), is

$$Nu_f = 7.0 + 0.025\ Pe_f^{0.8} \tag{1}$$

Cope (ref. 29) investigated the possibility of assuming that the "modified vorticity transfer analogy" applied to the turbulent core of the fluid, while the "momentum transfer analogy" applied to the boundary layer and buffer layer. Kennison (ref. 30) assumed that the heat transfer is analogous to the transfer of vorticity for turbulent fluid flow

in a long straight pipe. Deissler (ref. 31) modified the "momentum transfer analogy" to allow for heat transferred by conduction to or from a turbulent particle as it moves radially in the tube. Deissler's analysis is for a Prandtl number of 0.01.

Some of the results of these various investigations are shown in figure 1. The experimental results for fully developed heat transfer in a round tube with uniform heat input will be compared with Lyon's equation (eq. (1)) inasmuch as this is the equation recommended by the Liquid-Metals Handbook and most commonly used in practice.

(b) Uniform wall temperature; round tubes: The fully developed heat-transfer coefficient in turbulent flow in a round tube with a uniform wall temperature has been investigated by Seban and Shimazaki (ref. 32) using the "momentum transfer analogy"; they give, as an approximate relation, the equation

$$Nu_f = 5.0 + 0.025\ Pe_f^{0.8} \tag{2}$$

This equation is plotted in figure 1. The Liquid-Metals Handbook lists the equation as

$$Nu_f = 4.8 + 0.025\ Pe_f^{0.8} \tag{3}$$

and gives the work of Seban and Shimazaki as a reference. The experimental results for fully developed heat transfer in a round tube with a uniform wall temperature will be compared with Seban and Shimazaki's equation (eq. (2)).

(c) Uniform heat input; annuli: Very little theoretical work has been done on the fully developed heat-transfer coefficient in annuli. For thin annuli (diameter ratio less than or equal to 1.4), the Liquid-Metals Handbook recommends the use of the theoretical relation proposed by Seban (ref. 33) for heat transfer to parallel plates with heat through one side only.

$$Nu_f' = 5.8 + 0.020\ (Pe_f')^{0.8} \qquad \text{for } D_o/D_i \leq 1.4 \tag{4}$$

For annuli of diameter ratio greater than 1.4, the Liquid-Metals Handbook lists an equation which approximates the results of Bailey (ref. 34) and is of the form suggested by Werner, Tidball, and King (ref. 7).

$$Nu_f' = 0.75\ (D_o/D_i)^{0.3}\left[7.0 + 0.025\ (Pe_f')^{0.8}\right] \qquad \text{for } D_o/D_i > 1.4 \tag{5}$$

Equations (4) and (5) are plotted in figure 2. The experimental data on heat transfer in annuli will be compared with these equations.

Local heat-transfer coefficients in entrance region. - Heat-transfer coefficients in the entrance region have been calculated by several investigators for a number of different cases. Poppendiek, Palmer, and Harrison (refs. 26, 35, and 36) have analyzed the case of uniform wall temperature for various different entering velocity profiles; the analysis assumes the eddy diffusivity of heat is negligible when compared with the molecular diffusivity and consequently is intended only for low Reynolds numbers. The analysis is independent of Prandtl number. Deissler (ref. 37) analyzed the case of uniform heat input at the wall, with a fully developed velocity profile at the entrance; the numerical calculations were carried out only for a Prandtl number of 0.01. Seban and Shimazaki (ref. 38) have made calculations for the case of uniform wall temperature and fully developed velocity profile at the entrance for a Prandtl number of 0.01 and Reynolds numbers of 10^4 and 10^5. The results of the analyses of Poppendiek and Palmer and of Deissler are shown in figure 3.

Average heat-transfer coefficients. - Predictions of average heat-transfer coefficients can be made by integrating the predictions for local heat-transfer coefficients over the length-diameter ratio of the tube in question. Heat transfer in the entrance region, however, has been analyzed for only relatively specialized cases. Therefore, the experimental results for average heat-transfer coefficients will first be compared with equations (1) and (2), even though equations (1) and (2) are derived for fully developed heat-transfer coefficients. Later in the report, a comparison will be made with the average heat-transfer coefficients on the basis of the analytical evidence.

Temperature distribution. - The fully developed temperature distribution due to heat transfer to a liquid metal in turbulent flow in a round tube has been predicted on theoretical grounds by several investigators. The predictions of Martinelli (ref. 27) are shown in figure 4 for a Prandtl number of 0.022. Martinelli, using his own predicted values for the temperature distribution, calculated the ratio of the temperature differences $(t_w - t_m)/(t_w - t_c)$ as a function of Reynolds and Prandtl numbers. Martinelli's results are shown in figure 5 for Prandtl numbers pertinent to liquid metals. Martinelli also calculated values of $(t_w - t_m)/(t_w - t_c)$ for fully developed flow between flat plates with heat flow through both walls with uniform heat flux. These results are shown in figure 6.

Methods of Calculation

The heat-transfer parameters were evaluated using the same method of calculation for each individual reference as was used by the authors of that particular reference, with the following exceptions:

(a) All physical properties of liquid metals were taken from the second edition of the Liquid-Metals Handbook (ref. 28). These properties are shown in figures 7 to 10.

(b) When an investigator measured the combined liquid-metal heat-transfer coefficient in a tube and concentric annulus, the individual heat-transfer coefficients were obtained by assuming that the ratio of the Nusselt number in the tube to the Nusselt number in the annulus is determined by equations (1), (4), and (5).

$$\frac{Nu}{Nu'} = \frac{7.0 + 0.025\ Pe^{0.8}}{5.8 + 0.020\ Pe'^{0.8}} \qquad \text{for } D_o/D_i \leq 1.4 \qquad (6)$$

$$\frac{Nu}{Nu'} = \frac{7.0 + 0.025\ Pe^{0.8}}{0.75(D_o/D_i)^{0.3}\ (7.0 + 0.025\ Pe'^{0.8})} \qquad \text{for } D_o/D_i > 1.4 \qquad (7)$$

Because of the lack of theoretical work on average heat-transfer coefficients, particularly in annuli, the same ratios which have been assumed for the fully developed Nusselt numbers will be assumed for the average Nusselt numbers.

It is important to note that in most of those tests in which the combined coefficient in a tube and concentric annulus was measured, the Reynolds number in the annulus was smaller than the Reynolds number in the tube. Quite often the flow in the annulus was in the transition flow region, while the flow in the tube was in the turbulent flow region. Inasmuch as there are no predictions for liquid-metal heat transfer in the transition region, equations (6) and (7) will be used to separate the tube and annulus heat-transfer coefficients even when the flow in the annulus is in the transition region. This procedure is open to question, and the interpretation of the data calculated by this procedure may be inaccurate.

(c) In those tests in which the center-line temperature of the fluid was measured instead of the bulk temperature, the temperature difference between the wall and the bulk fluid will be calculated from Martinelli's relation for $(t_w - t_m)/(t_w - t_c)$ (figs. 5 and 6). Martinelli's prediction of $(t_w - t_m)/(t_w - t_c)$ for flat plates with heat flowing through both sides will be used for annuli inasmuch as no other predictions covering as broad a range of Reynolds and Prandtl numbers are available.

RE-EVALUATION OF EXPERIMENTAL DATA

The experimental investigations of references 1 to 26 will first be discussed individually and then compared with each other and with theory.

The experimental work of the various investigators will be discussed in a chronological order determined by the publication date of the original manuscript.

Styrikovich and Semenovker. - Styrikovich and Semenovker (ref. 1) investigated heat transfer to mercury as part of their investigation of the mercury-steam binary power cycle. Their test sections were a series of five tubes, each about 106 inches in length; the diameters were 0.63, 0.87, 1.58, 1.67, and 1.97 inches. The tubes were heated by external electric heaters. Thermocouples were placed 17.2 inches apart on the outside surface of each tube. The bulk fluid temperature in the test section was calculated by adding to the inlet temperature the temperature rise corresponding to the heat input. The velocity profile of the mercury entering the test section was essentially fully developed. The method of heating the mercury approximated uniform heat input to the wall. The heat-transfer coefficient was calculated for only the central portion of the tube. The coefficients presented are essentially the fully developed heat-transfer coefficients.

The physical properties used in evaluating the heat-transfer coefficients are not listed, but the Prandtl number is tabulated over a range of temperature from 32° to 1112° F. These Prandtl numbers are lower than the values in reference 28, which lists values of Prandtl number up to 600° F. The values of Prandtl number of Styrikovich and Semenovker and of reference 28 are shown in figure 11. Since the specific heat and viscosity in the temperature range used are essentially the same in reference 28 as those reported in the International Critical Tables (1929 edition), the inaccuracies in Prandtl number may be assumed due to incorrect values of thermal conductivity. It appears that Styrikovich and Semenovker used the thermal conductivity data of Gelhoff and Neumeier, which have been found to be high (ref. 12). It was deemed advisable to recalculate the data of Styrikovich and Semenovker using the values of thermal conductivity from reference 28. The precise temperature level of the various data points is not reported, but the average temperature level is given as about 932° F. At this temperature, Styrikovich and Semenovker list a Prandtl number of 0.0056. Reference 28 presents Prandtl number data up to 600° F which when extrapolated to 932° F give a Prandtl number between 0.006 and 0.007. The data points were reevaluated using a Prandtl number of 0.0065 at 932° F. This increased the Nusselt and Peclet numbers of the data by about 16 percent. The reevaluated data of Styrikovich and Semenovker are shown in figure 12; shown for comparison is equation (1).

Gilliland, Musser, and Page. - Gilliland, Musser, and Page (refs. 2 and 3) measured both heating and cooling coefficients for mercury. The heating test section was 0.319 inch in inside diameter by 14 inches in length; heat was added by dropwise condensation of steam on the outside of the test section. The cooling test section was 0.319 inch in inside

diameter by 51 inches in length; it was cooled by water flowing on the outside in a direction opposite to that of the inside flow. Both test sections were made of nickel. The mercury and water bulk temperatures entering and leaving the test sections and the stream temperature and pressure entering the test section were measured. The velocity profile of the mercury was fully developed at the entrance to both test sections. The methods of heating and cooling the mercury were such that the heating tests approximated a constant wall temperature, while the cooling tests were somewhere between a constant wall temperature and a constant heat input. The heat-transfer coefficient measured was an over-all average coefficient.

Inasmuch as no wall temperatures were measured, it was necessary to separate the mercury heat-transfer coefficients from those of the steam and water. This was done by the Wilson plot method (see refs. 2 and 3).

(a) Heating: Tests were run with water in the place of mercury and the Wilson plot method was used to determine the combined resistance of the steam film and the wall. The range of water flows covered was sufficiently small and the scatter of the points sufficiently great that values of the combined resistance could be chosen ranging from 40 percent greater to 15 percent smaller than the value selected. An increase of 40 percent in steam and wall resistance, however, would increase the mercury coefficient only about 8 percent. An attempt was made to use the results of the mercury runs to confirm the steam and wall resistance, but in this case the range of mercury flows and data scatter permit selecting a value of resistance ranging from 200 percent greater to 50 percent lower than the value chosen. The slope of the Wilson plot for the runs with water can be compared with the slope predicted by the standard empirical relation for heat transfer to water (ref. 39, p. 168)

$$Nu = 0.023\ Re^{0.8}\ Pr^{0.4} \tag{8}$$

The slope predicted by equation (8) turns out to be considerably higher than the slope best representing the experimental data.

(b) Cooling: At a given mercury flow rate, the water flow rate was varied and the combined mercury film and tube wall resistance determined by means of a Wilson plot. The range and scatter of the data are such that the resistance of the mercury and the wall could be chosen 20 percent lower or 15 percent higher than the value actually chosen. The corresponding variation in mercury coefficient would be somewhat greater. Alternatively, cooling coefficients for mercury were calculated by evaluating the coefficients for water in an annulus using the following equation (ref. 39, p. 202):

$$St\ Pr^{2/3} = \frac{0.020\ (D_o/D_i)^{0.53}}{Re^{0.2}} \tag{9}$$

The resulting mercury coefficients were approximately 40 percent lower than those derived by the Wilson plot method. The physical properties used by Gilliland, Musser, and Page are about the same as those of reference 29. In view of the possible inaccuracies in the method of evaluating the data, the reported results of Gilliland, Musser, and Page may not be very accurate. Their data are shown in figure 13 without change; shown for comparison are equations (1) and (2). The lower values for cooling coefficient may be due to the longer length-diameter ratio of the cooling section.

Elser. - Elser (ref. 4) measured cooling heat-transfer coefficients for mercury. Three different test sections were used: The test-section inner diameters were 0.317, 0.308, and 0.260 inch; the 0.317-inch-diameter test section was made of mild steel; the other test sections were made of stainless steel. The test sections were all over 38 inches long, but measurements were made between two stations 10.2 and 38.3 inches from the entrance. The mercury was cooled by water flowing in a concentric annulus in a direction opposite to the flow of mercury. Two thermocouples imbedded in the wall measured the wall temperature at the two stations. Two other thermocouples immersed in the stream measured a temperature close to the fluid center-line temperature. The velocity profile of the mercury at the first station was fully developed. The cooling water flow rate was such that a uniform heat input to the wall was approximated. The fully developed heat-transfer coefficient was measured.

The only mercury property listed by Elser is Prandtl number. These values are in agreement with the values of reference 28, and the other mercury properties will be assumed to be correct. The basic data are not presented by Elser. He presents a plot of Stanton number against Reynolds number showing his data points. The values of Stanton number have been corrected by Elser to a common Prandtl number by approximating the data with a curve of the form

$$Nu_f = a\, Re_f^{m}\, Pr_f^{n} \tag{10}$$

He gives no values of n so that it is impossible to return to the basic points.

Elser measured mercury flow by measuring the mercury pressure drop and assuming the following formula for friction factor:

$$4f = \frac{0.3164}{Re^{0.25}} \qquad Re < 80{,}000 \tag{11}$$

$$\frac{1}{\sqrt{4f}}\, 2 \log (Re\sqrt{4f}) - 0.8 \qquad Re > 80{,}000 \tag{12}$$

Equation (11) is due to Blasius; equation (12), to Kármán.

Elser's heat-transfer coefficients are based on the difference between wall and fluid center-line temperatures. He is not certain of the location (depth) of his wall thermocouples and states that the difference between a midwall and a wall surface location results in shifts of heat-transfer coefficients of 4, 7, and 18 percent, respectively, for the three tubes of 0.317, 0.308, and 0.260 inch diameters. In Elser's data, the wall thermocouple is assumed to be at the wall midpoint. Martinelli's predictions for the ratio of the temperature differences $(t_w - t_m)/(t_w - t_c)$ (see fig. 5) were used to change the heat-transfer coefficients of Elser so that they would be based on the difference between wall and fluid bulk temperatures. This increased the Nusselt number about 40 to 60 percent. In this re-evaluation, the wall thermocouples were assumed to be located at the wall midpoint. If the thermocouples were assumed at the wall surface, the Nusselt numbers would be somewhat increased. Figure 14 shows the re-evaluated data of Elser; shown for comparison is equation (1).

Bailey, Cope, and Watson. - Bailey, Cope, and Watson (ref. 5) measured cooling coefficients for mercury. The test section was a mild steel tube of 0.437 inch inner diameter. The central 18 inches of the tube was surrounded by a water jacket, with about 6 inches left projecting at each end. These ends were enclosed in chambers in such a manner that the inlet and outlet mercury passed along the outside of the ends before entering and after leaving the test section. Fluid temperatures were measured at the inlet and outlet of the test section; wall temperatures were measured at four stations along the length of the water-jacketed section of the tube.

There is considerable question as to just what temperature was measured at the test-section outlet. First, there was no provision made for mixing before the exit temperature was measured. Second, inasmuch as the mercury was being cooled, the temperature distribution of the mercury was such that the temperature near the wall was lower than the bulk temperature. The mercury was discharged from the test section into a larger chamber, turned 180°, and passed over the end of the test section which projected from the water jacket. Because of the mixing in the discharge and turning processes, the mercury on the outside of the projecting end had a temperature profile close to flat. Hence, the mercury on the outside of the projecting end of the test section was at about fluid bulk temperature, while the mercury on the inside of the projecting end (close to the wall) was at a temperature lower than fluid bulk temperature. Heat was therefore transferred from the outside to the inside; this tended to increase the measured mercury exit temperature and consequently decrease the observed heat-transfer coefficients. The combined effect on heat-transfer coefficient of the heat transferred through the projecting end and the lack of mixing before the exit temperature measurement is very difficult to estimate.

The velocity profile at the entrance to the water-jacketed section of the test section was close to fully developed. The method of cooling was such that uniform wall temperature was approximated at the lower mercury Peclet numbers, while uniform heat input to the wall was more nearly the case at high mercury Peclet numbers. Fully developed heat-transfer coefficients were measured.

The physical properties used by Bailey, Cope, and Watson were somewhat different from the values of reference 28; the Prandtl numbers were about 10 percent high. The data of Bailey, Cope, and Watson were therefore re-evaluated, using the physical properties of reference 28, in two ways: first, it was assumed that the measured mercury exit temperature was equal to the fluid bulk temperature; second, it was assumed that the measured mercury exit temperature was equal to the fluid center-line temperature and Martinelli's predictions of $(t_w - t_m)/(t_w - t_c)$ (fig. 5) were used to calculate the fluid bulk temperature. The results of both methods of computation are shown in figure 15; equations (1) and (2) are shown for comparison. Because of the uncertainties described in the measurement of mercury exit temperature, it is difficult to say whether either set of data in figure 15 is at all correct.

Lyon. - Lyon (ref. 6) used a tube and concentric annulus to measure the combined coefficient resulting from transferring heat from a sodium-potassium alloy (52 percent Na, 48 percent K) flowing in the annulus to the same fluid flowing in the tube. The weight flows in the tube and annulus are, necessarily, the same. This type of test section is often referred to as a "figure eight" and will be so referred to hereinafter. Lyon used four different test sections made of nickel and having the following dimensions:

Test section	A	B	C	D
Tube inner diameter, in.	0.432	0.703	0.434	0.434
Annulus inner diameter, in.	.500	.757	.500	.500
Annulus outer diameter, in.	.715	.931	.684	.684
Length, in.	48	69	33	69

Bulk fluid temperatures were measured at the inlet and outlet of the tube and annulus. The velocity profiles of the fluid entering the tube and the annulus were approximately flat (uniform velocity). The figure eight test section with counter flow gives approximately constant heat input to the wall. The heat-transfer coefficients measured were overall average coefficients.

Lyon used physical properties which were somewhat different from those of reference 28. The specific heat was about 12 percent higher and the thermal conductivity was about 6 percent higher. Use of the properties of reference 28 decreases both the Nusselt and Peclet numbers about 5 percent. Lyon assumed that the resistances of the walls of the four test sections were approximately constant, neglecting the differences in wall thickness. Lyon did not separate the experimental tube and annulus coefficients, but rather calculated a combined predicted coefficient using equation (1) for the tube and an equation approximating the results of Harrison and Menke (ref. 40)

$$Nu_f' = 4.9 + 0.0175\ (Pe_f')^{0.8} \qquad (13)$$

for the annulus. The Liquid-Metals Handbook (ref. 28) mentions equation (13), but prefers equations (4) and (5) for heat transfer in an annulus.

Lyon's data were re-evaluated using the physical properties of reference 28 and calculating exactly the resistance of the wall. The overall heat-transfer coefficient was divided into a tube coefficient and an annulus coefficient assuming that the Nusselt numbers in the tube and annulus are related as in equations (6) and (7), which are taken from equations (1), (4), and (5). The use of equations (4) and (5) rather than equation (13) for the annulus results in higher annulus heat-transfer coefficients and lower tube heat-transfer coefficients for the same overall heat-transfer coefficient. The re-evaluated data of Lyon are shown in figures 16 and 17; equations (1), (4), and (5) are shown for comparison.

Untermeyer. - The data of Untermeyer were obtained from unclassified material in a classified report. Untermeyer measured heating coefficients for a lead-bismuth eutectic with and without magnesium addition. The test section was a steel tube 0.25 inch in inner diameter and 18 inches in length. The test section was heated by passing electric current directly through it and the fluid it contained. Wall temperatures and fluid inlet and outlet temperatures were measured. The velocity profile at the test section entrance was closer to flat than to fully developed. The method of heating most nearly approximated uniform heat input to the wall. Local fully developed coefficients were measured.

The physical properties used by Untermeyer are different from those of reference 28. The thermal conductivity used by Untermeyer was about 15 percent low and the volumetric specific heat was about 8 percent high. It is difficult to determine from the data whether the heat generated directly in the fluid has been subtracted from the total heat input. It is also difficult to determine whether a mixing chamber was used in the measurement of the fluid bulk temperature leaving the test section. Figure 18 shows the data of Untermeyer re-evaluated using physical properties from reference 28.

Werner, King, and Tidball. - Werner, King, and Tidball (ref. 7 and unclassified data from a classified report) used a figure eight type of test section (tube and concentric annulus with same fluid in both) to measure heat-transfer coefficients for a sodium-potassium alloy. Cooling coefficients were measured in the tube and heating coefficients in the annulus. Two test sections having the following characteristics were used:

Test section	A	B
Tube inner diameter, in.	0.68	0.70
Annulus inner diameter, in.	.75	.75
Annulus outer diameter, in.	1.37	1.37
Length, in.	33.8	33.8
Material	304 Stainless steel	Nickel

The tests in test section A were all run with a 56 percent sodium, 44 percent potassium alloy. The tests in test section B were run with both 56 percent sodium, 44 percent potassium and 23 percent sodium, 77 percent potassium alloys. Fluid temperatures were measured at the inlet and outlet of the tube and of the annulus. In test section A no provision was made for mixing the fluid before measuring the outlet temperatures of the tube or the annulus, except that the fluid turned one right angle bend before each thermocouple. The outlet temperatures measured in exchanger A were therefore somewhere between fluid bulk temperature and fluid center-line temperature, probably closer to fluid center-line temperature. In test section B, mixing baffles were used to mix the fluid before measuring outlet temperatures, and the temperatures measured were fluid bulk temperatures. The velocity profiles of the fluid entering the tube and the annulus were essentially flat in test section B, and between flat and fully developed in test section A. The figure eight test section with counterflow gives approximately uniform heat input to the wall. The heat-transfer coefficients measured were over-all average coefficients.

Werner, King, and Tidball used physical properties which were about the same as those of reference 28. However, the relation used to divide the over-all heat-transfer coefficient in the test section into separate coefficients for the tube and annulus is somewhat different from that recommended by the Liquid-Metals Handbook (eq. (7)).

The experimental data of Werner, King, and Tidball were re-evaluated using equation (7) to separate the over-all heat-transfer coefficient into tube and annulus coefficients. In addition, the predictions of Martinelli for the ratio of the temperature differences $(t_w - t_m)/(t_w - t_c)$ for the tube and the annulus (figs. 5 and 6) were used to make allowance for the lack of mixing of the fluid before the outlet thermocouples of test section A. The re-evaluated data of Werner, King, and Tidball are shown in figures 19 to 22; equations (1) and (5) are shown for comparison.

Sineath. - Sineath (ref. 8) ran heat-transfer tests with mercury in rectangular channels. Sineath's test section was of the figure eight type except that instead of a tube and concentric annulus, he had two rectangular channels with one common wall. Heat was added to the mercury in one channel and removed from the mercury in the other. The common wall of the two channels was 4 inches high by 1/4 inch thick and was made of mild steel. The channel gap was 1/4 inch and the length, 25 inches. Fluid temperatures were measured at the inlet and outlet of the two channels. No attempt was made to provide any mixing of the fluid before the outlet temperatures were measured except that the abrupt transition from a 4- by 1/4-inch rectangular channel to the 3/4-inch pipes which carried the fluid to and away from the test section probably resulted in considerable mixing. The pipe entered the channels at right angles to the direction of flow in the channels; there was no smooth transition piece between the pipes and the channels. The fluid temperatures measured were probably close to the bulk temperature. However, the abrupt change of section at the entrance to the channels probably caused some of the heat-transfer surface to be relatively less effective as a result of poor local flow distribution. The figure eight test section with counterflow approximated uniform heat input to the wall. The heat-transfer coefficients measured were over-all average coefficients.

Sineath ran four sets of tests. The first three sets were inconclusive because of experimental difficulties with air entrainment and with the deposition of mercurous oxide on the wall through which heat was being transferred. These problems were partially eliminated in the fourth set of runs. There was probably no air entrainment during the fourth set of runs; the wall through which heat was being transferred was carefully cleaned at the beginning of the runs but was covered with a thin layer of scale at the end.

Sineath used physical properties similar to those of reference 28. The temperatures in the two channels were sufficiently close that the heat-transfer coefficients in both channels could be assumed the same.

The data of the fourth set of runs of Sineath are shown unchanged in figure 23; shown for comparison is equation (4). The data of Sineath are undoubtedly lower than they should be as a result of the deposit of an oxide film on the heat-transfer surface and of the abrupt change of

cross section at the entrance to the channels, which makes a portion of the heat-transfer surface ineffective. It is difficult, however, to estimate the magnitude of these effects.

English and Barrett. - English and Barrett (refs. 9 and 10) measured heating coefficients for mercury. The test sections were of nickel and stainless steel 0.051 inch in inner diameter and 0.059 inch in outer diameter. The test section length was approximately 1.9 inches. A copper coating was bonded to the outside of the test section; the outer diameter of the copper was 0.0825 inch. The test section was heated by passing electricity directly through it. The inlet and outlet mercury bulk temperatures were measured, as was the outside wall temperature along the test section; the voltage distribution along the test section was also measured. The velocity profile at the test section entrance was fully developed. The method of heating most nearly approximated uniform heat input to the wall. English and Barrett measured local heat-transfer coefficients along the test section and present the local fully developed coefficients for all runs. For one run, the local coefficient along most of the tube is presented.

The physical properties used by English and Barrett are the same as those of reference 28 except that the viscosity is slightly high at low temperatures. This will probably not affect the fully developed heat-transfer coefficients, but the entrance region Reynolds numbers should be increased 3 to 4 percent.

The fully developed heat-transfer coefficients of English and Barrett are shown unchanged in figure 24; equation (1) is shown for comparison. The entrance heat-transfer coefficients for the one run presented are shown in figure 25; Deissler's predicted curves for a Prandtl number of 0.01 and the same Peclet number range are shown for comparison.

Seban. - Seban (ref. 11) measured heat-transfer coefficients with lead-bismuth eutectic in two different types of test section. One was the figure eight type with a tube and concentric annulus; the other was a copper-coated tube heated by external electric heaters. Only combined heat-transfer coefficients for the tube and annulus of the figure eight test section are presented in reference 11. Not enough basic data (specifically fluid temperatures) are presented to separate the tube and annulus coefficients. Accordingly, only the electrically heated test section will be discussed. The test section was 0.652 inch in inner diameter by 48 inches in length. The copper coating was for the purpose of containing the wall thermocouples in a region of relatively low temperature gradient and of smoothing out the nonuniformities of heat input of the external electric heaters. The fluid bulk temperatures were measured at the inlet and outlet of the test section, and the wall temperatures were measured at eight stations along the tube. The velocity profile was close to fully developed at the entrance to the test section.

The method of heating approximates very closely uniform heat input to the wall. Local heat-transfer coefficients were measured. The local fully developed coefficients are presented for all the runs; entrance coefficients are presented for a few of the runs.

The physical properties of Seban are the same as those given in reference 28. Seban had some trouble with fouling, which caused the heat-transfer coefficients to decrease with time. Figure 26 shows unchanged the fully developed heat-transfer coefficients of Seban; equation (1) is shown for comparison. Those points taken immediately after cleaning have higher heat-transfer coefficients than the others. The entrance heat-transfer coefficients presented by Seban are shown in figure 27; predicted curves of Deissler (see fig. 3) for the same range of Peclet number and for a Prandtl number of 0.01 are shown for comparison.

Trefethen. - Trefethen (refs. 12 and 13) used a figure eight type of test section to measure heat-transfer coefficients with mercury. Six different tubes, described in the following table, were used in the tube and concentric annulus test section:

Test section	A	B	C	D	E	F
Tube inner diameter, in.	0.711	0.737	0.585	0.523	0.308	0.429
Annulus inner diameter, in.	.749	.748	.629	.627	.378	.500
Annulus outer diameter, in.	.874	.874	.874	.874	.874	.874
Length, in.	39.3	39.3	39.3	39.3	39.3	39.3
Tube material	Stainless steel	Stainless steel	Stainless steel	Copper	Copper	Copper

Heating and cooling tests were run in both the tube and the annulus. Trefethen measured the fluid bulk temperature at the inlet and outlet of the tube and annulus. He also measured the wall temperature of the outside of the annulus. The velocity profiles were between flat and fully developed at the entrance to the test section, probably a little closer to flat. The counterflow figure eight test section approximated a uniform heat input to the wall. Trefethen presents a fully developed heat-transfer coefficient for the central section of his tube (from 10.2 to 29.4 in. from the entrance). In his calculations he assumed that the temperature difference between the fluid in the tube and in the annulus remains the same as the temperature difference at the entrance to the tube and annulus, and that the fluid bulk temperature gradient along the length of the tube center section is the same as the temperature gradient along the annulus outer wall center section. Trefethen separates the tube and annulus coefficients in a manner different from that resulting from the use of equations (6) and (7).

The physical properties used by Trefethen are about the same as those of reference 28 for the range of temperature covered by his experiments. (The values of thermal conductivity at high temperature (extrapolated by Trefethen to correct the data of Styrikovich and Semenovker) are lower than those of the Liquid-Metals Handbook by about 6 percent at 212°, 14 percent at 392°, and 20 percent at 662° F.)

The data of Trefethen for fully developed heat-transfer coefficients were recalculated using equations (6) and (7) to separate the coefficients of the tube and annulus. The re-evaluated data for the tube are shown in figure 28; equation (1) is shown for comparison. Trefethen gives enough data to permit the calculation of over-all average heat-transfer coefficients for the tube and annulus. These coefficients also were calculated using equations (6) and (7) to separate the individual coefficients in the tube and annulus. These data are shown in figures 29 and 30; equations (1), (4), and (5) are shown for comparison.

Doody and Younger. - Doody and Younger (refs. 14 and 15) measured both heating and cooling coefficients for mercury with and without sodium additions. The test section was a steel tube 0.493 inch in inner diameter and 61 inches long. The test section was heated or cooled by water flowing in a concentric annulus. Both parallel and counterflow runs were made. The annulus was 61 inches long, but the annulus entrance and exit were each 6 inches from the ends of the test section; the length of the test section between the annulus entrance and exit was thus 49 inches. Tube wall temperatures were measured at five stations starting 1/2 inch downstream of the annulus inlet and ending 3 inches upstream of the annulus outlet (inlet and outlet refer to the parallel-flow case); the measurements covered $45\frac{1}{2}$ inches of the test section. The mercury temperature was measured at the inlet and outlet of the test section. The measurement of test-section exit temperature was made without any preliminary mixing of the fluid, and the exit temperature measured is closer to the fluid center-line temperature than to the fluid bulk temperature. The mercury velocity profile at the test section entrance was probably closer to flat than it was to fully developed. The method of heating resulted in a wall condition somewhere between uniform heat input and uniform wall temperature for the counterflow runs. The parallel flow runs resulted in a wall condition where the rate of heat input varied even more rapidly than for the conditioned uniform wall temperature.

The physical properties used by Doody and Younger are the same as those of reference 28 except for the thermal conductivity. The values of thermal conductivity used by Doody and Younger are low by about 1 to 14 percent in the temperature range of the investigation. Because of the location of the annulus entrance and exit as described, some effective length of test section between 49 inches and 61 inches must be selected. Doody and Younger used a method due to Sherwood and Petrie

(ref. 41) and arrived at an effective length of 56 inches. Since the wall temperatures at the ends of the test section were not measured, Doody and Younger extrapolated the wall temperature measurements to cover a length of 56 inches, the "effective" length of their test section. Inasmuch as this extrapolation necessarily neglects end effects, the data of Doody and Younger represent something between over-all average and fully developed heat-transfer coefficients.

The heat balances of Doody and Younger show deviations as great as 140 percent, with deviations between 40 and 100 percent being quite common. Flow was measured by an orifice, and the orifice calibration showed variations as great as 50 percent. The end temperature differences between the wall and the fluid found by the previously mentioned extrapolation were very small, varying from about 0.3° to 8° F, with values of 2° F or less being extremely common. Small errors in temperature measurement can therefore result in large errors in log mean temperature difference.

Doody and Younger attempted to check their experimental apparatus by running heat-transfer experiments with butanol. Unfortunately, most of these data were in the transition region. Some of the data were in the laminar flow region, and these data were 25 to 75 percent higher than the predictions of the Colburn equation for laminar flow (ref. 39, p. 191).

In view of the difficulties mentioned, the data of Doody and Younger may not be very accurate. The data of Doody and Younger were re-evaluated using the physical properties of reference 28 and the predictions of Martinelli for the ratio $(t_w - t_m)/(t_w - t_c)$ to determine the value of the temperature differences between the wall temperature and the fluid bulk temperature at the test-section exit. The original data on wall temperature are not presented in reference 14 or 15; therefore the extrapolated end temperature will be used for the wall temperature at the test-section inlet and outlet. The re-evaluated data of Doody and Younger are shown in figures 31 and 32; equations (1) and (2) are shown for comparison.

Lubarsky. - Lubarsky (ref. 16) used a figure eight type of test section to measure heating coefficients in a tube and cooling coefficients in a concentric annulus for lead-bismuth eutectic with and without magnesium additions. The test section was 40.2 inches long, with a tube inner diameter of 0.402 inch, an annulus diameter of 0.50 inch, and an annulus outer diameter of 0.625 inch. The fluid bulk temperatures at the inlet and outlet of the tube and annulus were measured. The entering velocity profile was approximately flat. The figure eight type heat exchanger with counterflow approximated uniform heat input to the wall. Over-all average heat-transfer coefficients were measured.

Lubarsky used physical properties which were the same as those of reference 28. He used equation (6) to separate the heat-transfer coefficients in the tube and the annulus. Lubarsky's data are shown unchanged in figures 33 and 34; equations (1) and (4) are shown for comparison.

Johnson, Hartnett, and Clabaugh (lead-bismuth tests). - Johnson, Hartnett, and Clabaugh (refs. 17 and 18) measured heating coefficients for lead-bismuth eutectic in an aluminum-coated tube heated externally by electric heaters. The test section is very similar to that of Seban (ref. 11) described above except that an aluminum coating has been used instead of a copper one. The test section inner diameter was 0.652 inch and its length, 48 inches. The fluid bulk temperature was measured at the inlet and the outlet of the test section, and the wall temperature was measured at eight stations along the wall. The inlet velocity profile was very close to fully developed. The method of heating very closely approximated uniform heat input to the wall. Local heat-transfer coefficients are presented for both the fully developed region and the entrance region.

Physical properties the same as those of reference 28 were used. The data on fully developed heat-transfer coefficients are shown unchanged in figure 35; equation (1) is shown for comparison. The data on entrance heat-transfer coefficients are shown unchanged in figure 36; predicted curves of Deissler (fig. 3(b)) for the same x/D and a Prandtl number of 0.01 are shown for comparison; the predictions of Poppendiek and Palmer (fig. 3(b)) for low Reynolds numbers are also shown in figure 36. From the local data of Johnson, Hartnett, and Clabaugh, it is possible to determine an approximate over-all average coefficient by plotting and integrating the local coefficients. The results of this procedure are shown in figure 37; equation (1) is shown for comparison.

Isakoff and Drew. - Isakoff and Drew (refs. 19 and 20) measured heating coefficients with mercury. The test section was a stainless steel tube, 0.127 inch in wall thickness, 1.5 inches in inner diameter, by about 223 inches in length, heated externally by electric heaters. The fluid bulk temperature was measured at the test section inlet and outlet and the outside wall temperature was measured at seven stations along the tube. Velocity and temperature profiles in the fluid were measured at three stations along the tube (x/D = 58, 98, and 138). The entrance velocity profile was very close to flat. The method of heating approximated very closely uniform heat input to the wall. Local fully developed heat-transfer coefficients were measured at the stations of x/D equal to 98 and 138. The heat-transfer coefficients measured at x/D equal to 58 are still in the entrance region.

The physical properties used by Isakoff and Drew are the same as those of reference 28. The inside wall temperature was calculated in two ways: one was to extrapolate the temperature profile in the fluid to the wall; the other was to use the measured outside wall temperature

to calculate the temperature drop through the wall. When this calculation was made, the two inside wall temperatures were found to coincide for only three of the total of twelve experimental runs. For the other nine runs, the inside wall temperature calculated from the outside wall temperatures was higher than the inside wall temperature as extrapolated from the fluid temperature profile. Fluid and wall temperatures for two typical runs are shown in figure 38.

This discrepancy between the two methods of determining inside wall temperature may be due to inaccuracies in the measurement of outside wall temperature. The outside wall temperature was measured by eight thermocouples at each station. The temperature readings of these thermocouples varied as much as 25 percent from one another in the high flux region. The deviation may have been due to the proximity of the thermocouples to the electric heaters. At any rate, the order of magnitude of the variation of the thermocouple readings on the outside wall is as great as the magnitude of the differences in temperature resulting from the two methods of calculating inside wall temperature. It is interesting to note, however, that the inside wall temperature as calculated from the outside wall temperature is greater (for nine cases out of twelve) than that extrapolated from the fluid temperature profile. This effect is that which would be noted if there were some form of interfacial resistance between the fluid and the tube. However, because of the circumferential variation of outside wall temperature and because three of the runs showed no difference in the inside wall temperature calculated by the two methods, no conclusions can be reached.

Figure 39 shows the data of Isakoff and Drew for the fully developed heat-transfer coefficient ($x/D = 138$); the coefficient is shown for both methods of calculating inside wall temperature; equation (1) is shown for comparison. The entrance data at x/D equal to 58 are shown in figure 40; inasmuch as the ordinate in figure 40 is a ratio, both methods of calculating the inside wall temperature give the same results; Deissler's predicted curves (fig. 3) are shown for comparison. The outside wall temperature was measured at a sufficient number of stations along the tube (see fig. 38) to permit the estimate of an over-all average heat-transfer coefficient. The average over-all coefficient from $x/D = 6.4$ to $x/D = 138$, based on inside wall temperatures calculated from the outside temperature, is shown in figure 41. These average coefficients are actually lower than the fully developed coefficients because the average outside wall temperature at the second station ($x/D = 98$) from the test section entrance is higher than might be expected from the other measured temperatures. Whether this might be a result of the local temperature gradients caused by the external electric heaters cannot be determined.

The temperature profiles in the fluid at x/D equal to 138 are shown in figure 42 and compared with the predictions of Martinelli (ref. 27).

Stromquist. - Stromquist (ref. 21) measured heating coefficients for mercury with and without sodium additions. The test section was a steel tube heated by passing electricity directly through the tube. The following four different test sections were used:

Test section	A	B	C	D
Inner diameter, in.	0.380	0.488	0.753	0.787
Outer diameter, in.	.753	1.002	1.500	1.501
Length, in.	47.25	48.25	50.25	50.25

Fluid bulk temperatures were measured at the test-section inlet and outlet and the outside wall temperatures were measured at twelve stations along the length of the test section. The entrance velocity profile to the test section was somewhere between flat and fully developed. The method of heating more nearly approximated uniform heat input than it did uniform wall temperature. Local heat-transfer coefficients, both entrance and fully developed, were measured.

Stromquist used physical properties which were the same as those of reference 28. Figure 43 shows, unchanged, the fully developed heat-transfer coefficients of Stromquist; equation (1) is included for comparison. Figure 44 shows, unchanged, the entrance heat-transfer coefficient data of Stromquist; Deissler's predicted curves (fig. 3(a)) are shown for comparison. The predictions of Poppendiek and Palmer (fig. 3(a)) for low Reynolds numbers are shown in figure 44(a).

MacDonald and Quittenton. - MacDonald and Quittenton (refs. 22 and 23) measured heating coefficients with sodium. The test section consisted of a monel tube with a copper jacket bonded to the outside. The test section was 0.625 inch in inner diameter by 60.05 inches in length and was heated externally by electric heaters. The purpose of the copper jacket was the same as the purpose of the copper coating used by Seban (ref. 11) and described in a previous section entitled "Seban." The fluid bulk temperature was measured at the inlet and outlet of the test section, and the wall temperatures were measured at eleven stations along the test section. The entrance velocity profile was close to fully developed if the length of piping in the diagram shown in figure 1 of reference 23 is to scale. The method of heating very closely approximated uniform heat input to the walls. Local heat-transfer coefficients were measured; the authors present fully developed heat-transfer coefficients for a length of the tube from 47.3 inches to 54.8 inches downstream of the tube entrance.

MacDonald and Quittenton used the same physical properties as reference 28. The data for fully developed heat-transfer coefficients are

shown, unchanged, in figure 45; equation (1) is shown for comparison. The data show a great amount of scatter. Consecutive runs at identical Peclet numbers and similar temperature levels vary as much as 120 percent in Nusselt number, with variations of 30 to 60 percent in consecutive runs being common. In view of this scatter, the entrance coefficients and over-all average coefficients have not been calculated, although the data were sufficient to make these calculations possible.

Johnson, Clabaugh, and Hartnett (mercury tests). - Johnson, Clabaugh, and Hartnett (ref. 24) measured heating coefficients for mercury. The test section was almost identical to the test section described previously under "Johnson, Hartnett, and Clabaugh (lead-bismuth tests)." The test section was an aluminum-coated tube 0.652 inch in inner diameter and 48 inches in length. The fluid bulk temperatures were measured at the inlet and outlet of the test section; the wall temperatures were measured at eight stations along the test section. The entrance velocity profile was close to fully developed. The method of heating approximated very closely uniform heat input to the wall. Local heat-transfer coefficients, both fully developed and entrance, are presented.

The physical properties used by Johnson, Clabaugh, and Hartnett are the same as those of reference 28. Figure 46 shows, unchanged, the fully developed heat-transfer coefficients of Johnson, Clabaugh, and Hartnett; equation (1) is shown for comparison. The entrance heat-transfer coefficients are shown in figure 47. Deissler's predicted curves (fig. 3(b)) are shown for comparison; the predictions of Poppendiek and Palmer (fig. 3(b)) for low Reynolds number are also shown in figure 47. From the experimentally determined entrance and fully developed heat-transfer coefficients, it is possible to determine by integration the over-all average coefficient. The resulting over-all average heat-transfer coefficients are shown in figure 48; equation (1) is shown for comparison.

Johnson, Hartnett, and Clabaugh (laminar and transition flow). - Johnson, Hartnett, and Clabaugh (ref. 25) have measured heating coefficients for lead-bismuth eutectic and mercury in the laminar and transition flow regions. The test section used was identical to the test sections used in the investigations of lead-bismuth and mercury in the turbulent flow region by Johnson, Hartnett, and Clabaugh (see the preceding sections entitled "Johnson, Hartnett, and Clabaugh (lead-bismuth)" and "Johnson, Clabaugh, and Hartnett (mercury)"). The test section was an aluminum-coated tube 0.652 inch in inner diameter by 48 inches in length. The fluid bulk temperatures were measured at the inlet and outlet of the test section and the wall temperatures were measured at eight stations along the test section. The entrance velocity profile was in doubt since the flow was mostly in the transition region. The method of heating approximated very closely uniform heat input to the wall. Local heat-transfer coefficients, both fully developed and entrance, were measured.

The physical properties used by Johnson, Hartnett, and Clabaugh are the same as those of reference 28. The fully developed heat-transfer coefficients are shown in figure 49; equation (1) is shown for comparison. The entrance region heat-transfer coefficients are shown in figure 50. There has been no theoretical work on entrance region heat transfer in the transition flow region, therefore no curves can be shown for purposes of comparison.

Poppendiek and Harrison. - Poppendiek and Harrison (ref. 26) have measured average heating coefficients with mercury in very short test sections. The test section was a small hole along the axis of a copper disk of 3-inch outer diameter heated on the outside with water. An unheated starting length was used so that the entrance velocity profile was very close to fully developed. Three different test sections were used:

Test section	A	B	C
Inner diameter, in.	1/8	1/16	1/8
Length, in.	1/8	1/16	1/16

The fluid bulk temperatures of the mercury were measured at the inlet and outlet of the test section. Wall temperatures were measured at several radial stations in the test section. The method of heating approximated constant wall temperature.

The properties used by Poppendiek and Harrison are the same as those of reference 28. The over-all average heat-transfer coefficients are shown in figure 51. Also shown is a predicted curve of Poppendiek and Harrison (ref. 26) for average coefficients. They obtained the curve by integrating the local coefficients predicted by Poppendiek and Palmer for low Peclet numbers (fig. 3).

So that the data could be compared with the predictions of Deissler (fig. 3), the local heat-transfer predictions of Deissler were integrated to obtain predictions for average Nusselt number for short length-diameter ratios. In figure 52, the data of Poppendiek and Harrison for average Nusselt number are compared with the predictions of Deissler for the average Nusselt number for small length-diameter ratios.

INTERCOMPARISON OF EXPERIMENTAL RESULTS AND COMPARISON WITH THEORY

The experimental results of the various investigators will be compared with each other and with theoretical predictions. The arrangement of the subjects to be considered will be the same as in the section "Theoretical Investigation of Liquid-Metal Heat Transfer" under "PROCEDURE."

Fully developed heat-transfer coefficients. - Fully developed heat-transfer coefficients for the case of uniform heat input to the wall were measured by the following investigators from the group of twenty investigations reviewed: Styrikovich and Semenovker; Elser; Untermeyer; English and Barrett; Seban; Trefethen; Johnson, Hartnett and Clabaugh (lead-bismuth); Isakoff and Drew; Stromquist; MacDonald and Quittenton; Johnson, Clabaugh, and Hartnett (mercury); and Johnson, Hartnett, and Clabaugh (laminar and transition flow). Curves representing mean lines through the data of these various investigators are shown in figure 53(a); when the amount of scatter of a set of data is so great that no mean line can be drawn through it, a cross-hatched area is used to represent the data; equation (1) is shown in figure 53(a) for purposes of comparison. The spread of all the data in figure 53(a) is extremely great. However, the following data are not considered:

(a) Data below a Peclet number of 200: These data, being below a Reynolds number of 10,000 and therefore in the transition flow region, are not intended to be represented by equation (1).

(b) Data of Elser and of MacDonald and Quittenton: These are less reliable because of the very large scatter of the data.

(c) Data of Untermeyer: Severe corrosion throughout the duration of the tests caused large changes in the physical dimensions of the test section, as well as possibly contaminating the fluid and the heat-transfer surface.

The Nusselt number of remaining data can be compared with the predicted values of equation (1) as follows:

Peclet number	200	500	1000	2000	5000	9000
Range of ratio of measured values to predicted values	0.54 to 0.69	0.55 to 0.75	0.57 to 0.96	0.57 to 1.04	0.55 to 1.13	0.50 to 1.26

Another method of comparing the data for the fully developed heat transfer is to show on a single plot the actual corrected data of all the investigators. Figure 53(b) is such a plot. If the same data are considered valid in this figure as in figure 53(a), a line given by the following equation would best represent most of the data:

$$Nu = 0.625\ Pe^{0.4} \tag{14}$$

This equation is purely empirical and does not in any way suggest that the theoretical predictions are faulty. However, inasmuch as there is a considerable amount of scatter and since most of the data agree fairly

well with this line, it would seem preferable for the designer to use equation (14) until further experiment reduces the uncertainty as to the precise values of liquid-metal heat-transfer coefficients.

Local heat-transfer coefficients in entrance region. - Entrance region heat-transfer coefficients have been measured by the following investigators from the group of twenty investigations reviewed: English and Barrett; Seban; Johnson, Hartnett, and Clabaugh (lead-bismuth); Isakoff and Drew; Stromquist; Johnson, Clabaugh, and Hartnett (mercury); Johnson, Hartnett, and Clabaugh (laminar and transition flow); and Poppendiek and Harrison. The bulk of the data on heat transfer in the entrance region is in the reports of Johnson, Hartnett, and Clabaugh (lead-bismuth); Stromquist; Johnson, Clabaugh, and Hartnett (mercury); and Poppendiek and Harrison; and is presented in figures 36, 44, 47, and 52.

There is considerable scatter in most of the entrance heat-transfer data presented. The predictions of Deissler (fig. 3) agree well with the data of Stromquist (fig. 44), but fall slightly low when compared with the remaining data (figs. 36, 47, and 52).

English and Barrett, Seban, and Isakoff and Drew present a small amount of entrance region heat-transfer data. As may be seen from figure 25, the data of English and Barrett are considerably lower than the predictions of Deissler. The data of Seban (fig. 27) agree reasonably well with the predictions of Deissler. The data of Isakoff and Drew (fig. 40) are considerably higher than the predictions of Deissler, which may be in part due to the fact that the entrance velocity profile of Isakoff and Drew was very nearly flat, while in the analyses of Deissler a fully developed velocity profile is assumed at the entrance.

Average heat-transfer coefficients. - Theoretical predictions of the over-all average heat-transfer coefficient can be made from the information on local heat-transfer coefficients. The predictions of Deissler for the ratio Nu_f/Nu_x were integrated mechanically, and the values of the ratio of average Nusselt number to fully developed Nusselt number Nu_a/Nu_f are shown plotted against length-diameter ratio x/D for various Peclet numbers in figure 54.

Values of average Nusselt number were determined from the values of the ratio Nu_a/Nu_f in figure 54 and the values of fully developed Nusselt number Nu_f of equation (1). The results are shown in figure 55, which gives the variation of average Nusselt number with Peclet number for several length-diameter ratios.

The measured average heat transfer coefficients are described.

(a) Uniform heat input to the wall; round tubes: Average heat-transfer coefficients in round tubes with constant heat input to the walls were measured by the following investigators: Lyon; Werner, King, and Tidball; Trefethen; Lubarsky; Johnson, Hartnett, and Clabaugh (lead-bismuth); Isakoff and Drew; and Johnson, Clabaugh, and Hartnett (mercury). Curves representing mean lines through the data of these various investigators are shown in figure 56. Also shown is the relation for average Nusselt number (L/D = 100) from figure 55. The Nusselt numbers of the data compare with the predicted values for a length-diameter ratio of 100 as follows (values below a Peclet number of 200 are not considered because they fall in the transition flow region):

Peclet number	200	500	1000	2000	5000	9000
Range of ratio of measured values to predicted values	0.64 to 0.88	0.75 to 1.03	0.54 to 1.10	0.61 to 1.21	0.75 to 0.83	0.70 to 0.88

(b) Uniform wall temperature; round tubes: Average heat-transfer coefficients in round tubes with uniform wall temperatures or with wall conditions somewhere between uniform wall temperature and uniform heat input were measured by Gilliland, Musser, and Page and by Doody and Younger. In figure 57 are curves representing mean lines through the data of Gilliland, Musser, and Page; the data of Doody and Younger are represented by a cross-hatched area because of scatter. Also shown in figure 57 are the relations for average Nusselt number (L/D = 100) calculated from equations (1) and (2) and figure 55. The following data are not considered:

(a) Data below a Peclet number of 200: These data are in the transition flow region.

(b) Data of Doody and Younger: The scatter is large.

The Nusselt number of the remaining data can be compared with the predicted values for an L/D of 100 as follows (values of Nusselt number halfway between the values of the two theoretical curves in fig. 57 will be used for comparison):

Peclet number	500	1000
Range of ratio of measured values to predicted values	0.63 to 0.69	0.61 to 0.72

(c) Annuli: Average heat-transfer coefficients in annuli or between flat plates with constant heat input to the wall were measured by Lyon; Werner, King, and Tidball; Sineath; Trefethen; and Lubarsky. Figure 58 shows curves representing mean lines through the data of these various investigators; also shown are the relations for average Nusselt number ($L/D = 100$) calculated from equations (4) and (5) and figure 55. The Nusselt numbers of the data compare with the predicted Nusselt numbers (average of the Nusselt numbers of the two theoretical curves of fig. 58) as follows (values below a Peclet number of 200 are not considered because they fall in the transition flow region):

Peclet number	200	500	1000
Range of ratio of measured values to predicted values	0.69 to 1.21	0.39 to 1.37	0.39 to 0.67

Temperature distribution. - The only experimental data on temperature distribution is the work of Isakoff and Drew. Plots of the temperature distributions measured by Isakoff and Drew are shown in figure 42; Martinelli's predicted temperature distributions are shown for comparison. It is possible to use Isakoff and Drew's temperature and velocity profiles (the measured velocity profiles check quite well with the predicted velocity profiles) to calculate the values of the ratio $(t_w - t_m)/(t_w - t_c)$ shown in figure 59. Martinelli's predictions (fig. 5) for the ratio $(t_w - t_m)/(t_w - t_c)$ are also shown. The measured values are smaller than the predicted values. The predicted values of Martinelli for $(t_w - t_m)/(t_w - t_c)$ were used to calculate the fluid bulk temperature in those cases in which fluid center-line temperature was measured (Elser; Doody and Younger; Werner, King, and Tidball (test section A)). If the values of $(t_w - t_m)/(t_w - t_c)$ are actually lower than predicted by Martinelli, the Nusselt numbers of these cases would increase.

Final comparison of heat-transfer data. - The experimental data of all the investigators for fully developed and average heat-transfer coefficients have been compared with the appropriate prediction and the results are shown in table I.

Figure 60 shows the variation of the ratio of measured to predicted Nusselt number with Peclet number for some of the data of table I. The results which are not shown in figure 60 were not included for the following reasons:

(a) There is large scatter of data.

(b) Obvious uncertainties exist as to the accuracy of the data.

(c) The measurements are of average heat-transfer coefficients which were made concurrently with the measurement of fully developed coefficients; the fully developed coefficients are shown in figure 60.

(d) The measurements are of annulus heat-transfer coefficients which were made concurrently with the measurement of round tube coefficients; the round tube coefficients are shown in figure 60.

On the basis of the results shown in table I and figure 60, it can be seen that most of the measured values of fully developed and average Nusselt numbers for turbulent flow (as given by eqs. (1), (2), (4), and (5) and fig. 54) fall between 60 to 80 percent of their predicted values.

SUGGESTED EXPERIMENTAL WORK

It is suggested that the type of experiment most likely to reduce the uncertainties with respect to liquid-metal heat transfer would be one in which velocity and temperature profiles were measured in the fluid, somewhat like the experiment of Isakoff and Drew. The experiment of Isakoff and Drew could be improved by the use of a thick, high conductivity, metallic coating around the test section similar to the one used by Seban or Johnson, Hartnett, and Clabaugh; this would probably eliminate the uncertainties as the measurements of outside wall temperature.

The experimental data are insufficient to lead to any conclusion concerning liquid-metal heat transfer in the laminar and transition flow region. Such data are greatly needed because the small amount of data in these flow regions disagree considerably with theoretical predictions.

CONCLUDING REMARKS

The review of the experimental investigations of liquid-metal heat transfer may be summarized as follows:

(1) The experimental data of the various investigators were re-evaluated using as consistent assumptions and methods as possible, and the results were compared with each other and with theory.

(2) The re-evaluated experimental data for fully developed Nusselt number in the turbulent flow region were found still to have considerable spread, and most of the data are lower than predicted by theory.

(3) An equation based on empirical grounds, which best represents most of the fully developed heat-transfer data, is

$$Nu = 0.625\ Pe^{0.4}$$

where Nu and Pe represent Nusselt number and Peclet number, respectively.

(4) The theoretical predictions of heat transfer in the entrance region were found to give lower values, in most cases, than those found in the experimental work.

(5) Integrating the theoretical and experimental results for the ratio Nu_x/Nu_f gave predictions for the value of the ratio Nu_a/Nu_f over a range of Peclet number and length-diameter ratio.

(6) The small amount of data on temperature distribution disagreed with the theoretical predictions, the discrepancy increasing with decreasing Reynolds number.

(7) The experimental evidence is insufficient to lead to any conclusion about liquid-metal heat transfer in the laminar and transition flow region.

Lewis Flight Propulsion Laboratory
National Advisory Committee for Aeronautics
Cleveland, Ohio, November 4, 1954

REFERENCES

1. Styrikovich, M. A., and Semenovker, I. E.: Heat Exchange at Very Low Prandtl Numbers. Jour. Tech. Phys. (USSR), vol. X, no. 16, 1940, pp. 1324-1330.

2. Gilliland, E. R., Musser, R. J., and Page, W. R.: Heat Transfer to Mercury. General Discussion on Heat Transfer, Inst. Mech. Eng. and A.S.M.E., 1951, pp. 402-404.

3. Musser, R. J., and Page, W. R.: Heat Transfer to Mercury. M.S. Thesis, M.I.T., 1947.

4. Elser, D. (Ronald Kay, trans.): Heat Transfer Measurements with Mercury. Eng. Res. Proj., Univ. Calif., May 10, 1949.

5. Bailey, D. L. R., Cope, W. F., and Watson, G. G.: Heat Transfer to Mercury. Heat Div. Paper No. 13, Mech. Eng. Res. Lab., East Kilbride (Glasgow), July 1952.

6. Lyon, Richard N.: Forced Convection Heat Transfer Theory and Experiments with Liquid Metals. ORNL 361, Tech. Div., Eng. Res. Section, Oak Ridge Nat. Lab., Apr. 1949. (Contract No. W-7405, eng. 26.)

7. Werner, Robert C., King, Earle C., and Tidball, Robert A.: Heat Transfer with Sodium-Potassium Liquid Alloys. Paper presented at meeting of Am. Inst. Chem. Eng., Pittsburgh (Penn.), Dec. 5, 1949.

8. Sineath, Henry H.: Heat Transfer to Mercury - The Asymmetric Case. M.S. Thesis, Univ. of Tenn., 1949.

9. English, D., and Barrett, T.: Heat Transfer Properties of Mercury. A.E.R.E. E/R 547, Atomic Energy Res. Est., Ministry of Supply, Harwell, Berks, June 1950.

10. English, D., and Barrett, T.: Heat-transfer Properties of Mercury. General Discussion of Heat Transfer, Inst. Mech. Eng. and A.S.M.E., 1951, pp. 458-460.

11. Seban, R. A.: Heat Transfer Measurements on Lead Bismuth Eutectic in Turbulent Pipe Flow. Inst. Eng. Res., Univ. Calif., June 15, 1950. (Contract N7-onr-29523, Phase (2), Proj. NR 035 324.)

12. Trefethen, Lloyd MacGregor: Heat Transfer Properties of Liquid Metals. NP 1788, Tech. Info. Service, United States Atomic Energy Comm., July 1, 1950.

13. Trefethen, Lloyd M.: Liquid Metal Heat Transfer in Circular Tubes and Annuli. General Discussion on Heat Transfer, Inst. Mech. Eng. and A.S.M.E., 1951, pp. 436-438.

14. Doody, T. C., and Younger, Andrew H.: Heat Transfer Coefficients for Liquid Mercury and Dilute Solutions of Sodium in Mercury in Forced Convection. Preprints of papers presented at meeting of Am. Inst. Chem. Eng., Atlantic City (New Jersey), Dec. 5, 1951, pp. 77-98.

15. Younger, A. H.: Heat Transfer for Liquid Mercury and Dilute Solutions of Sodium in Mercury. Doctoral Thesis, Purdue Univ., Jan. 1951.

16. Lubarsky, Bernard: Experimental Investigation of Forced-Convection Heat-Transfer Characteristics of Lead-Bismuth Eutectic. NACA RM E51G02, 1951.

17. Johnson, H. A., Hartnett, J. P., and Clabaugh, W. J.: Heat Transfer to Molten Lead-Bismuth Eutectic in Turbulent Pipe Flow. Final Rep., Univ. Calif., Inst. Eng. Res., Nov. 15, 1951. (Contract A.E.C. No. AT-(40-1)-1061 Pt. 2.)

18. Johnson, H. A., Hartnett, J. P., and Clabaugh, W. J.: Heat Transfer to Molten Lead-Bismuth Eutectic in Turbulent Pipe Flow. Trans. A.S.M.E., vol. 75, no. 6, Aug. 1953, pp. 1191-1198.

19. Isakoff, Sheldon E., and Drew, Thomas B.: Heat and Momentum Transfer in Turbulent Flow of Mercury. General Discussion on Heat Transfer, Inst. Mech. Eng. and A.S.M.E., 1951, pp. 405-409.

20. Isakoff, Sheldon E.: Heat and Momentum Transfer in Turbulent Flow of Mercury. Ph. D. Thesis, Columbia Univ., May 1952.

21. Stromquist, W. K.: Effect of Wetting on Heat Transfer Characteristics of Liquid Metals. ORO-93, Tech. Info. Service, U. S. Atomic Energy Commission, Mar. 1953. (Contract No. AT-(40-1)-1310.)

22. MacDonald, W. C., and Quittenton, R. C.: A Critical Analysis of Metal "Wetting" and Gas Entrainment in Heat Transfer to Molten Metals. Preprint No. 8, Am. Inst. Chem. Eng., 1953.

23. Quittenton, Richard Charles: The Direct Measurement of the Film Coefficient of Heat Transfer to Molten Sodium Metal in Forced Convection. Ph. D. Thesis, Univ. of Toronto, 1953.

24. Johnson, H. A., Clabaugh, W. J., and Hartnett, J. P.: Heat Transfer to Mercury in Turbulent Pipe Flow. Inst. Eng. Res., Univ. Calif., July 1953. (Contract AT-11-1-GEN 10, Proj. 5, Phase II.)

25. Johnson, H. A., Hartnett, J. P., and Clabaugh, W. J.: Heat Transfer to Lead-Bismuth and Mercury in Laminar and Transition Pipe Flow. Inst. Eng. Res., Univ. Calif., Aug. 1953. (Contract AT-11-1-GEN 10, Proj. 5, Phase II.)

26. Poppendiek, H. F., and Harrison, W. B.: Remarks on Thermal Entrance-Region Heat Transfer in Liquid-Metal Systems. Preprint No. 7, Am. Inst. Chem. Eng., 1953.

27. Martinelli, R. C.: Heat Transfer to Molten Metals. Trans. A.S.M.E., vol. 69, no. 8, Nov. 1947, pp. 947-959.

28. Lyon, Richard N., ed.: Liquid-Metals Handbook. Second ed., Atomic Energy Comm., Dept. Navy, June 1952.

29. Cope, W. F.: Heat Transfer to Mercury. General Discussion on Heat Transfer, Inst. Mech. Eng. and A.S.M.E., 1951, pp. 453-458.

30. Kennison, R. G.: Vorticity Heat Transfer in Molten Metals. Knolls Atomic Power Lab., General Electric Co., Apr. 11, 1952.

31. Deissler, Robert G.: Analysis of Fully Developed Turbulent Heat Transfer at Low Peclet Numbers in Smooth Tubes with Application to Liquid Metals. NACA RM E52F05, 1952.

32. Seban, R. A., and Shimazaki, T. T.: Heat Transfer to a Fluid Flowing Turbulently in a Smooth Pipe with Walls at Constant Temperature. Paper No. 50-A-128, A.S.M.E., 1950.

33. Seban, R. A.: Heat Transfer to a Fluid Flowing Turbulently Between Parallel Walls with Asymmetric Wall Temperatures. Trans. A.S.M.E., vol. 72, no. 6, Aug. 1950, pp. 789-795.

34. Bailey, Raymond V.: Heat Transfer to Liquid Metals in Concentric Annuli. ORNL 521, Tech. Div., Eng. Res. Section, Oak Ridge Nat. Lab., June 13, 1950. (Contract No. W-7405, eng. 26.)

35. Poppendiek, H. F.: Forced Convection Heat Transfer in Thermal Entrance Regions, Pt. I. ORNL 913, Reactor Tech. Div., Oak Ridge Nat. Lab., Mar. 1951. (Contract No. W-7405, eng. 26.)

36. Poppendiek, H. F., and Palmer, L. D.: Forced Convection Heat Transfer in Thermal Entrance Regions, Pt. II. ORNL 914, Reactor Exp. Eng. Div., Oak Ridge Nat. Lab., May 26, 1952. (Contract No. W-7405, eng. 26.)

37. Deissler, Robert G.: Analysis of Turbulent Heat Transfer and Flow in Entrance Regions of Smooth Passages. NACA TN 3016, 1953.

38. Seban, R. A., and Shimazaki, T.: Calculations Relative to the Thermal Entry Length for Fluids of Low Prandtl Number. Inst. Eng. Res., Univ. Calif., Jan. 10, 1950. (Contract No. N7-onr-29523, Phase (2), NR 035 324.)

39. McAdams, William H.: Heat Transmission. Second ed., McGraw-Hill Book Co., Inc., 1942.

40. Harrison, W. B., and Menke, J. R.: Heat Transfer to Liquid Metals Flowing in Asymmetrically Heated Channels. Trans. A.S.M.E., vol. 71, no. 7, Oct. 1949, pp. 797-803.

41. Sherwood, T. K., and Petrie, J. M.: Heat Transmission to Liquids Flowing in Pipes. Ind. and Eng. Chem., vol. 24, no. 7, July 1932, pp. 736-745.

TABLE I. - COMPARISON OF HEAT-TRANSFER DATA

Investigation	Reference	Type of heat-transfer coefficient measured	Theoretical equation used for comparison	Ratio of measured Nusselt number to predicted Nusselt number for Peclet number of					
				200	500	1000	2000	5000	9000
Styrikovich and Semenovker	1	Round tube; fully developed; uniform heat input	$Nu_f = 7.0 + 0.025\ Pe_f^{0.8}$			0.80	0.77		
Gilliland, Musser, and Page (heating data)	2, 3	Round tube; over-all average; uniform wall temperature	$Nu_f = 5.0 + 0.025\ Pe_f^{0.8}$ [a]corrected for L/D = 44		0.69	0.72			
Gilliland, Musser, and Page (cooling data)	2, 3	Round tube; over-all average; between uniform heat input and uniform wall temperature	$Nu_f = 6.0 + 0.025\ Pe_f^{0.8}$ (average of eqs. (1) and (2)) corrected for L/D = 160		0.63	0.61			
Elser	4	Round tube; fully developed; uniform heat input	$Nu_f = 7.0 + 0.025\ Pe_f^{0.8}$				0.17-.40		
Bailey, Cope, and Watson	5	Round tube; fully developed; between uniform heat input and uniform wall temperature	$Nu_f = 6.0 + 0.025\ Pe_f^{0.8}$ (average of eqs. (1) and (2))	0.36	0.46	0.39	0.35		
Lyon (tube data)	6	Round tube; over-all average; uniform heat input	$Nu_f = 7.0 + 0.025\ Pe_f^{0.8}$ corrected for L/D = 110	0.63	0.72	0.80			
Lyon (annulus data)	6	Annulus; over-all average; uniform heat input	$Nu_f' = 5.8 + 0.020(Pe_f')^{0.8}$ corrected for L/D = 225	0.74	0.90				
Untermeyer (without magnesium additions)		Round tube; fully developed; uniform heat input	$Nu_f = 7.0 + 0.025\ Pe_f^{0.8}$		0.16	0.23	0.48		
Untermeyer (with magnesium additions)		Round tube; fully developed; uniform heat input	$Nu_f = 7.0 + 0.025\ Pe_f^{0.8}$		0.92	0.80			
Werner and King (heat exchanger A; tube data)		Round tube; over-all average; uniform heat input	$Nu_f = 7.0 + 0.025\ Pe_f^{0.8}$ corrected for L/D = 49	0.69	0.76	0.79			
Werner and King (heat exchanger A; annulus data)		Annulus; over-all average; uniform heat input	$Nu_f' = 0.75\ (D_o/D_1)^{0.3}\left[7.0 + 0.025(Pe_f')^{0.8}\right]$ $D_o/D_1 = 1.83$ corrected for L/D = 55	0.90					
Werner, King, and Tidball (heat exchanger B; tube data)	7	Round tube; over-all average; uniform heat input	$Nu_f = 7.0 + 0.025\ Pe_f^{0.8}$ corrected for L/D = 49		0.97	1.04	1.14		
Werner, King, and Tidball (heat exchanger B; annulus data)	7	Annulus, over-all average; uniform heat input	$Nu_f' = 0.75\ (D_o/D_1)^{0.3}\left[7.0 + 0.025(Pe_f')^{0.8}\right]$ $D_o/D_1 = 1.83$; corrected for L/D = 55	1.15	1.29				
Sineath	8	Rectangular ducts; over-all average; uniform heat input	$Nu_f' = 5.8 + 0.020(Pe_f')^{0.8}$ corrected for L/D = 50		0.41	0.40			
English and Barrett	9, 10	Round tube; fully developed; uniform heat input	$Nu_f = 7.0 + 0.025\ Pe_f^{0.8}$	0.61	0.74				
Seban	11	Round tube; fully developed; uniform heat input	$Nu_f = 7.0 + 0.025\ Pe_f^{0.8}$			0.67	0.58		
Trefethen (fully developed tube data)	12, 13	Round tube; fully developed; uniform heat input	$Nu_f = 7.0 + 0.025\ Pe_f^{0.8}$	0.68	0.77	0.78	0.76		
Trefethen (over-all average tube data)	12, 13	Round tube; over-all average; uniform heat input	$Nu_f = 7.0 + 0.025\ Pe_f^{0.8}$ corrected for L/D = 65	0.74	0.83	0.86	0.87		

[a]"Corrected for L/D" means that the fully developed Nusselt number found from the equation was multiplied by the ratio Nu_a/Nu_f from fig. 54.

TABLE I. - Concluded. COMPARISON OF HEAT-TRANSFER DATA

Investigation	Reference	Type of heat-transfer coefficient measured	Theoretical equation used for comparison	Ratio of measured Nusselt number to predicted Nusselt number for Peclet number of					
				200	500	1000	2000	5000	9000
Trefethen (over-all average annulus data)	12, 13	Annulus; over-all average; uniform heat input	Average of $Nu_f = 5.8 + 0.020\ Pe_f^{0.8}$ and $Nu_f = 0.75\ (D_o/D_i)^{0.3}\left[7.0 + 0.025\ (Pe_f)^{0.8}\right]$, $\frac{D_o}{D_i} = 2$, corrected for L/D = 200	0.81	0.87				
Doody and Younger (data with no sodium additions)	14, 15	Round tube; over-all average; between uniform heat input and uniform wall temperature	$Nu_f = 6.0 + 0.025\ Pe_f^{0.8}$ (average of eqs. (1) and (2)), corrected for L/D = 114	0.22 .51	0.33 .53				
Doody and Younger (data with sodium additions)	14, 15	Round tube; over-all average; between uniform heat input and uniform wall temperature	$Nu_f = 6.0 + 0.025\ Pe_f^{0.8}$ (average of eqs. (1) and (2)), corrected for L/D = 114	0.50 .92					
Lubarsky (tube data)	16	Round tube; over-all average; uniform heat input	$Nu_f = 7.0 + 0.025\ Pe_f^{0.8}$ corrected for L/D = 100			0.54	0.61		
Lubarsky (annulus data)	16	Annulus; over-all average; uniform heat input	$Nu_f = 5.8 + 0.020(Pe_f)^{0.8}$ corrected for L/D = 320		0.59	0.72			
Johnson, Hartnett, and Clabaugh (lead-bismuth; fully developed data)	17, 18	Round tube; fully developed; uniform heat input	$Nu_f = 7.0 + 0.025\ Pe_f^{0.8}$			0.76	0.70		
Johnson, Hartnett, and Clabaugh (lead-bismuth; over-all average data)	17, 18	Round tube; over-all average; uniform heat input	$Nu_f = 7.0 + 0.025\ Pe_f^{0.8}$ corrected for L/D = 74			0.77	0.72		
Isakoff and Drew (fully developed data; inside wall temperature calculated from fluid temperature profile)	19, 20	Round tube; fully developed; uniform heat input	$Nu_f = 7.0 + 0.025\ Pe_f^{0.8}$			0.97	1.05	1.14	1.25
Isakoff and Drew (fully developed data; inside wall temperature calculated from outside wall temperature)	19, 20	Round tube; fully developed; uniform heat input	$Nu_f = 7.0 + 0.025\ Pe_f^{0.8}$			0.95	0.94	0.90	0.91
Isakoff and Drew (over-all average data; inside wall temperature calculated from outside wall temperature)	19, 20	Round tube; over-all average; uniform heat input	$Nu_f = 7.0 + 0.025\ Pe_f^{0.8}$ corrected for L/D = 138			0.93	0.84	0.84	0.86
Stromquist	21	Round tube; fully developed; uniform heat input	$Nu_f = 7.0 + 0.025\ Pe_f^{0.8}$	0.54	0.55	0.57	0.58	0.54	0.51
MacDonald and Quittenton	22, 23	Round tube; fully developed; uniform heat input	$Nu_f = 7.0 + 0.025\ Pe_f^{0.8}$	1.0- .26					
Johnson, Clabaugh, and Hartnett (mercury; fully developed data)	24	Round tube; fully developed; uniform heat input	$Nu_f = 7.0 + 0.025\ Pe_f^{0.8}$	0.68	0.70	0.71	0.70	0.65	0.60
Johnson, Clabaugh, and Hartnett (mercury; over-all average data)	24	Round tube; over-all average; uniform heat input	$Nu_f = 7.0 + 0.025\ Pe_f^{0.8}$ corrected for L/D = 74	0.70	0.73	0.75	0.76	0.76	0.69
Johnson, Hartnett and Clabaugh (laminar and transition flow)	25	Round tube; fully developed; uniform heat input	$Nu_f = 7.0 + 0.025\ Pe_f^{0.8}$	0.68					

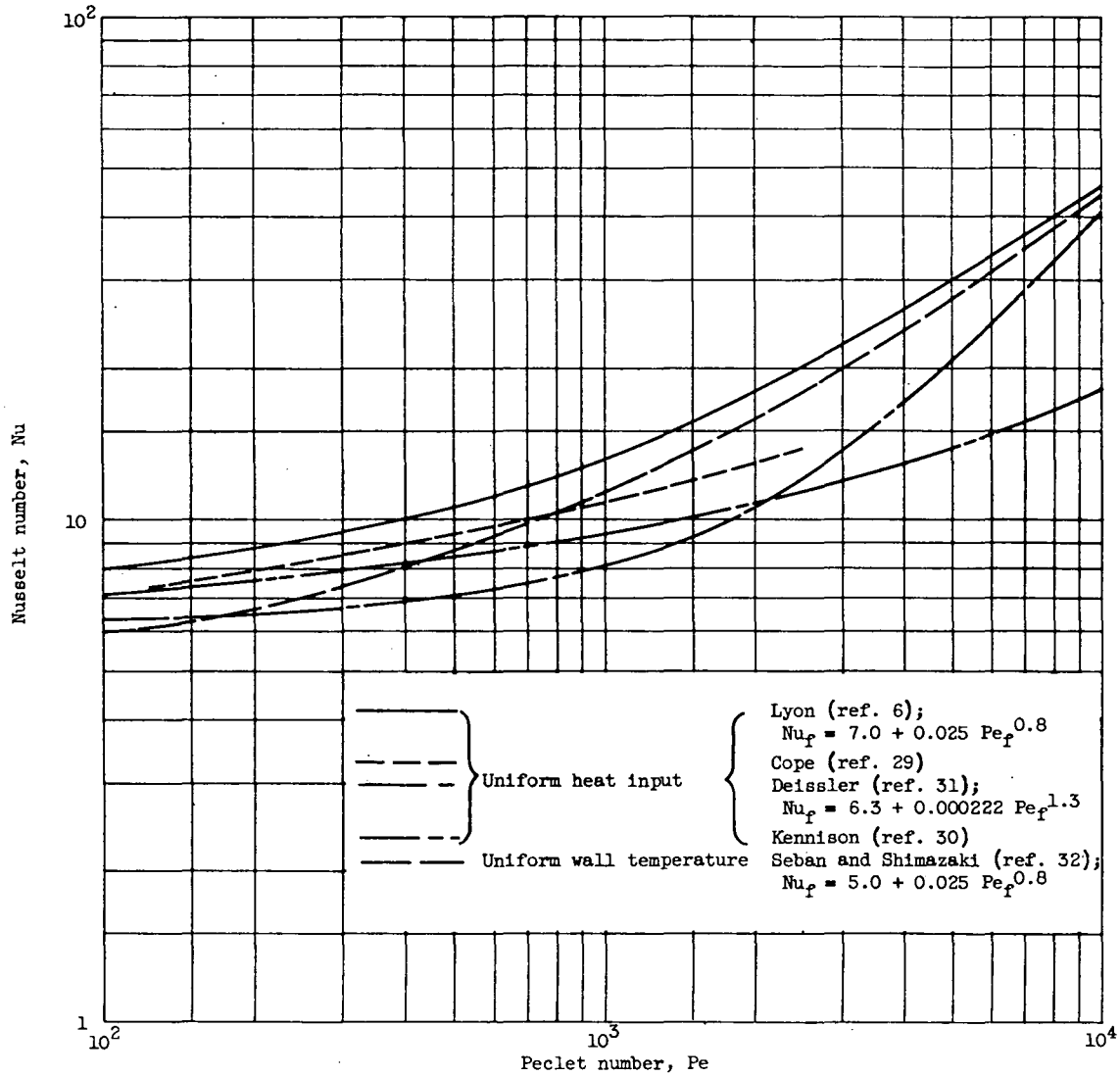

Figure 1. - Theoretical predictions of fully developed Nusselt numbers for heat transfer to liquid metals in turbulent flow in round tubes.

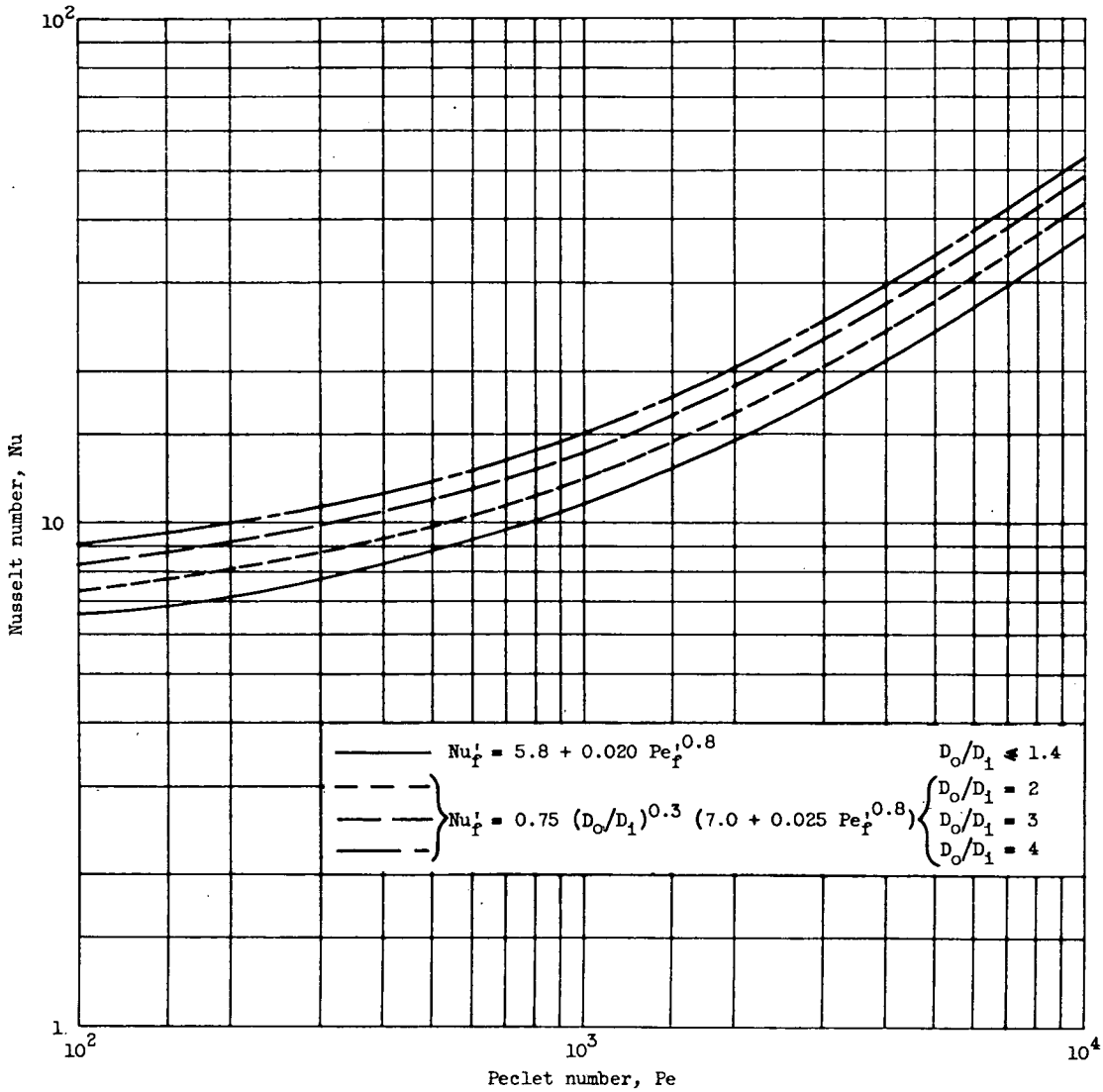

Figure 2. - Theoretical predictions of fully developed Nusselt numbers for heat transfer to liquid metals in turbulent flow in annuli and between flat plates.

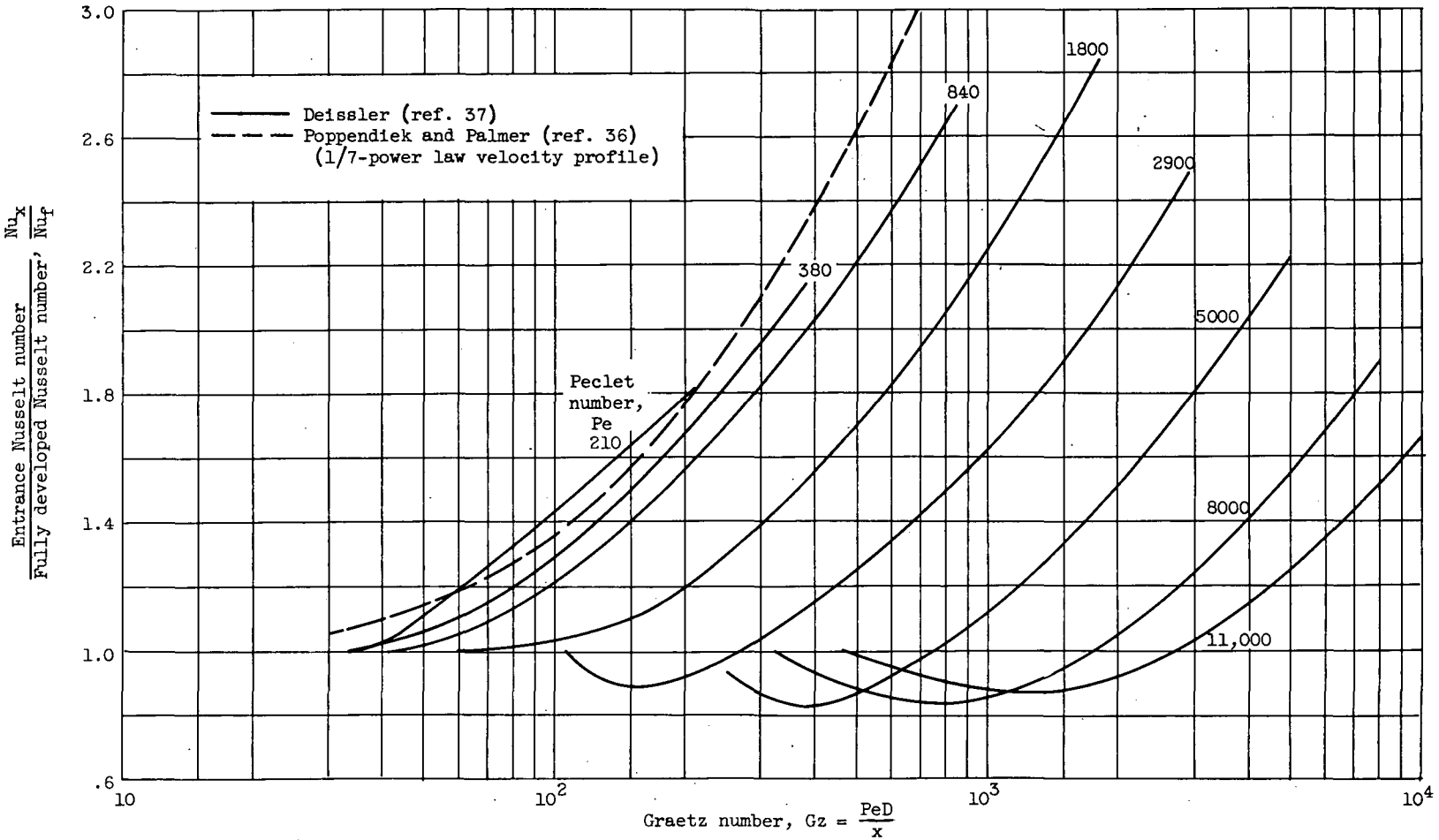

(a) Ratio of entrance Nusselt number to fully developed Nusselt number against Graetz number.

Figure 3. - Theoretical predictions of heat transfer to liquid metals in turbulent flow in round tubes.

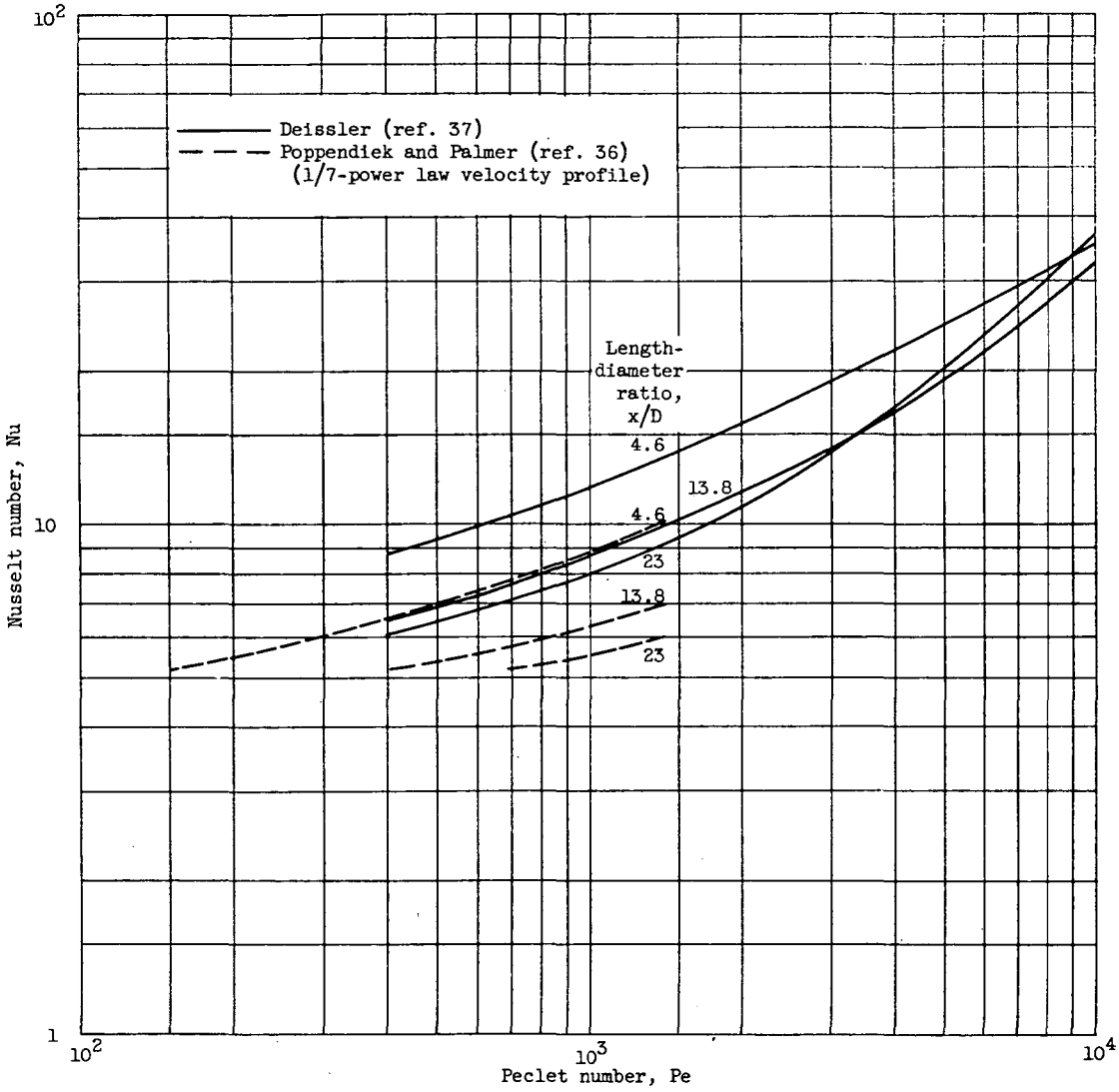

(b) Nusselt number against Peclet number.

Figure 3. - Concluded. Theoretical prediction of heat transfer to liquid metals in turbulent flow in round tubes.

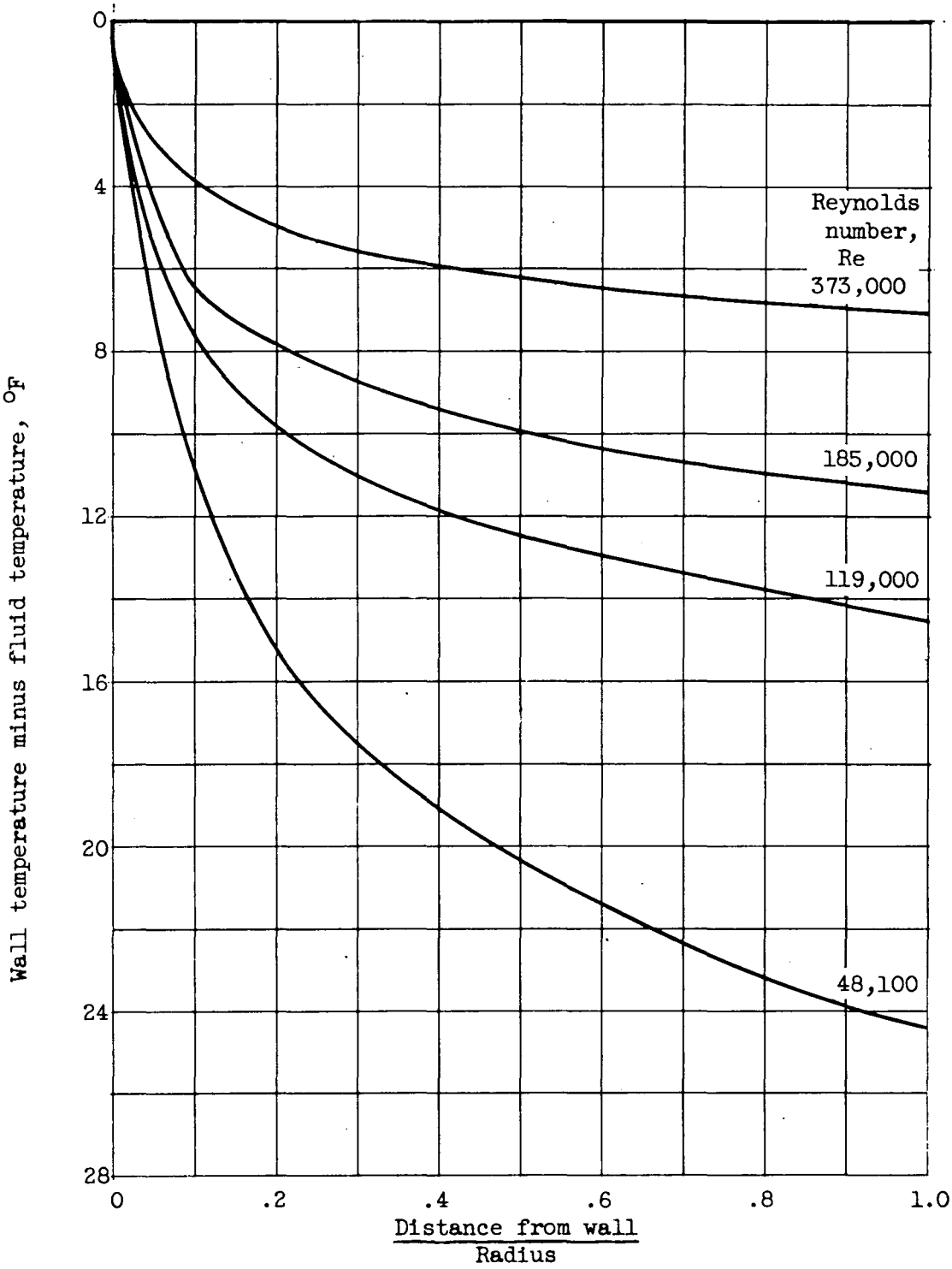

Figure 4. - Theoretical predictions of Martinelli (ref. 27) for fully developed temperature profiles for heat transfer to liquid metals in round tubes. Prandtl number, 0.022.

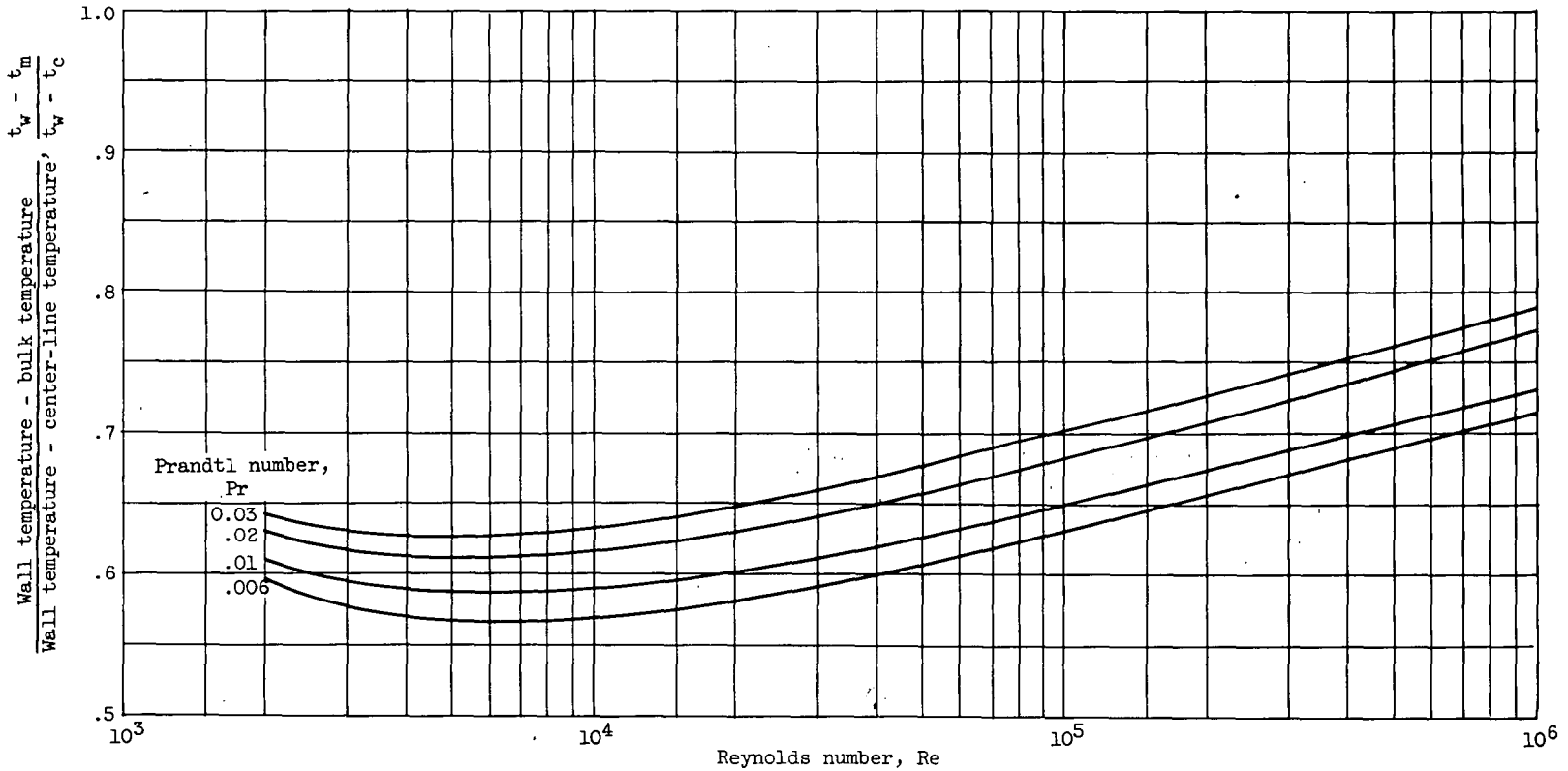

Figure 5. - Theoretical predictions of Martinelli (ref. 27) of ratio $(t_w - t_m)/(t_w - t_c)$ for heat transfer to liquid metals in round tubes.

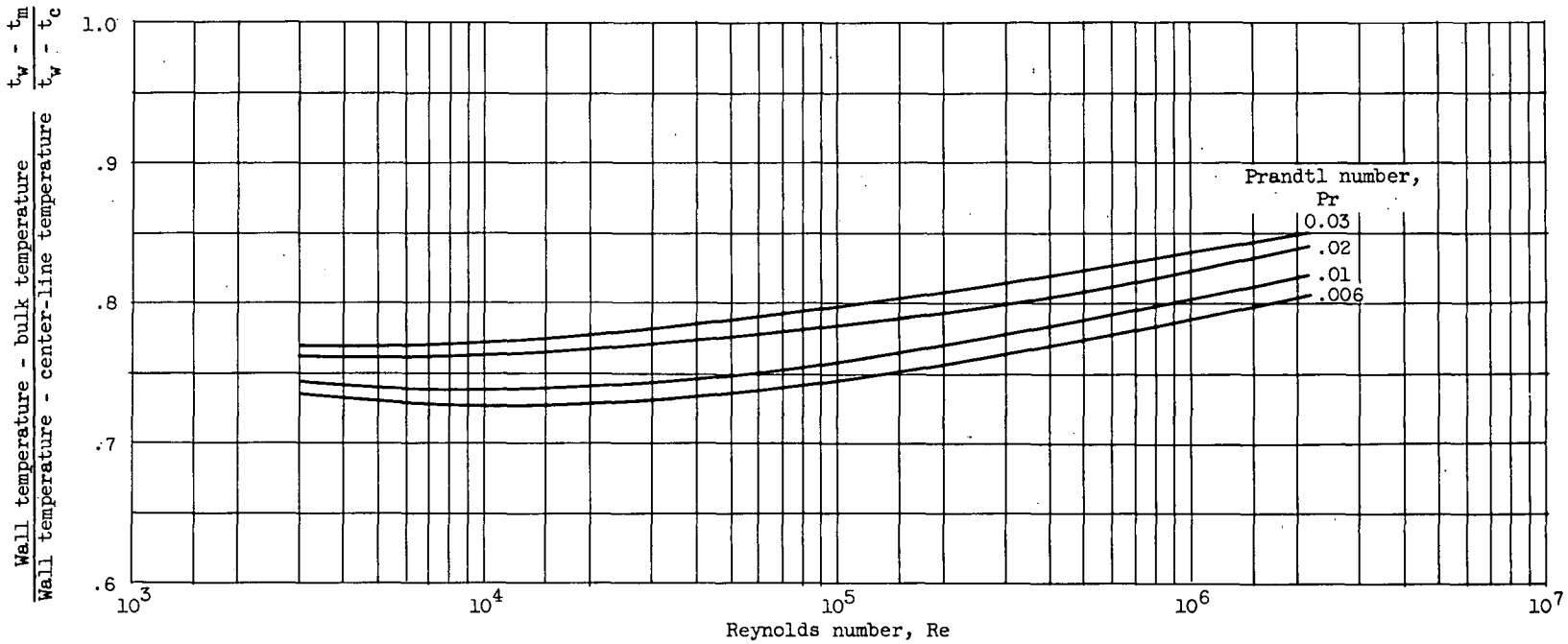

Figure 6. - Theoretical predictions of Martinelli (ref. 27) of ratio $(t_w - t_m)/(t_w - t_c)$ for heat transfer to liquid metals between flat plates.

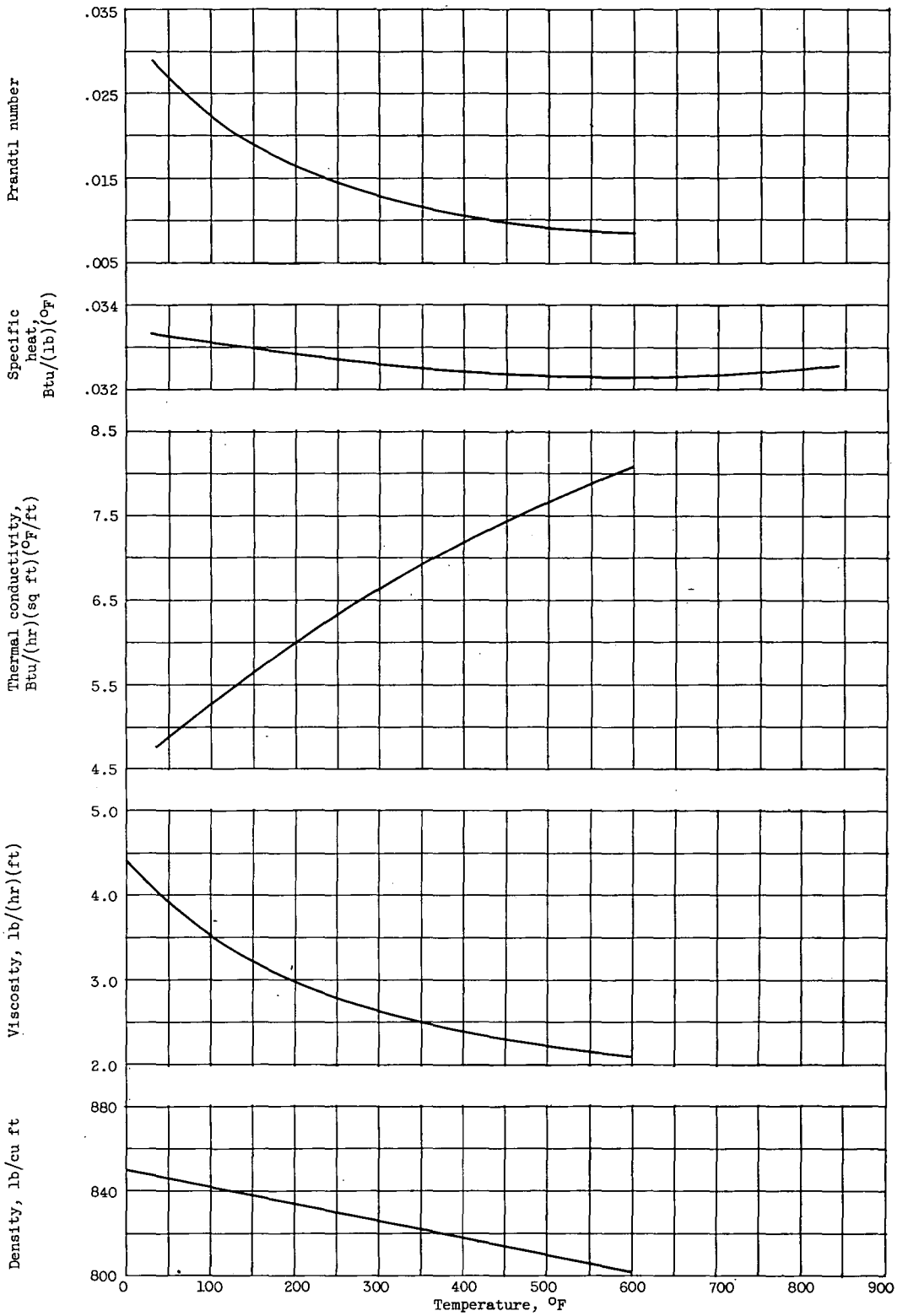

Figure 7. - Physical properties of mercury (ref. 28).

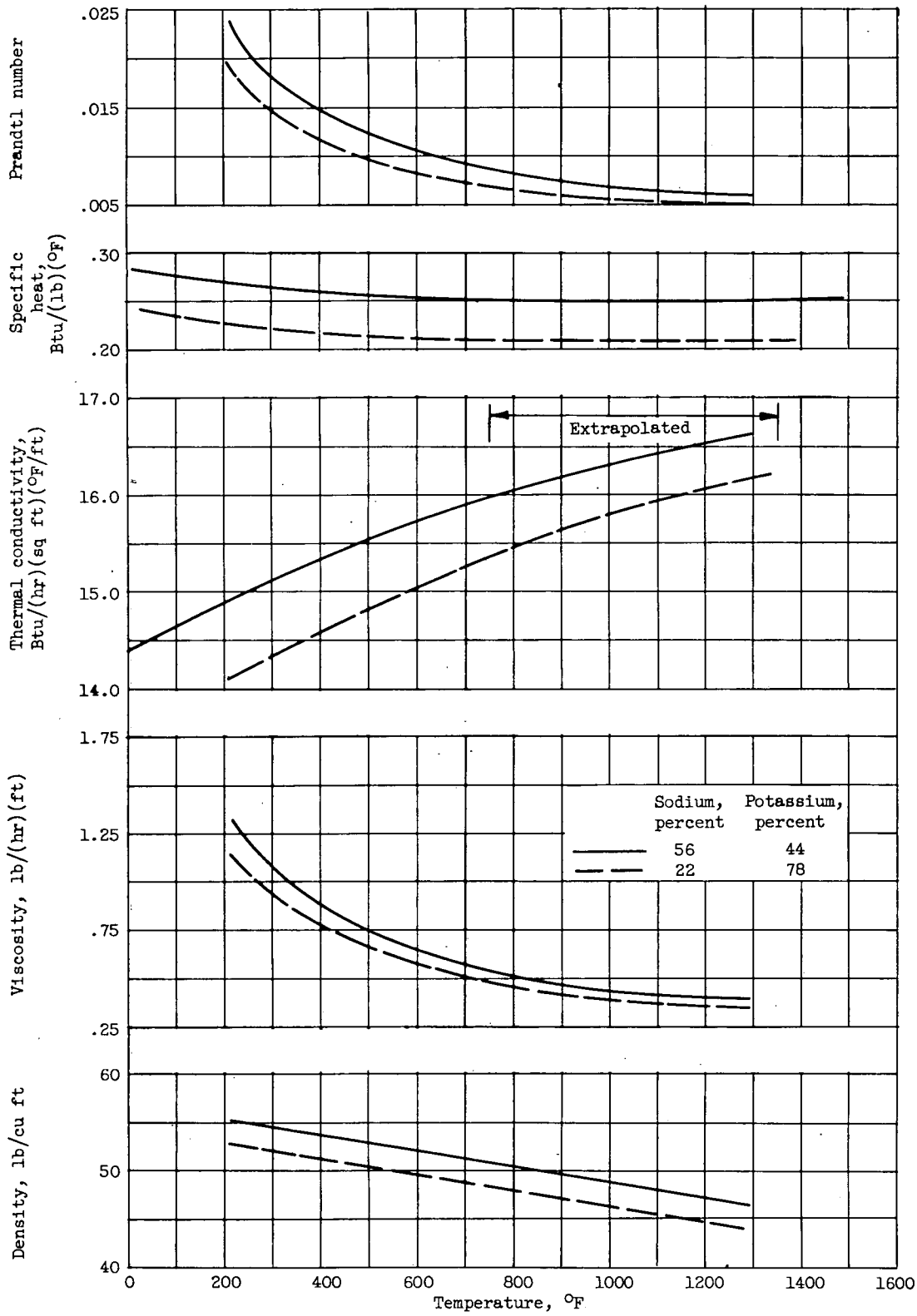

Figure 8. - Physical properties of sodium-potassium alloy (ref. 28).

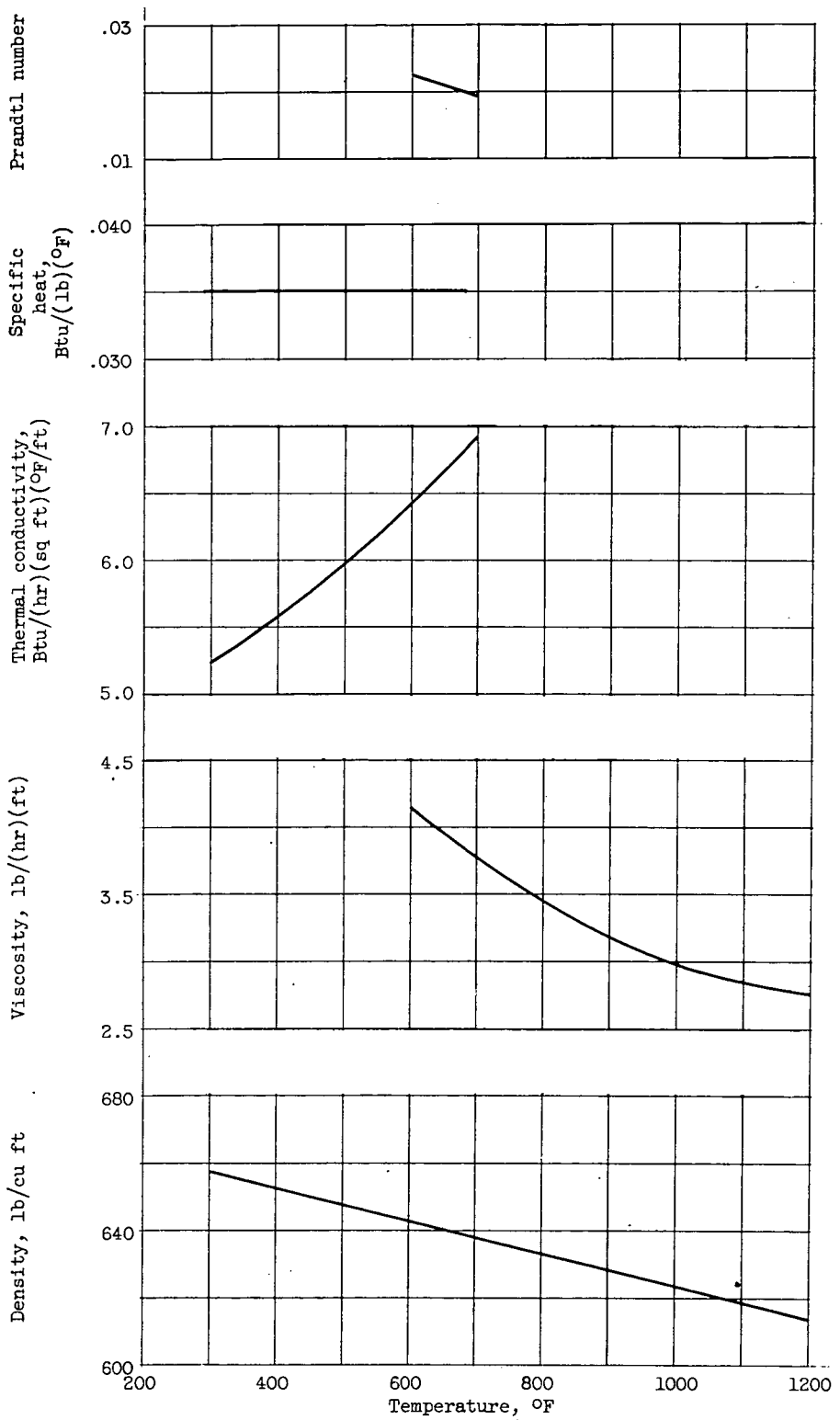

Figure 9. - Physical properties of lead-bismuth eutectic (ref. 28).

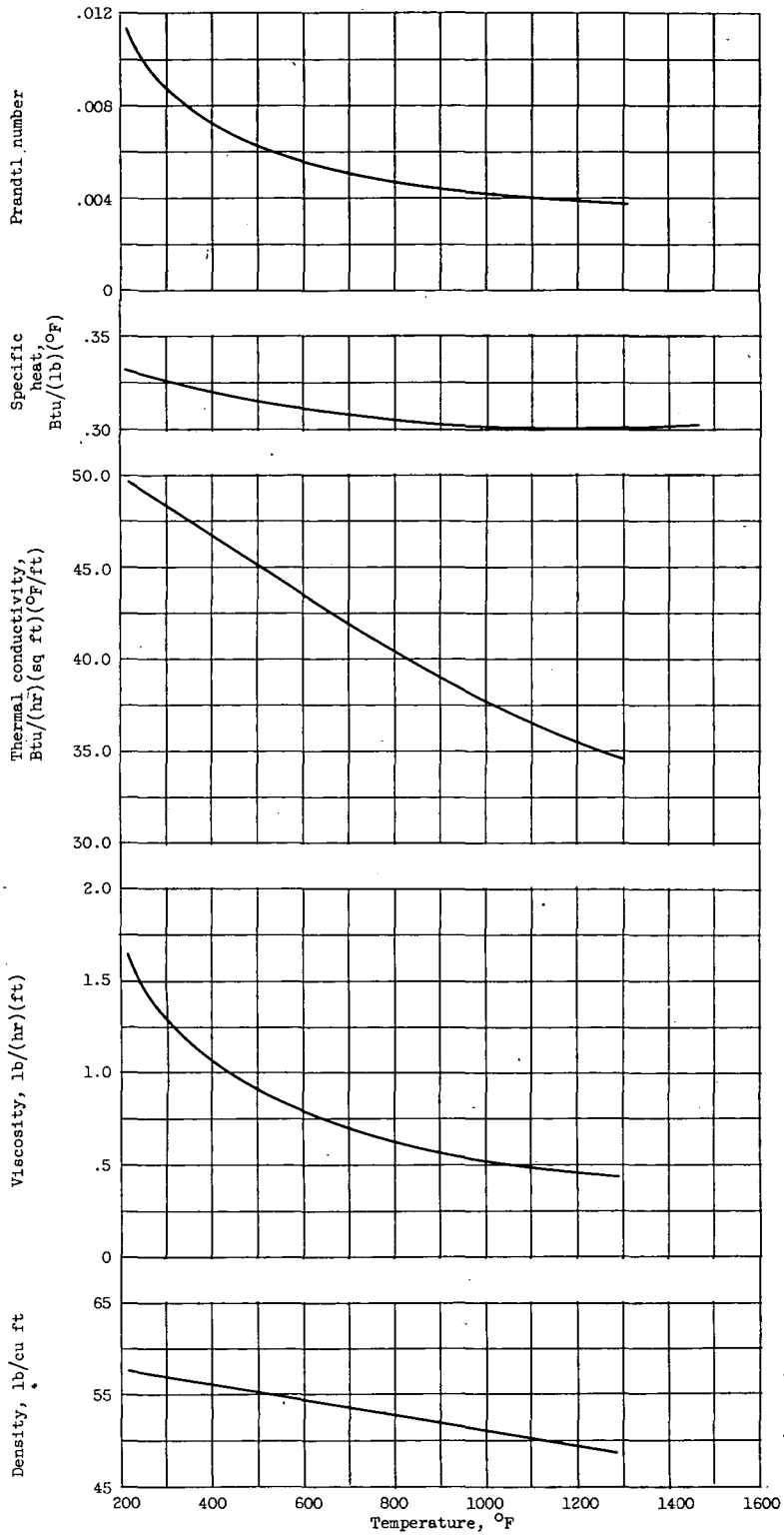

Figure 10. - Physical properties of sodium (ref. 28).

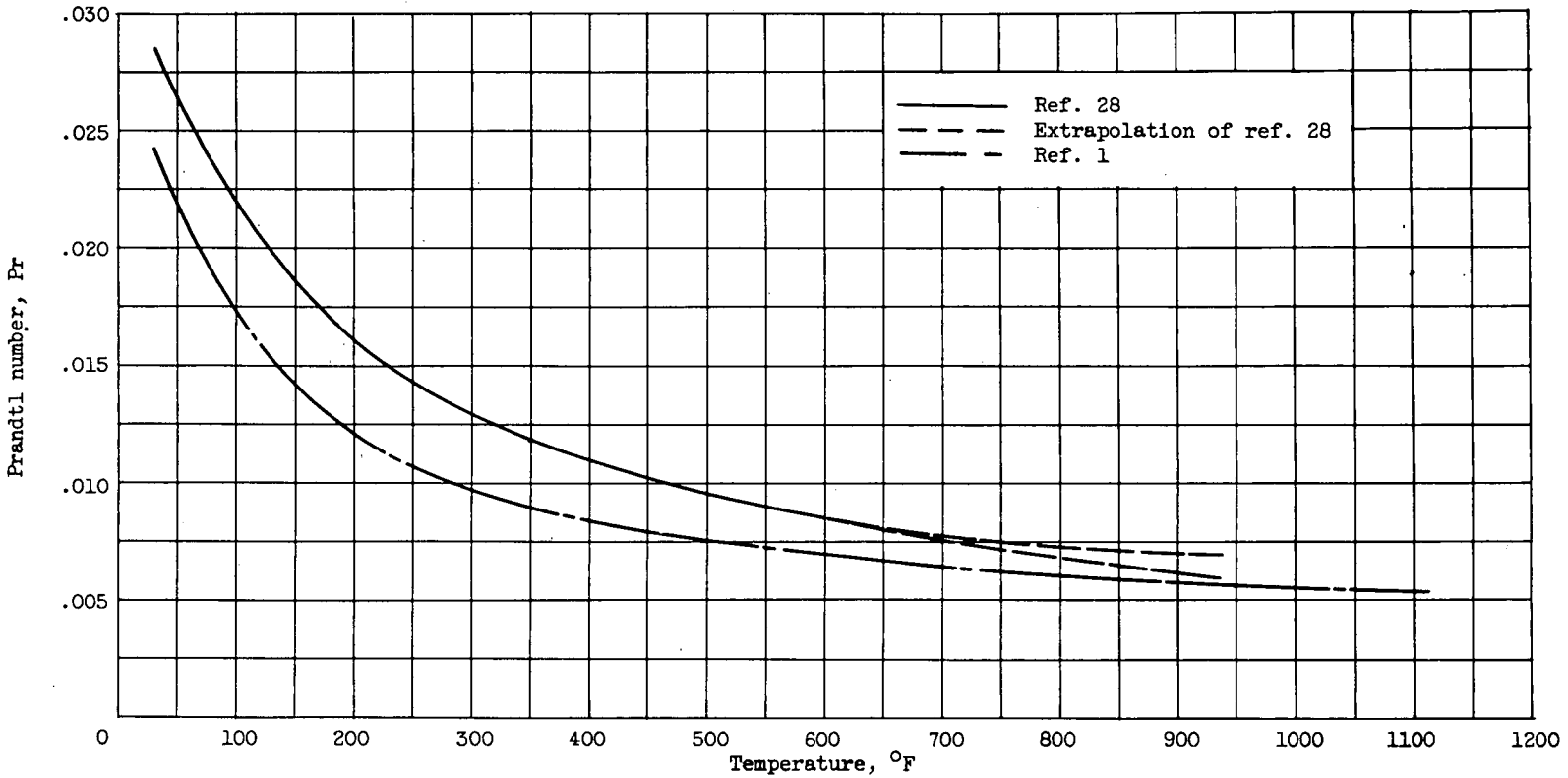

Figure 11. - Comparison of variation of Prandtl number of mercury with temperature of Liquid-Metals Handbook (ref. 28) and of Styrikovich and Semonovker (ref. 1).

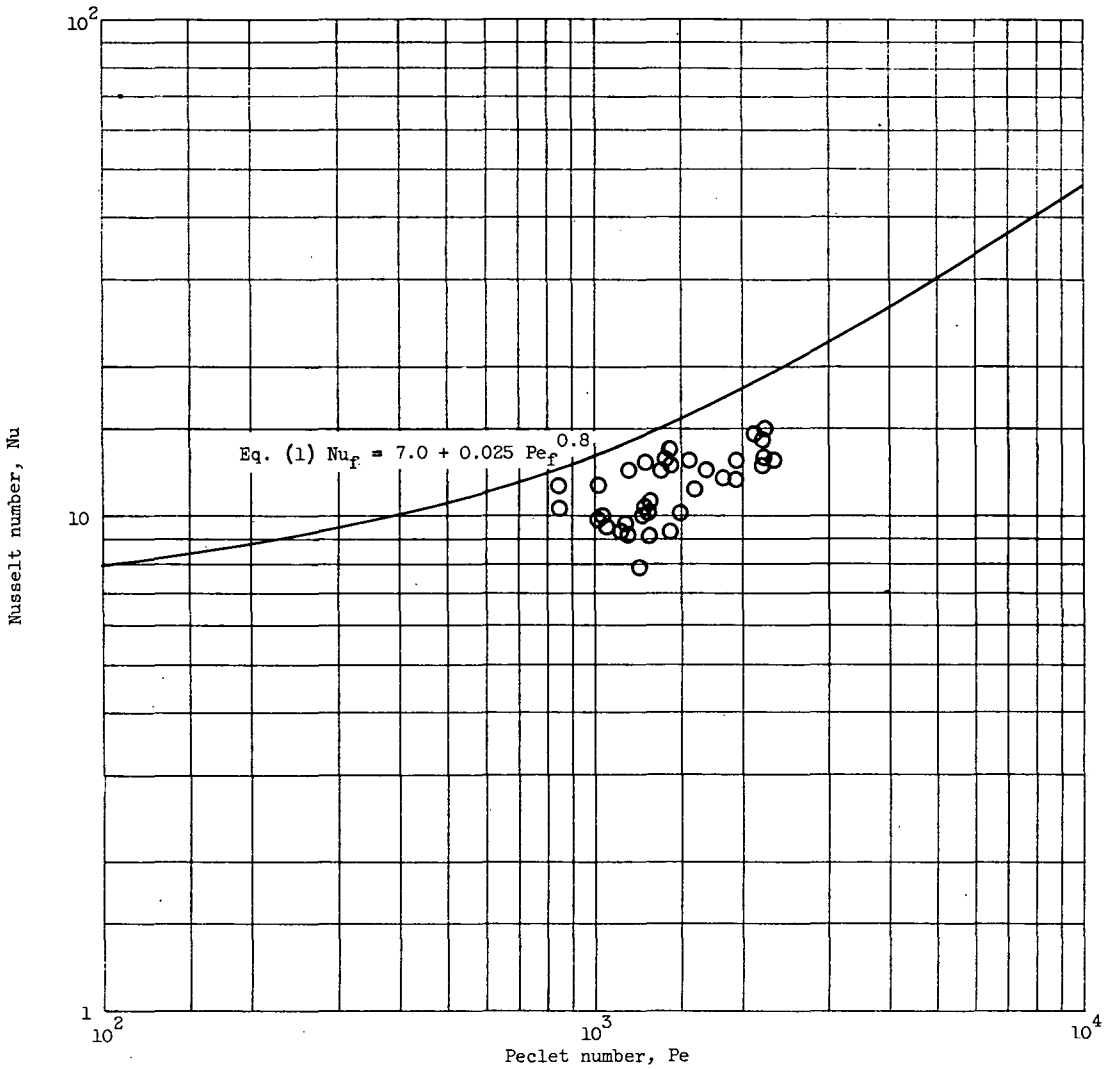

Figure 12. - Re-evaluated data of Styrikovich and Semenovker (ref. 1) for fully developed heat transfer to mercury in round tubes.

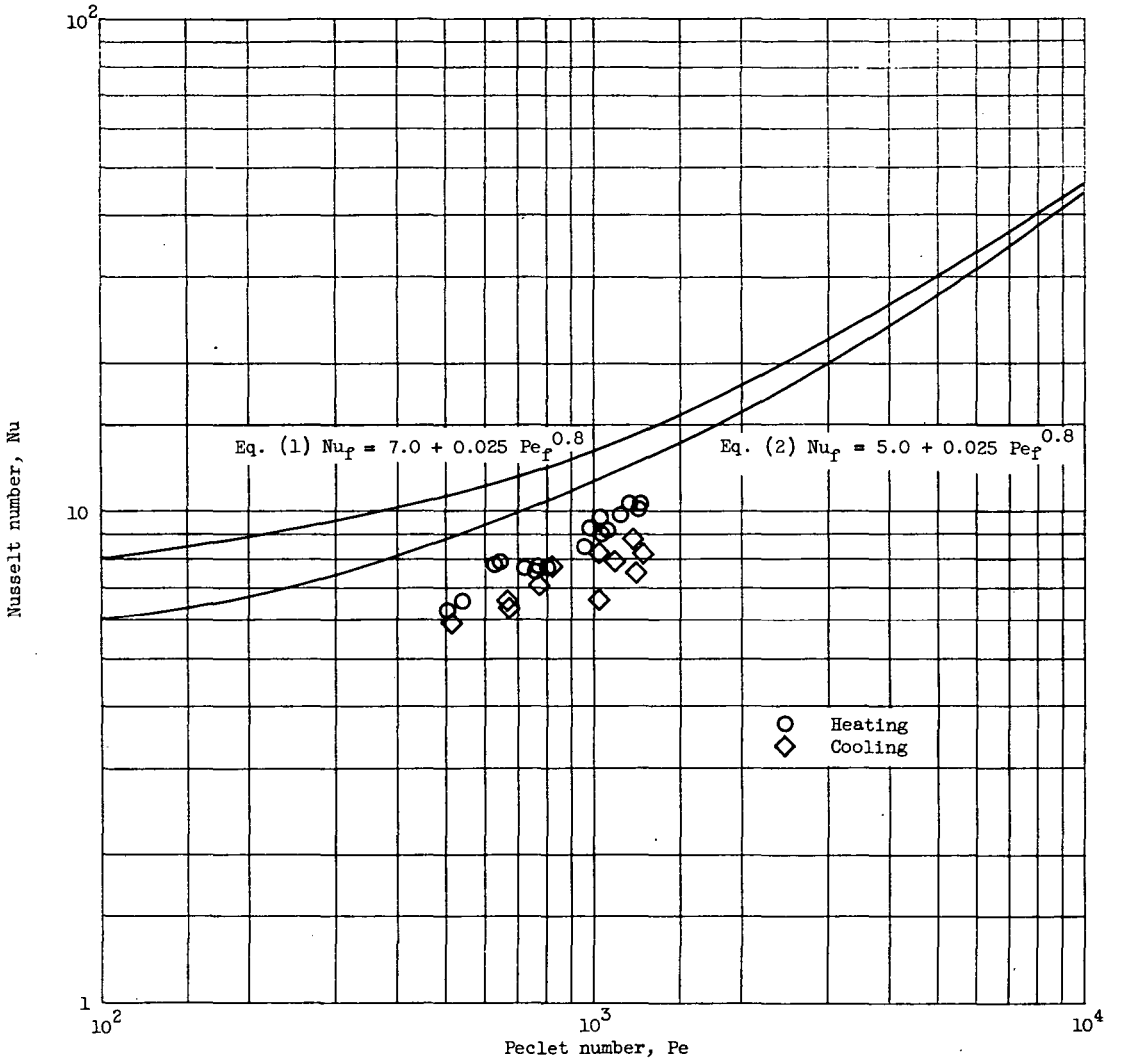

Figure 13. - Data of Gilliland, Musser, and Page (refs. 2 and 3) for average heat transfer to mercury in round tubes. Length-diameter ratio of heating section, 45; of cooling section, 160.

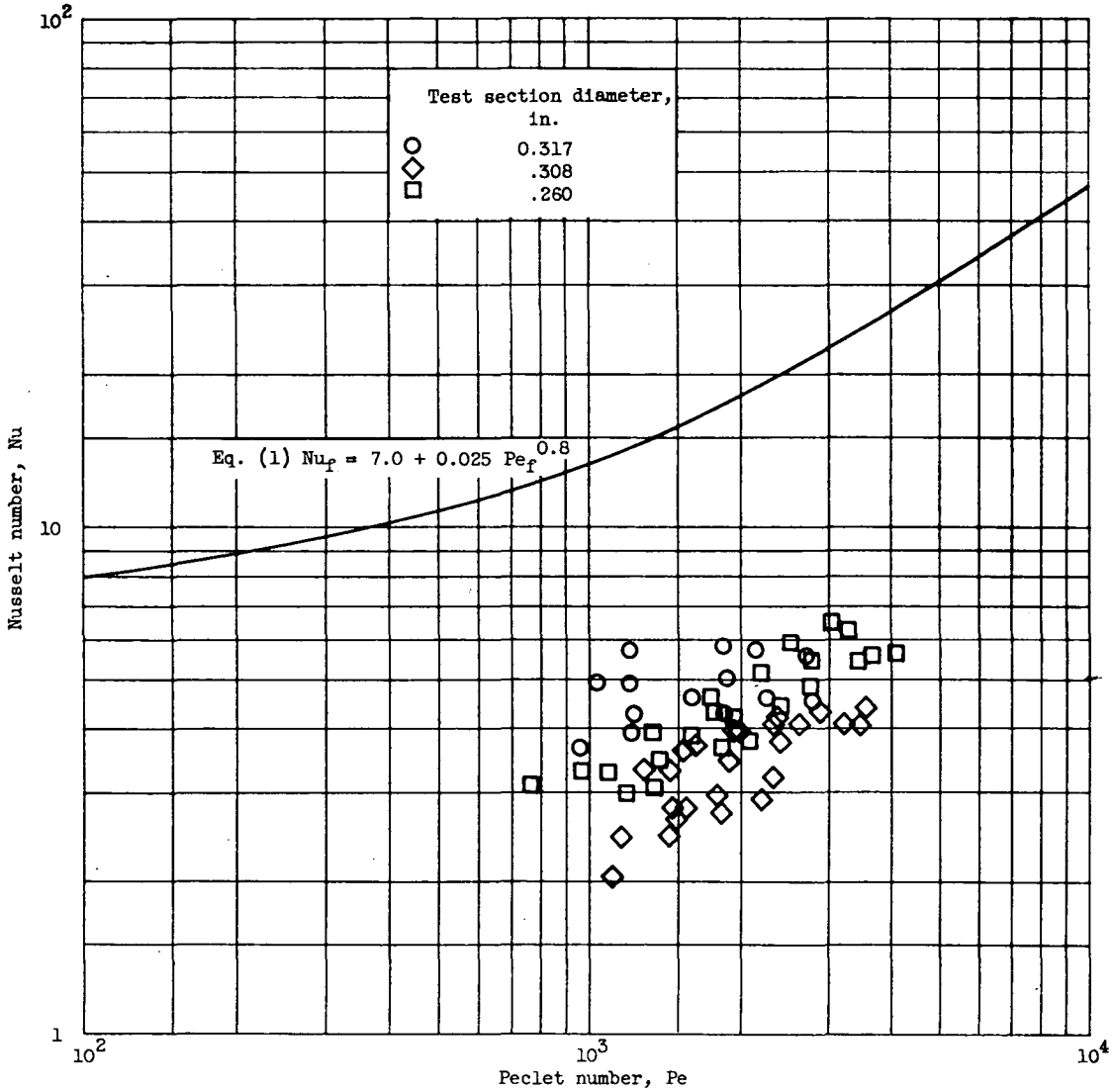

Figure 14. - Re-evaluated data of Elser (ref. 4) for fully developed heat transfer to mercury in round tubes.

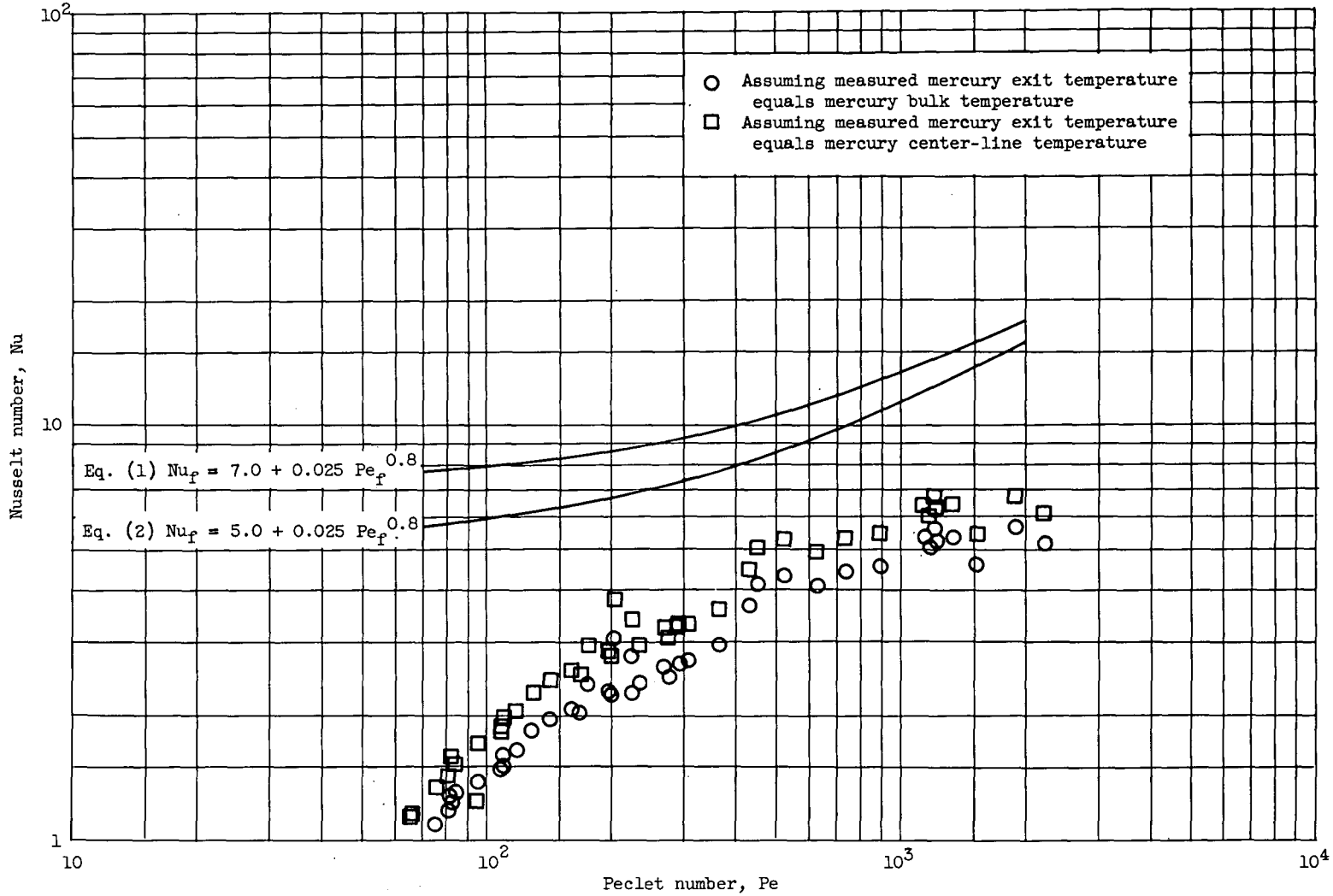

Figure 15. - Re-evaluated data of Bailey, Cope, and Watson (ref. 5) for fully developed heat transfer to mercury in round tubes.

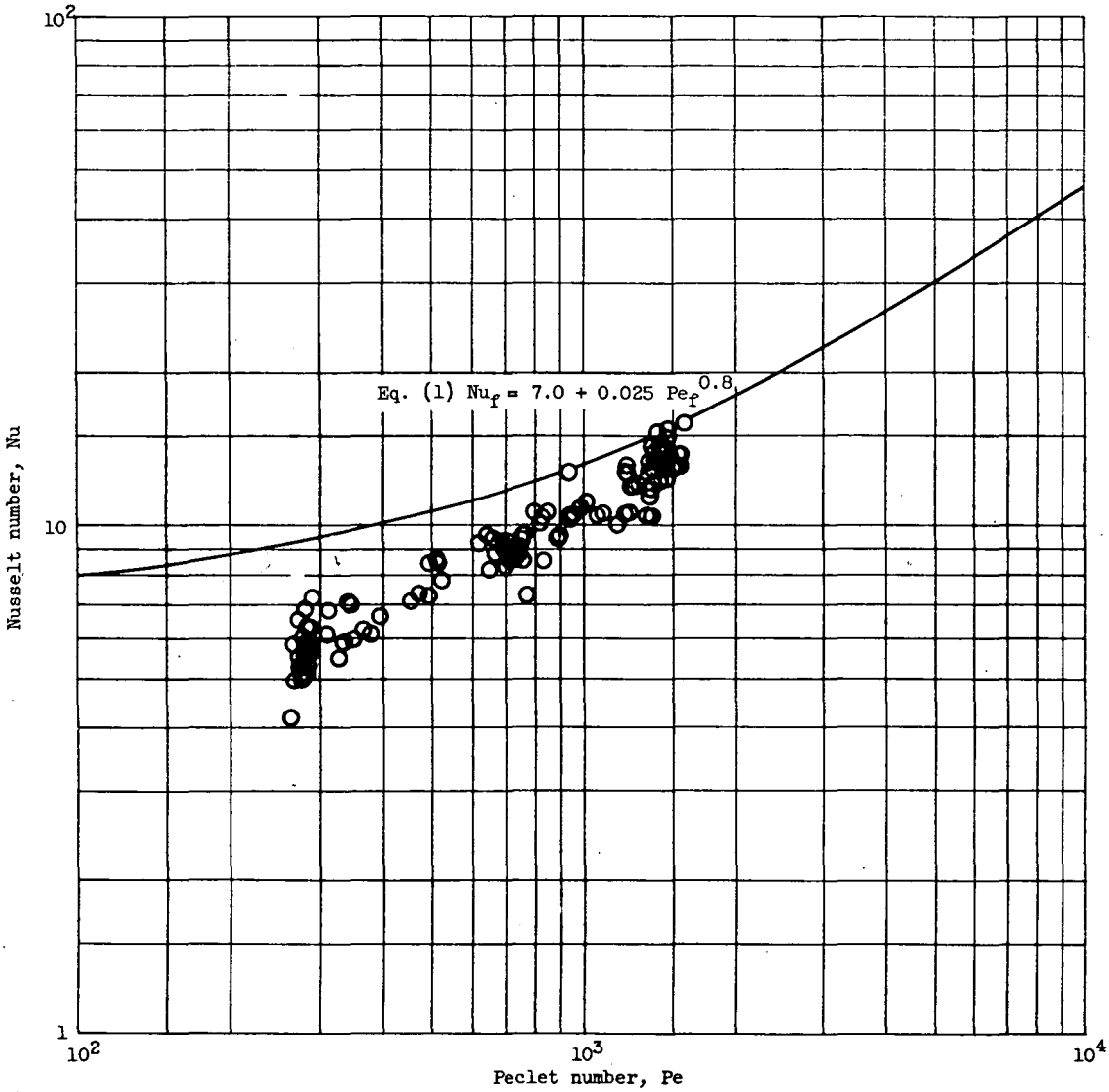

(a) Test section A (length-diameter ratio, 111).

Figure 16. - Re-evaluated data of Lyon (ref. 6) for average heat transfer to a sodium-potassium alloy in round tubes.

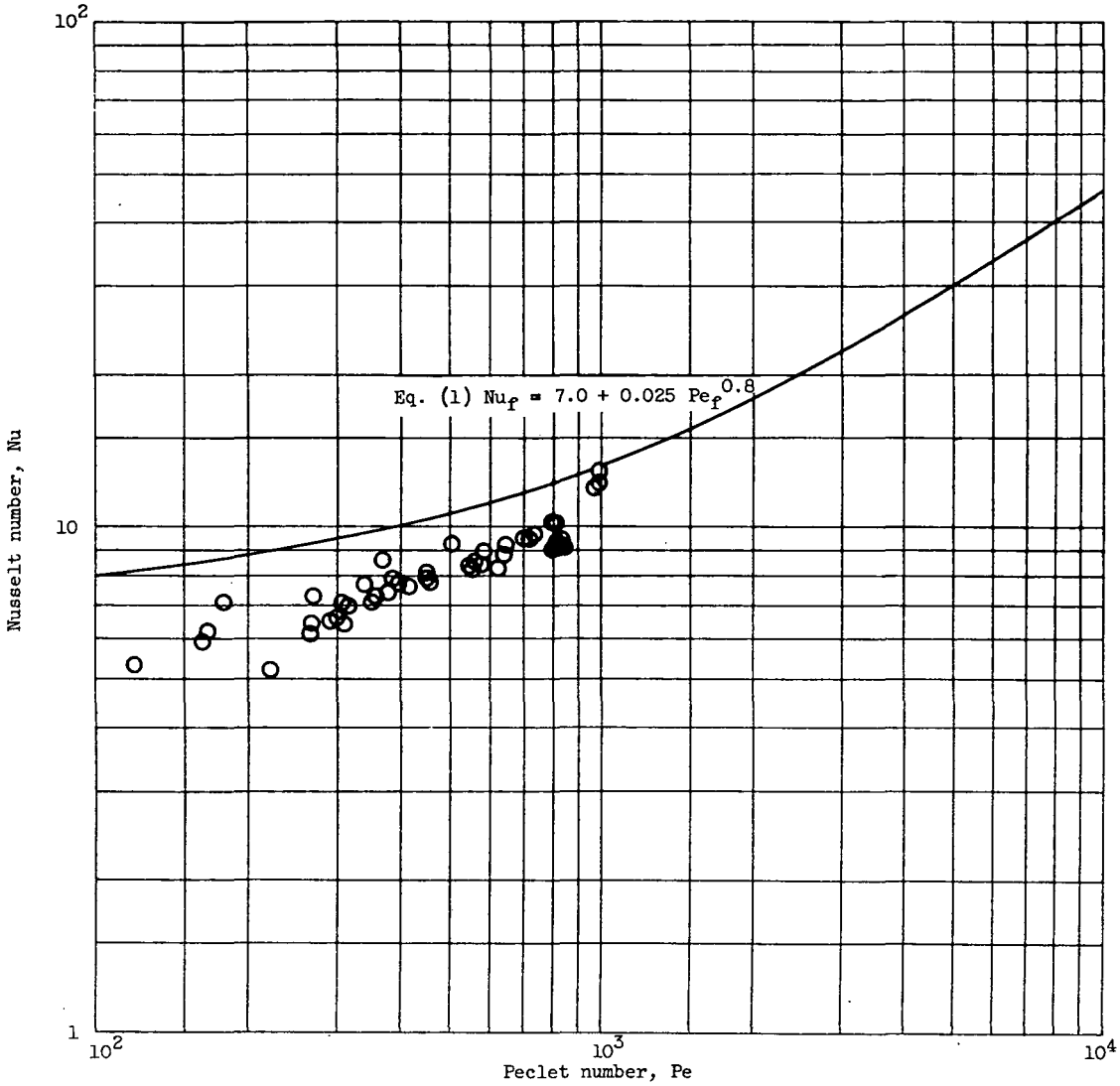

(b) Test section B (length-diameter ratio, 98).

Figure 16. - Continued. Re-evaluated data of Lyon (ref. 6) for average heat transfer to a sodium-potassium alloy in round tubes.

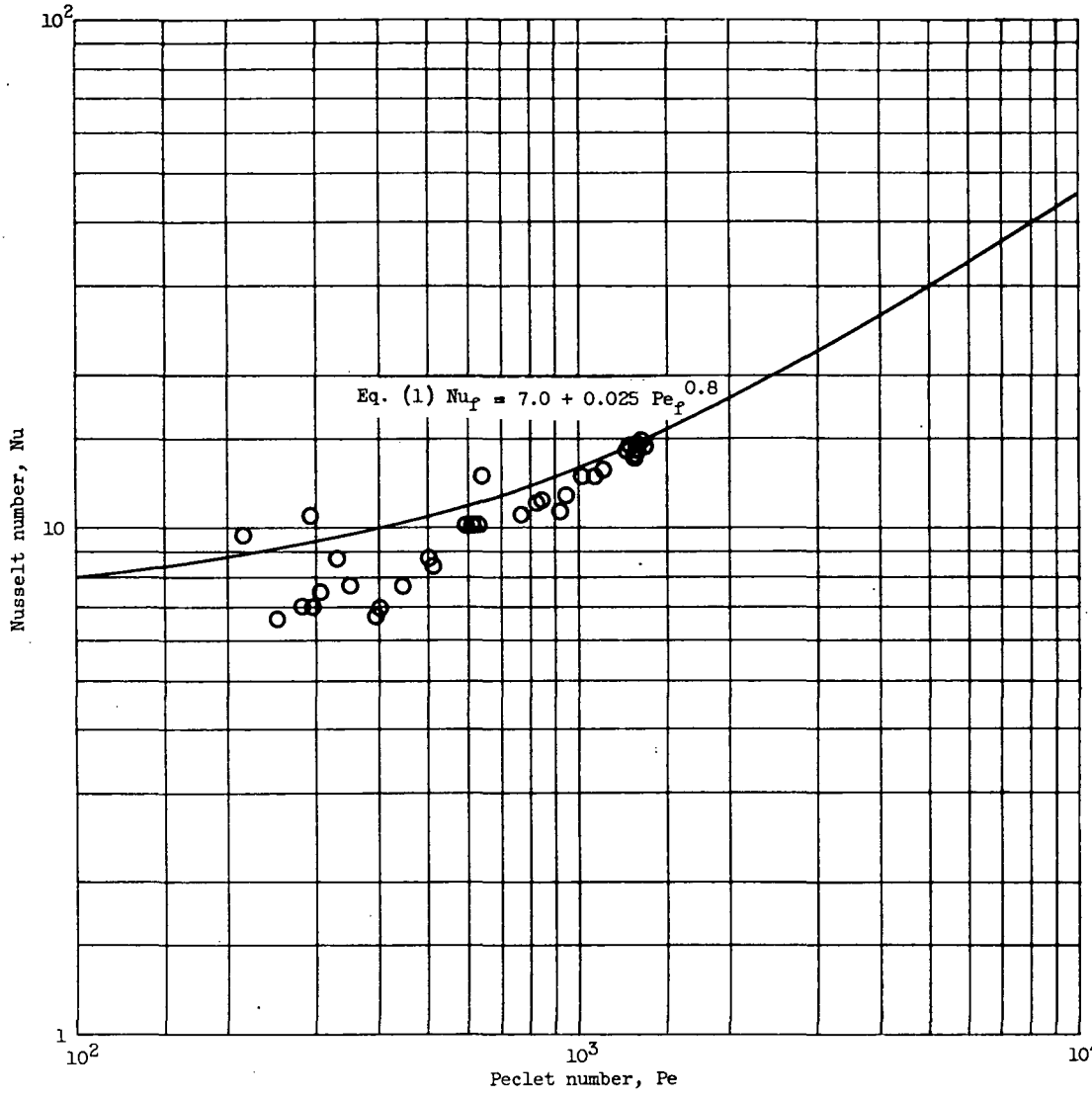

(c) Test section C (length-diameter ratio, 76).

Figure 16. - Continued. Re-evaluated data of Lyon (ref. 6) for average heat transfer to a sodium-potassium alloy in round tubes.

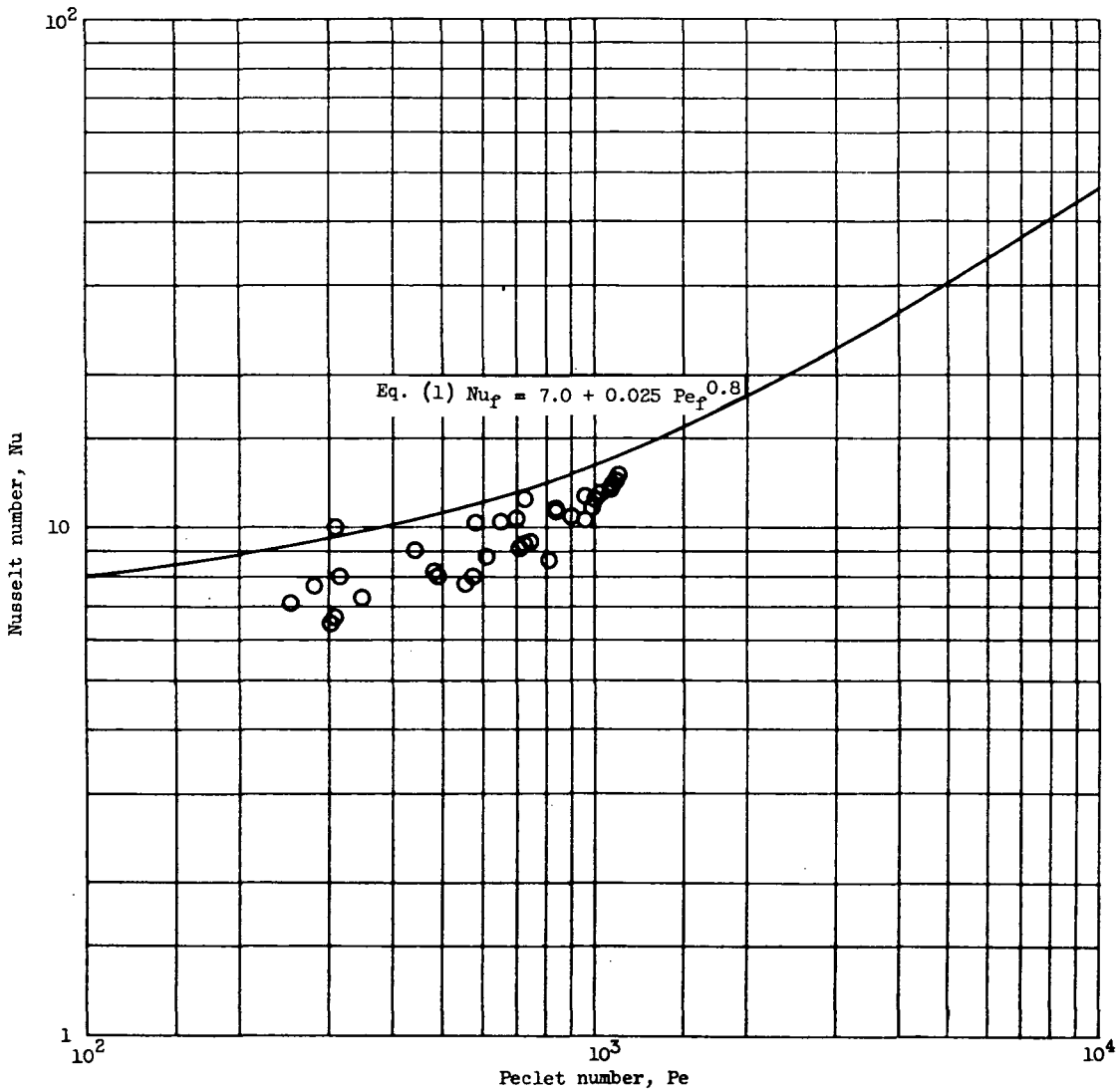

(d) Test section D (length-diameter ratio, 159).

Figure 16. - Concluded. Re-evaluated data of Lyon (ref. 6) for average heat transfer to a sodium-potassium alloy in round tubes.

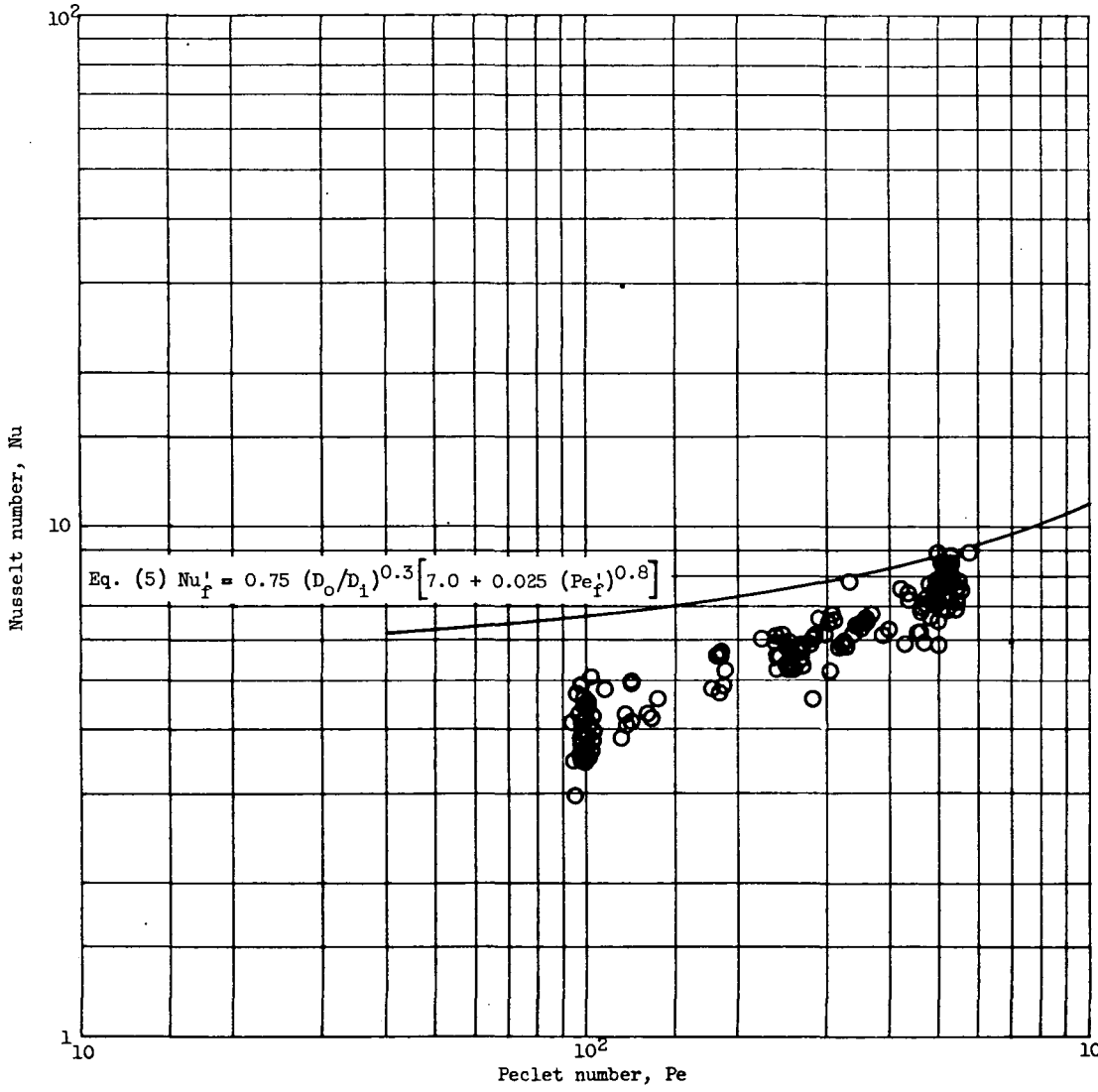

(a) Test section A (D_o/D_i, 1.43; length-diameter ratio, 223).

Figure 17. - Re-evaluated data of Lyon (ref. 6) for average heat transfer to a sodium-potassium alloy in annuli.

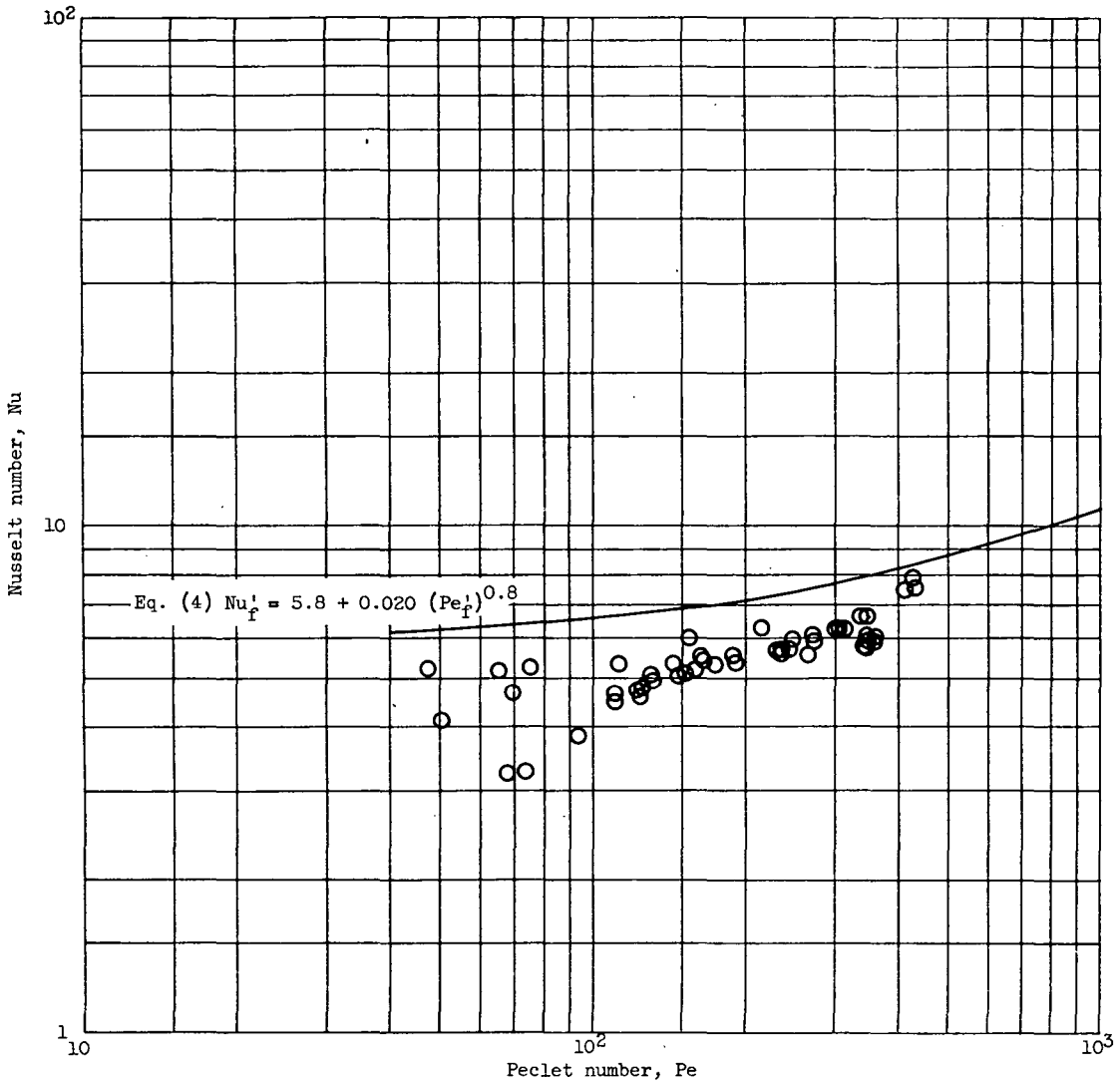

(b) Test section B (D_o/D_i, 1.23; length-diameter ratio, 397).

Figure 17. - Continued. Re-evaluated data of Lyon (ref. 6) for average heat transfer to a sodium-potassium alloy in annuli.

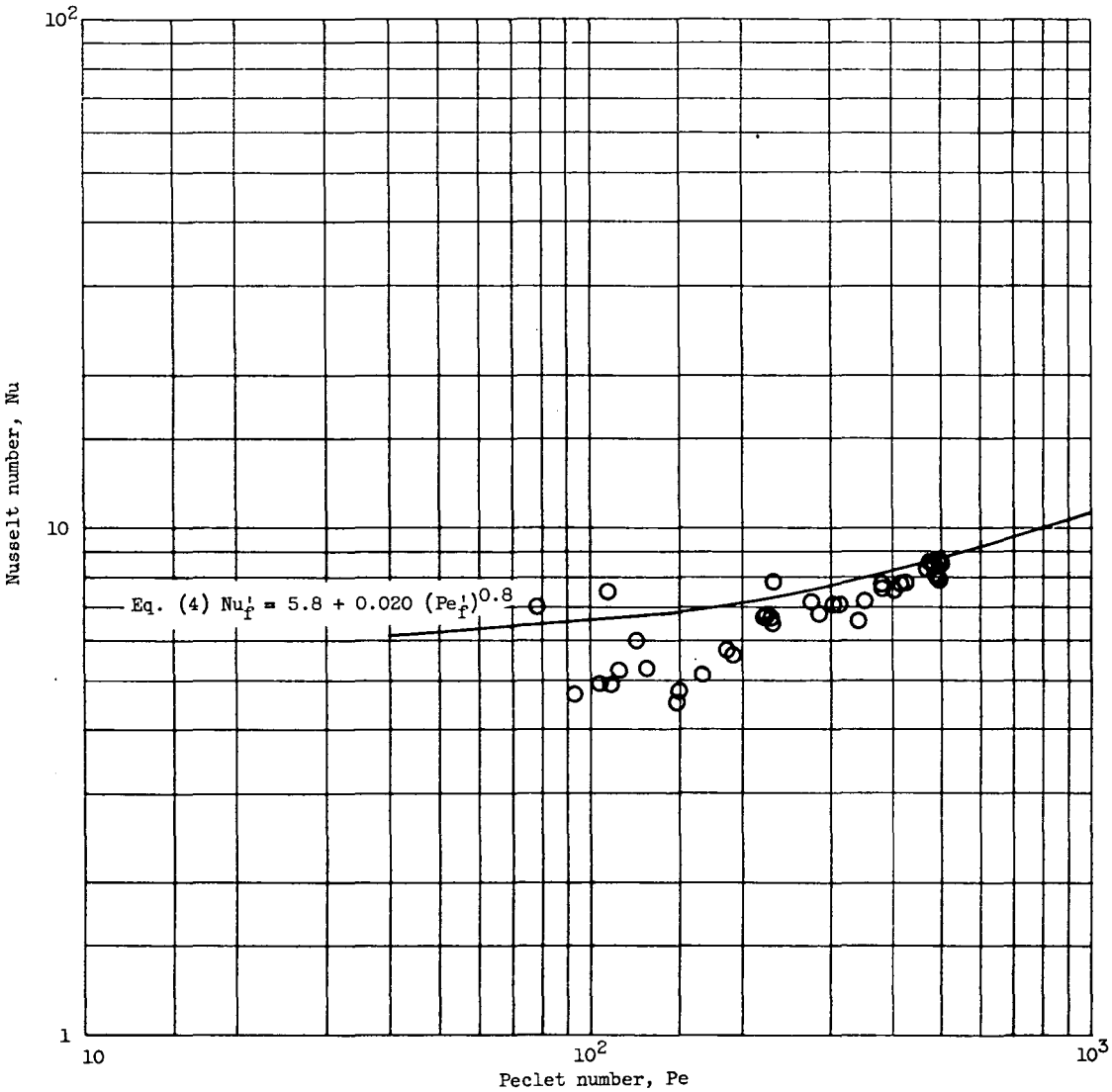

(c) Test section C (D_o/D_i, 1.37; length-diameter ratio, 179).

Figure 17. - Continued. Re-evaluated data of Lyon (ref. 6) for average heat transfer to a sodium-potassium alloy in annuli.

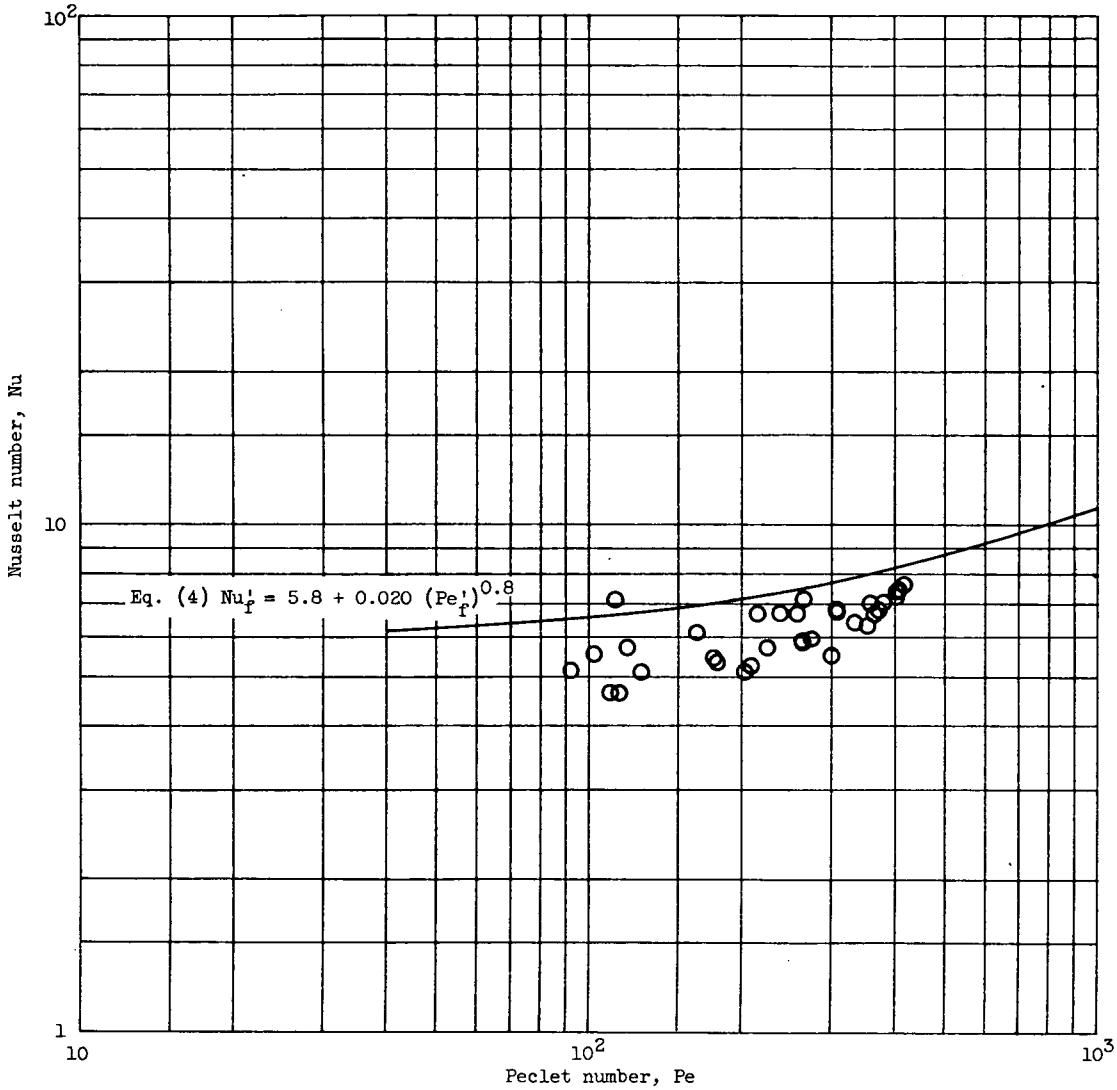

(d) Test section D (D_o/D_i, 1.37; length-diameter ratio, 375).

Figure 17. - Concluded. Re-evaluated data of Lyon (ref. 6) for average heat transfer to a sodium-potassium alloy in annuli.

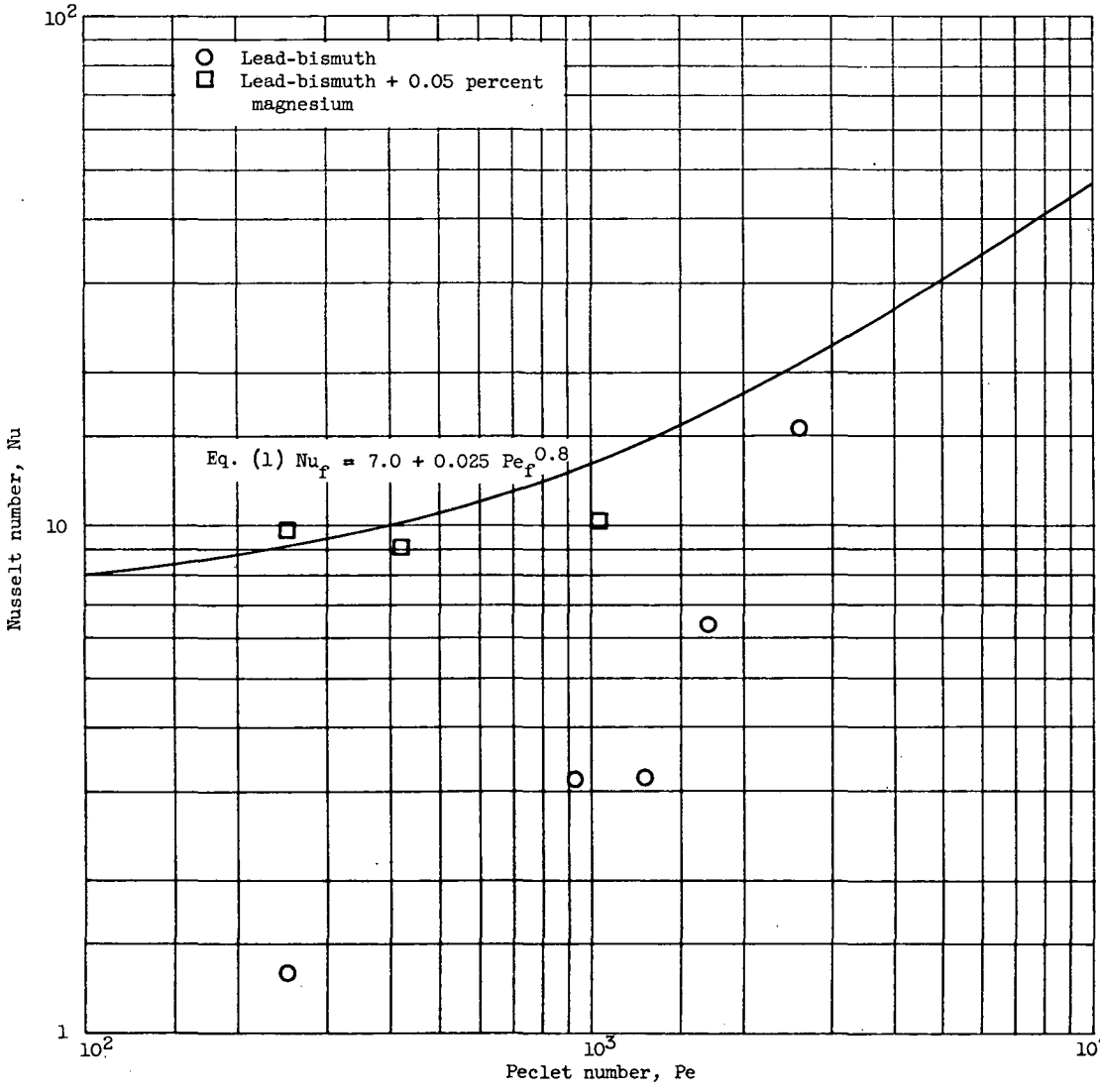

Figure 18. - Re-evaluated data of Untermeyer for fully developed heat transfer to lead-bismuth, with and without magnesium addition, in round tubes.

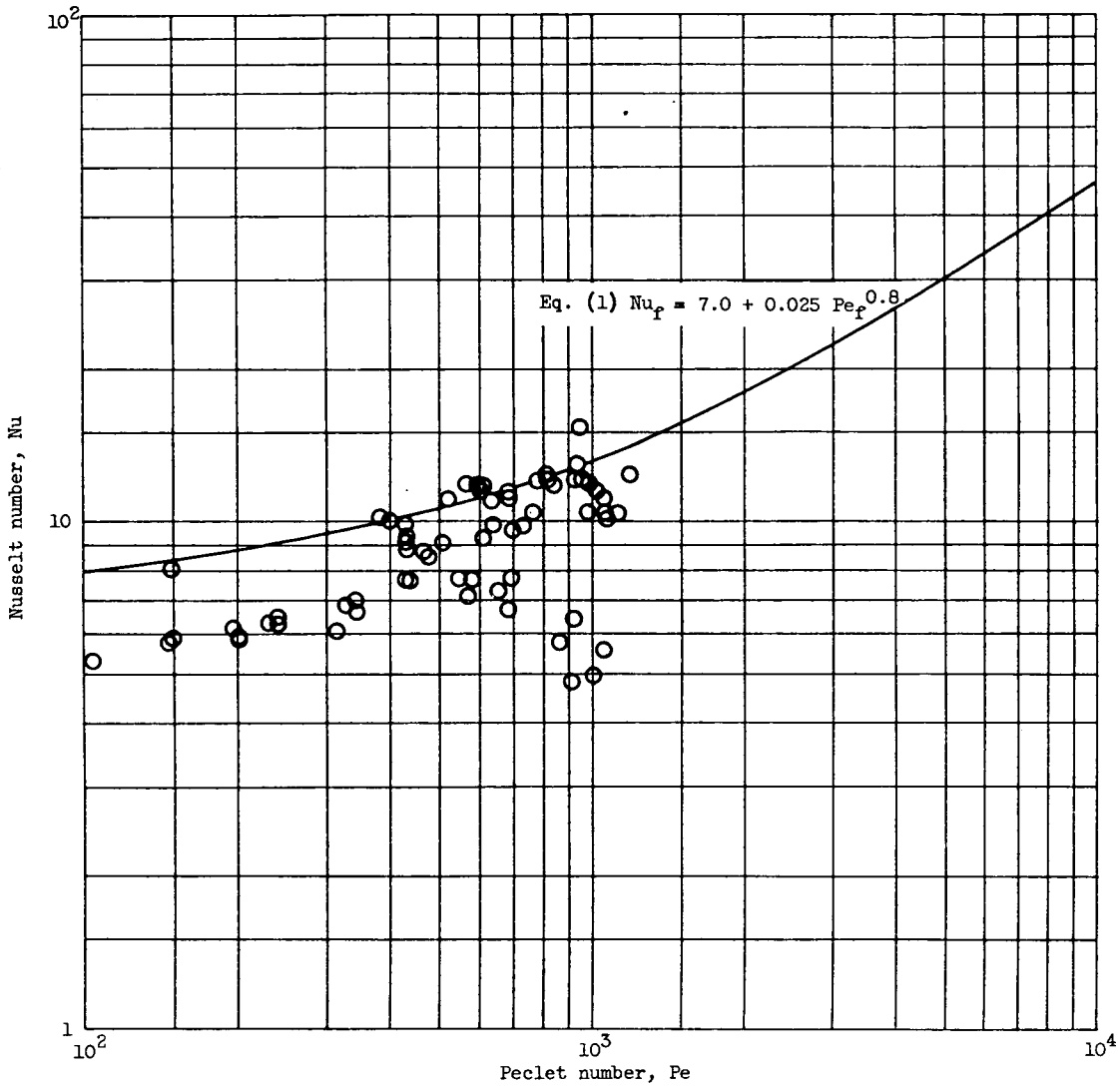

Figure 19. - Re-evaluated data of Werner, King, and Tidball for average heat transfer to sodium-potassium in round tubes. Test section A; length-diameter ratio, 50.

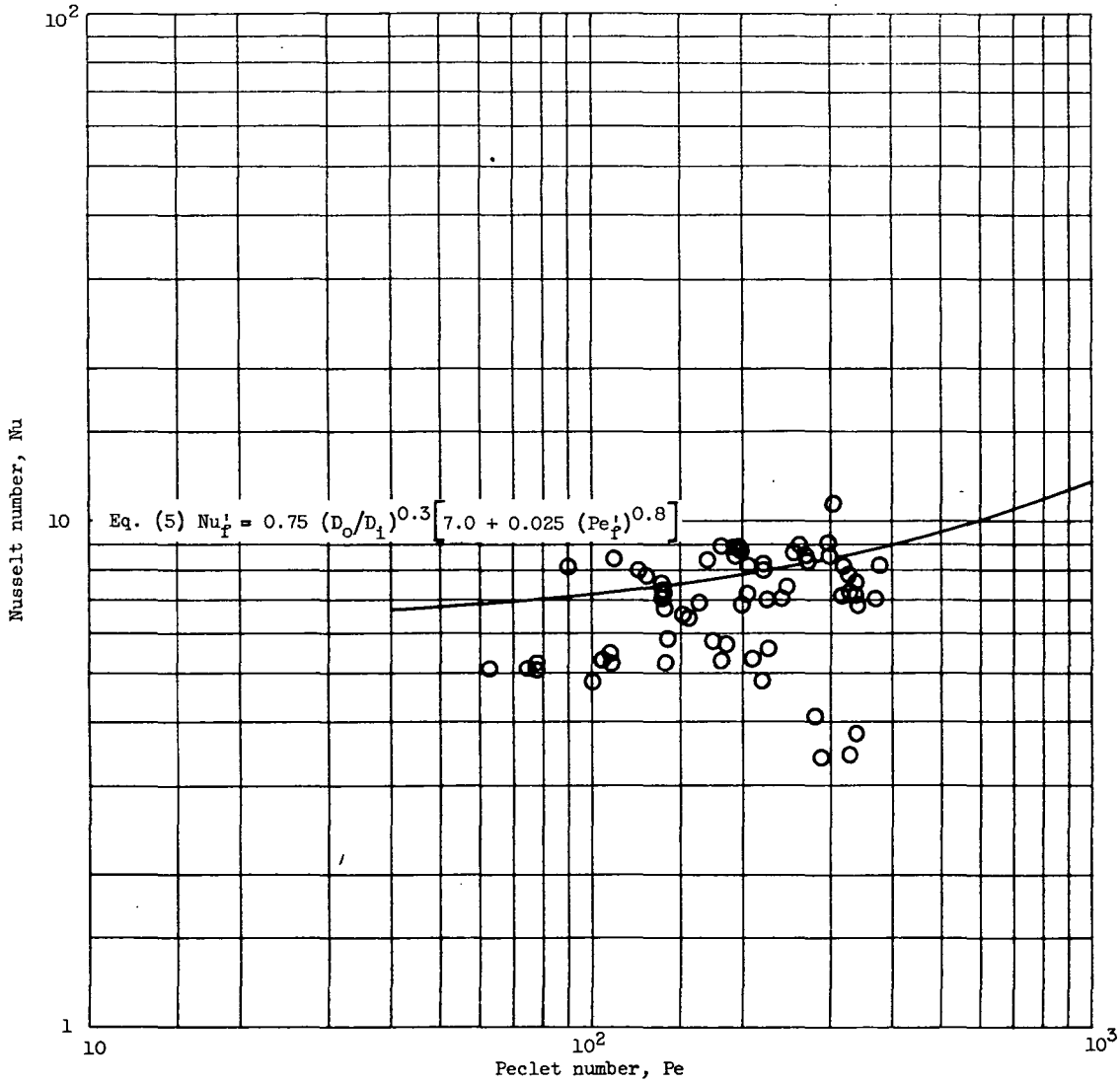

Figure 20. - Re-evaluated data of Werner, King, and Tidball for average heat transfer to sodium-potassium in annuli. Test section A; length-diameter ratio, 54; ratio of outer to inner diameter, 1.83.

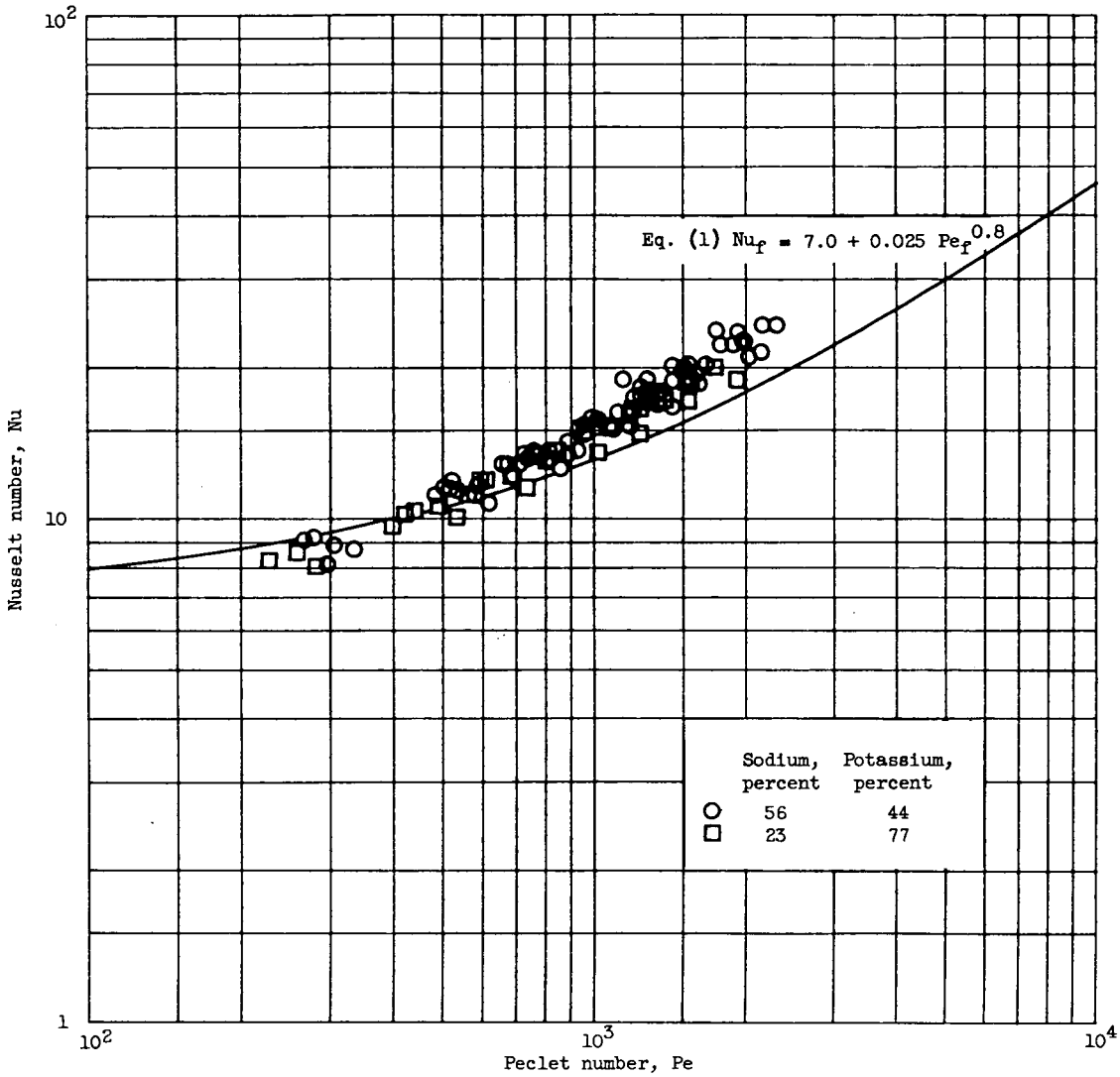

Figure 21. - Re-evaluated data of Werner, King, and Tidball (ref. 7) for average heat transfer to sodium-potassium in round tubes. Test section B; length-diameter ratio, 48.

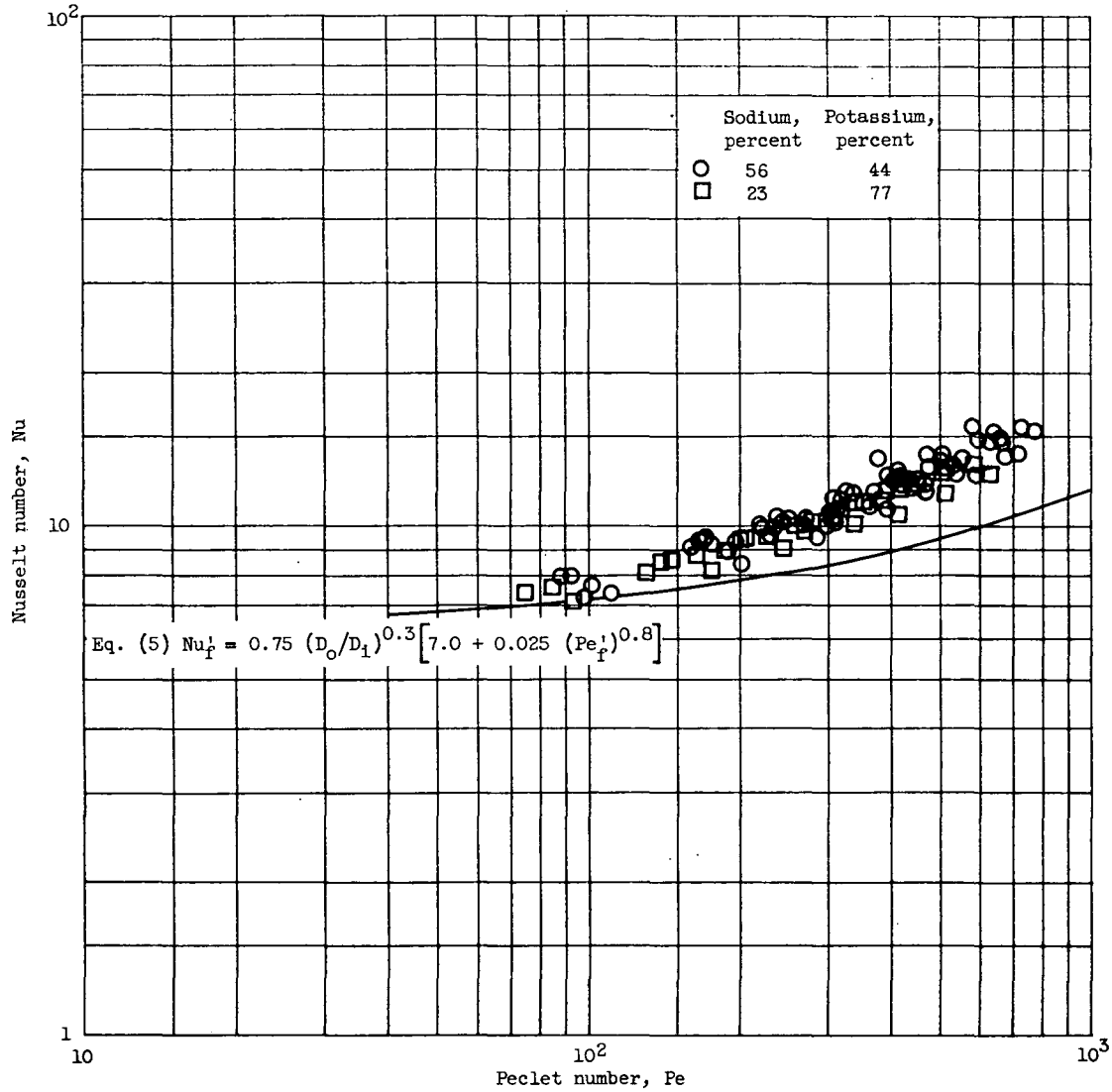

Figure 22. - Re-evaluated data of Werner, King, and Tidball (ref. 7) for average heat transfer to sodium-potassium in annuli. Test section B; length-diameter ratio, 54; ratio of outer to inner diameter, 1.83.

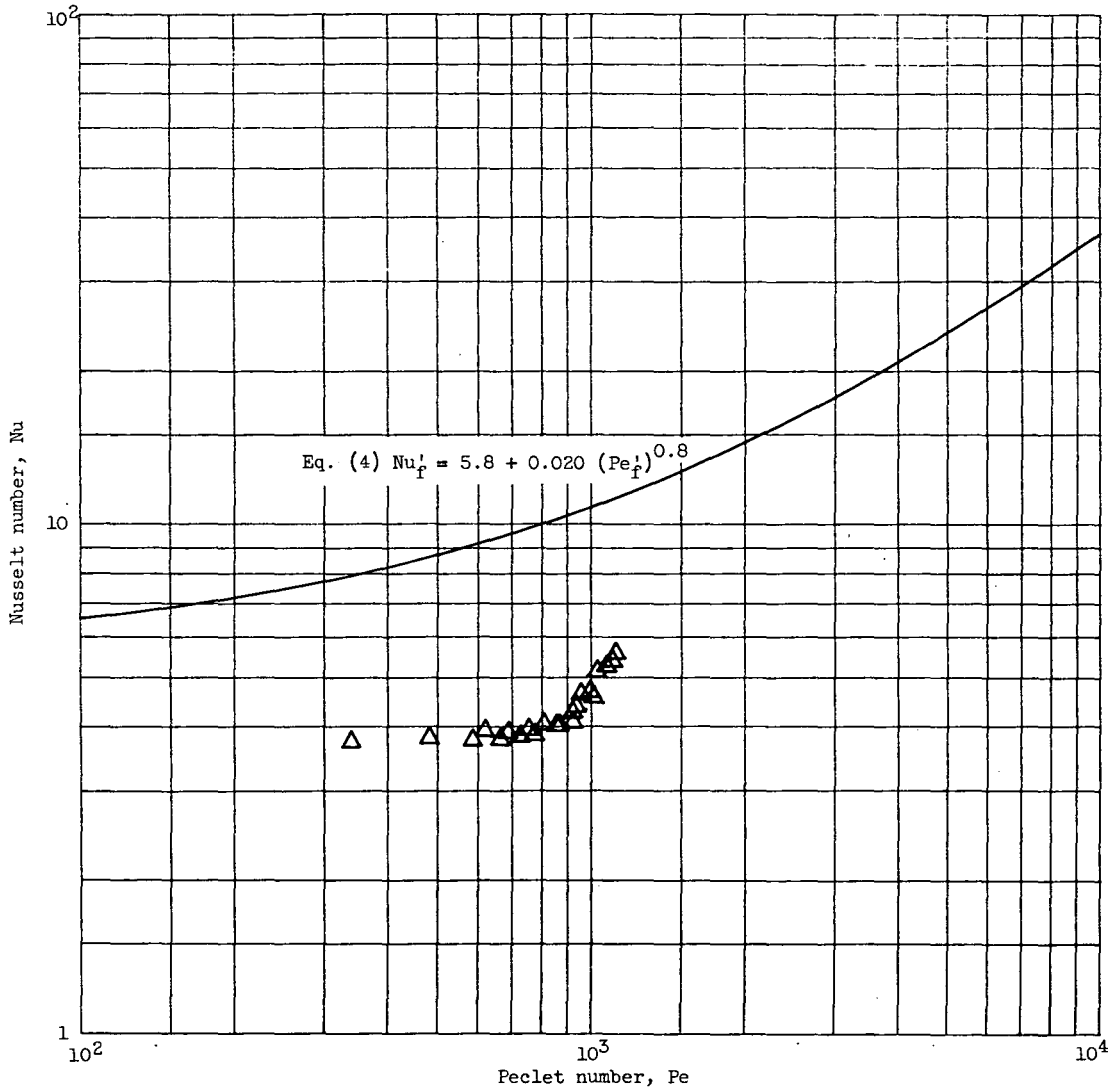

Figure 23. - Data of Sineath (ref. 8) for average heat transfer to mercury in rectangular ducts. Length-diameter ratio, 50.

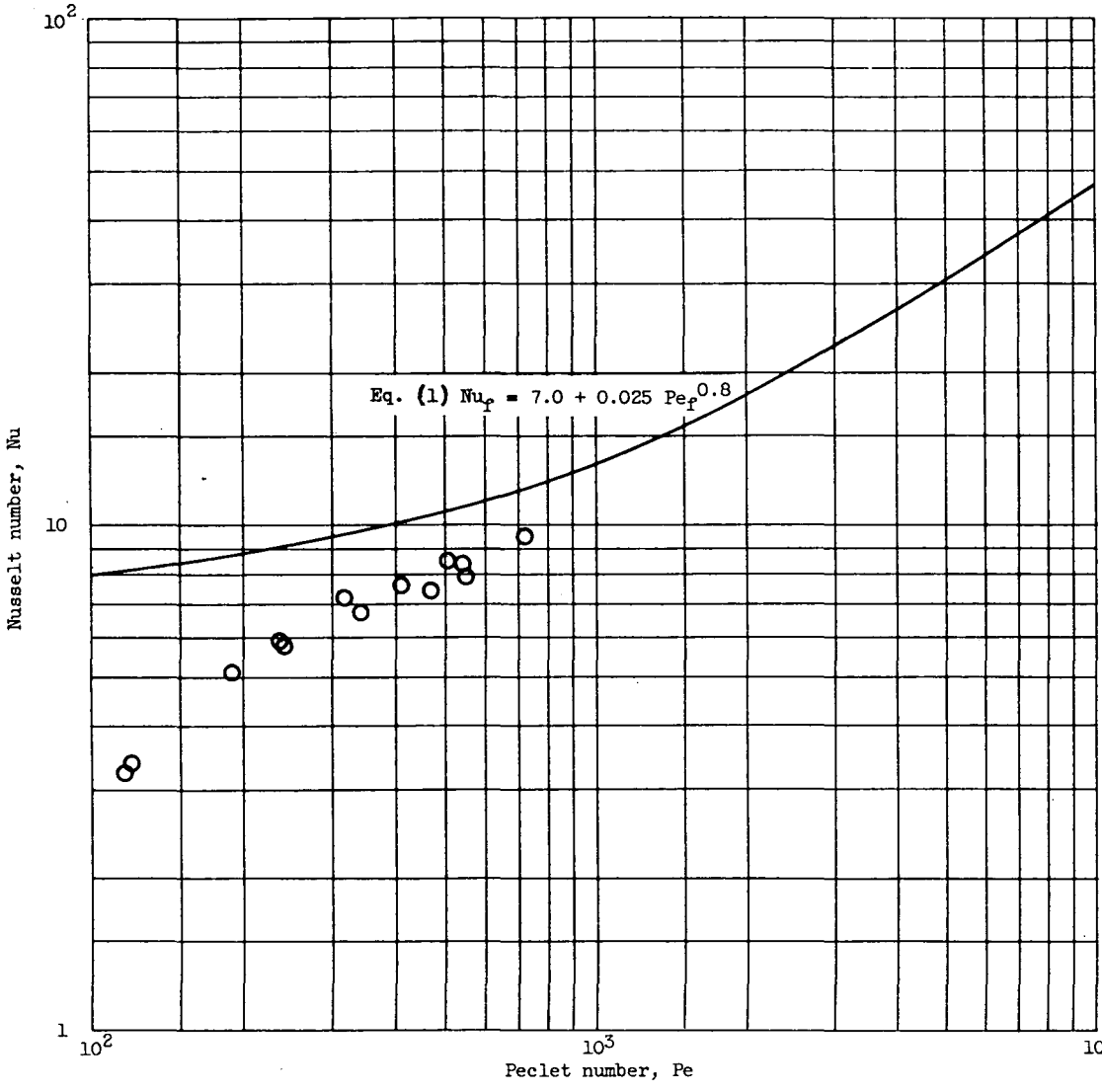

Figure 24. - Data of English and Barrett (refs. 9 and 10) for fully developed heat transfer to mercury in round tubes.

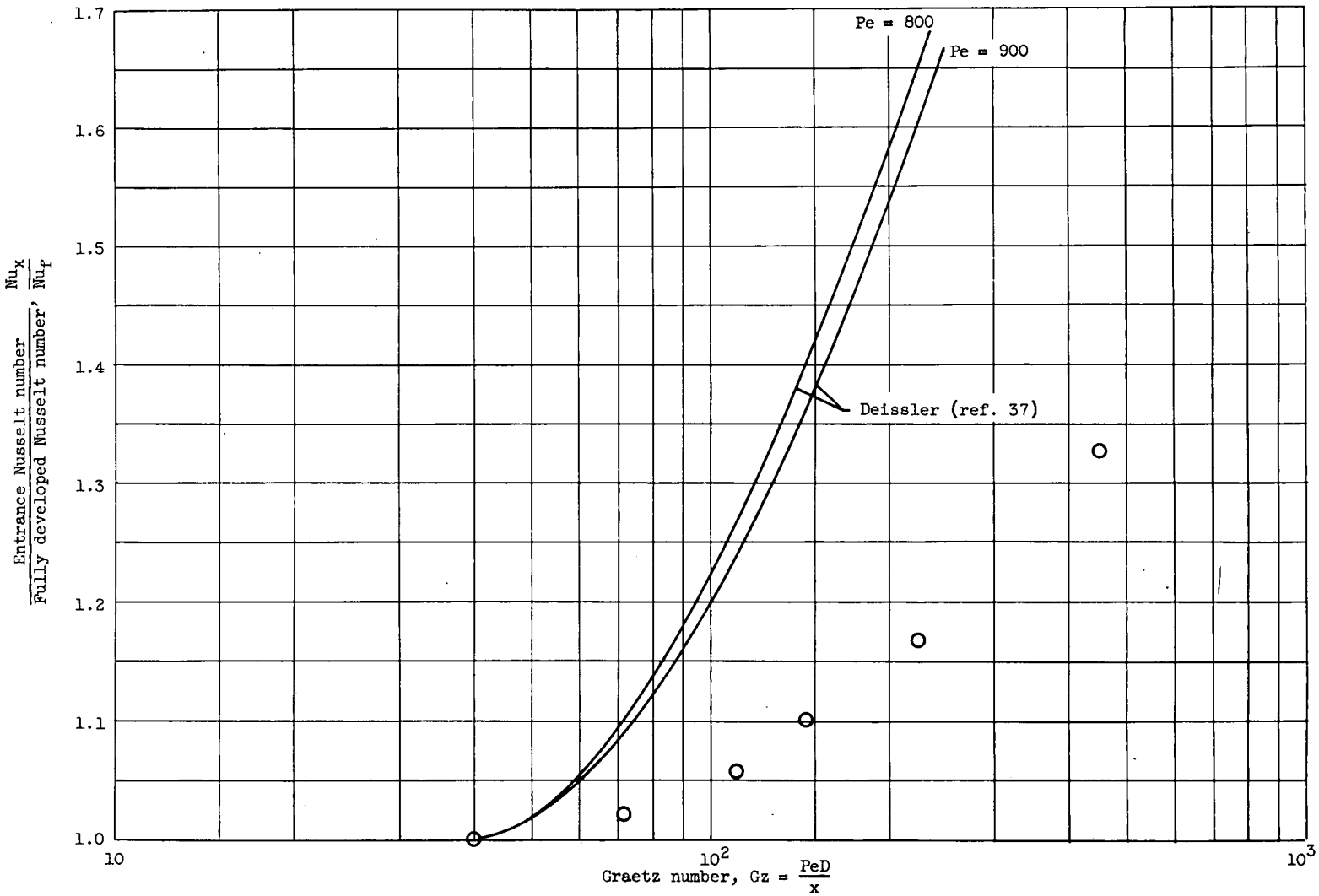

Figure 25. - Data of English and Barrett (ref. 9) for entrance region heat transfer to mercury in round tubes. Peclet number, 800 to 900.

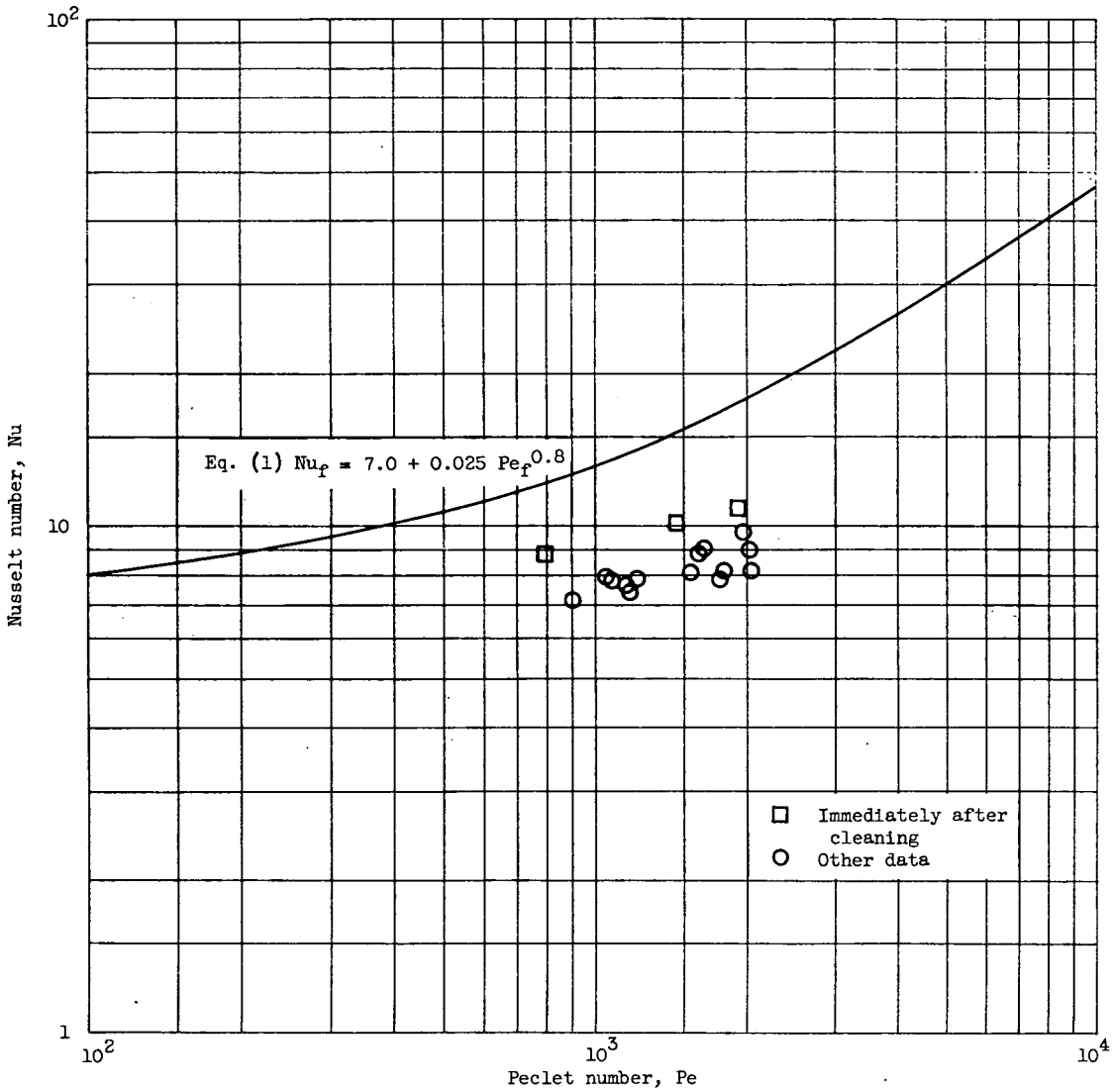

Figure 26. - Data of Seban (ref. 11) for fully developed heat transfer to lead-bismuth eutectic in round tubes.

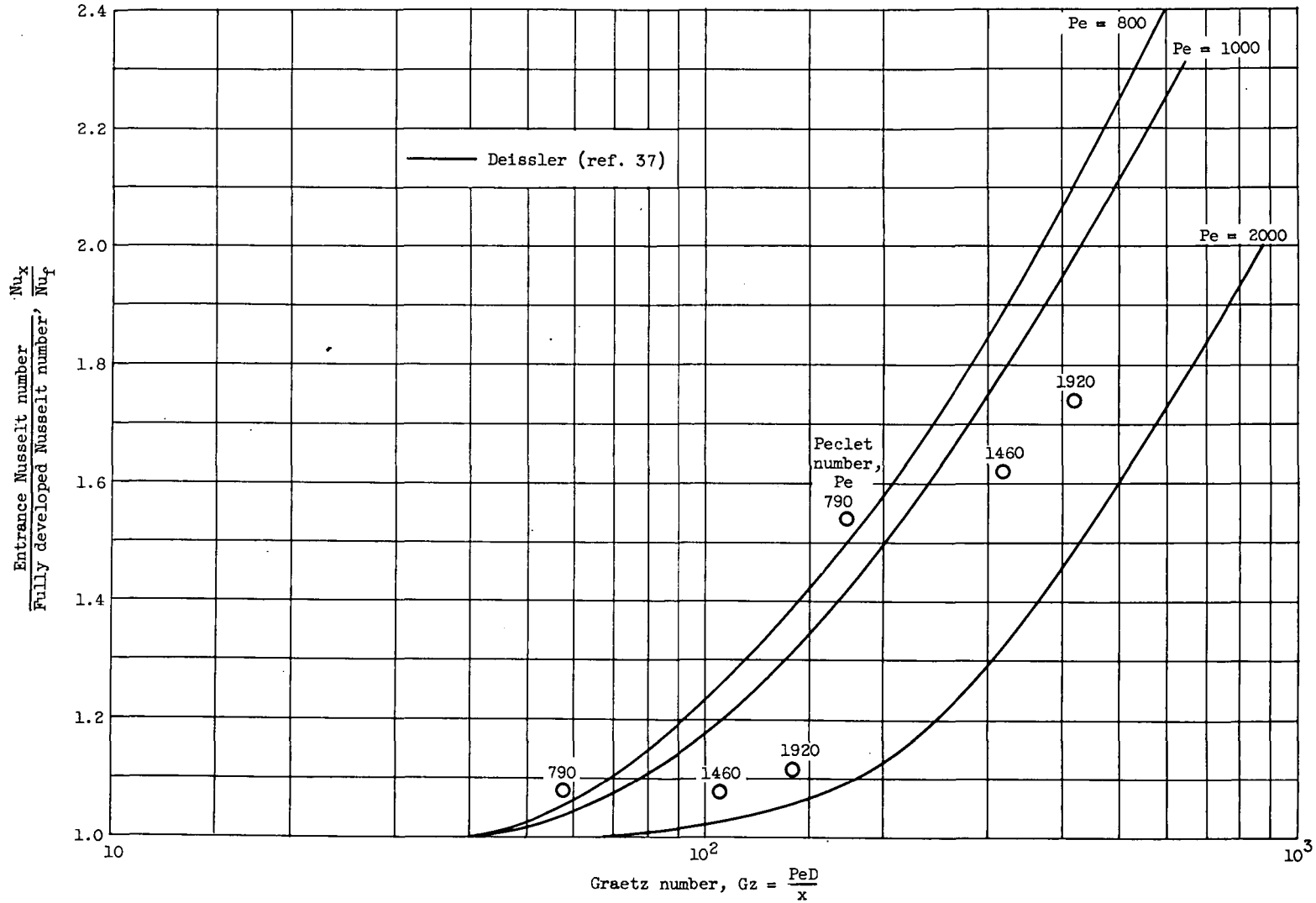

Figure 27. - Data of Seban (ref. 11) for entrance region heat transfer to lead-bismuth eutectic in round tubes.

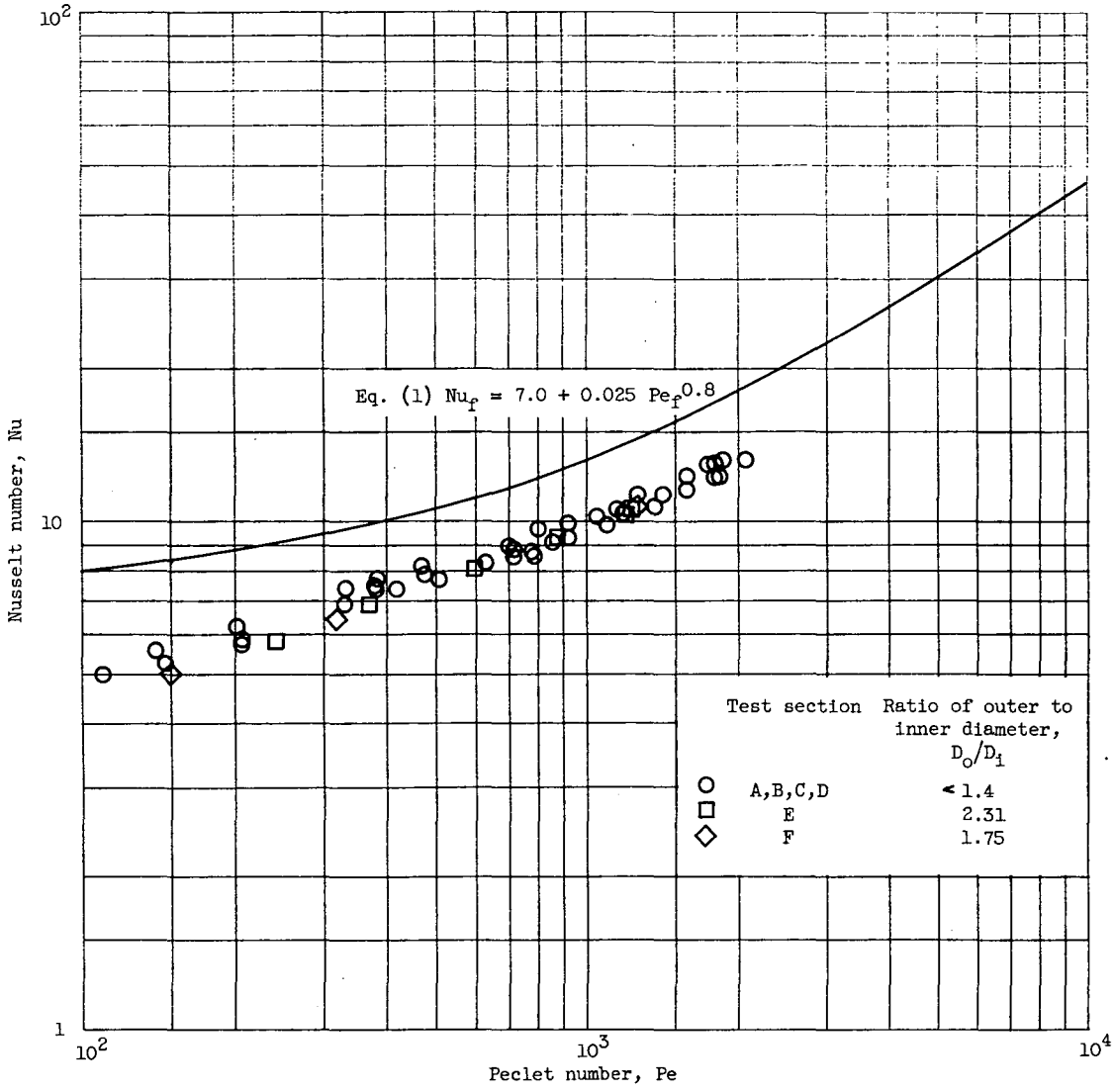

Figure 28. - Re-evaluated data of Trefethen (refs. 12 and 13) for fully developed heat transfer to mercury in round tubes.

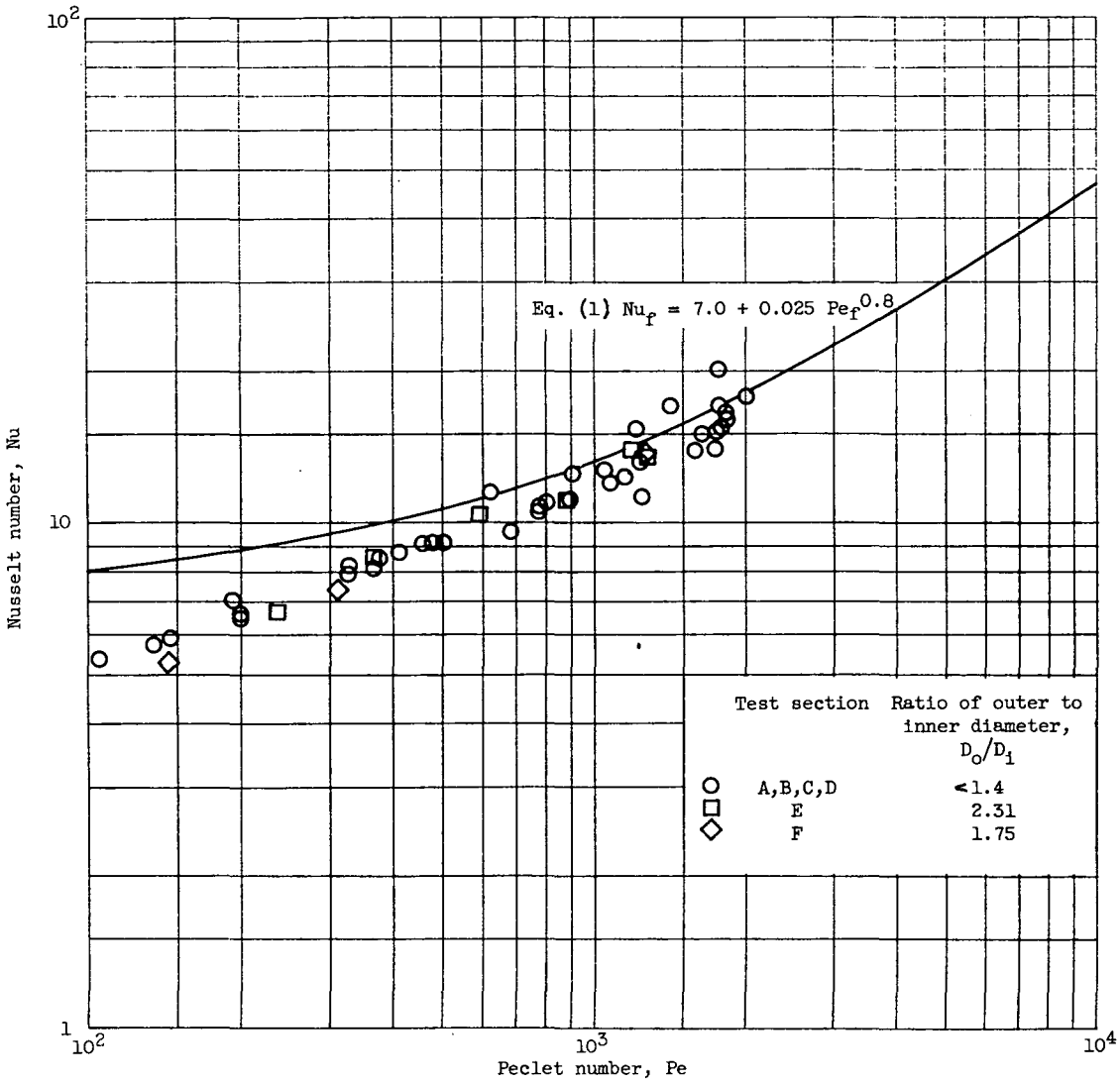

Figure 29. - Re-evaluated data of Trefethen (refs. 12 and 13) for average heat transfer to mercury in round tubes. Length-diameter ratio, 53 to 128.

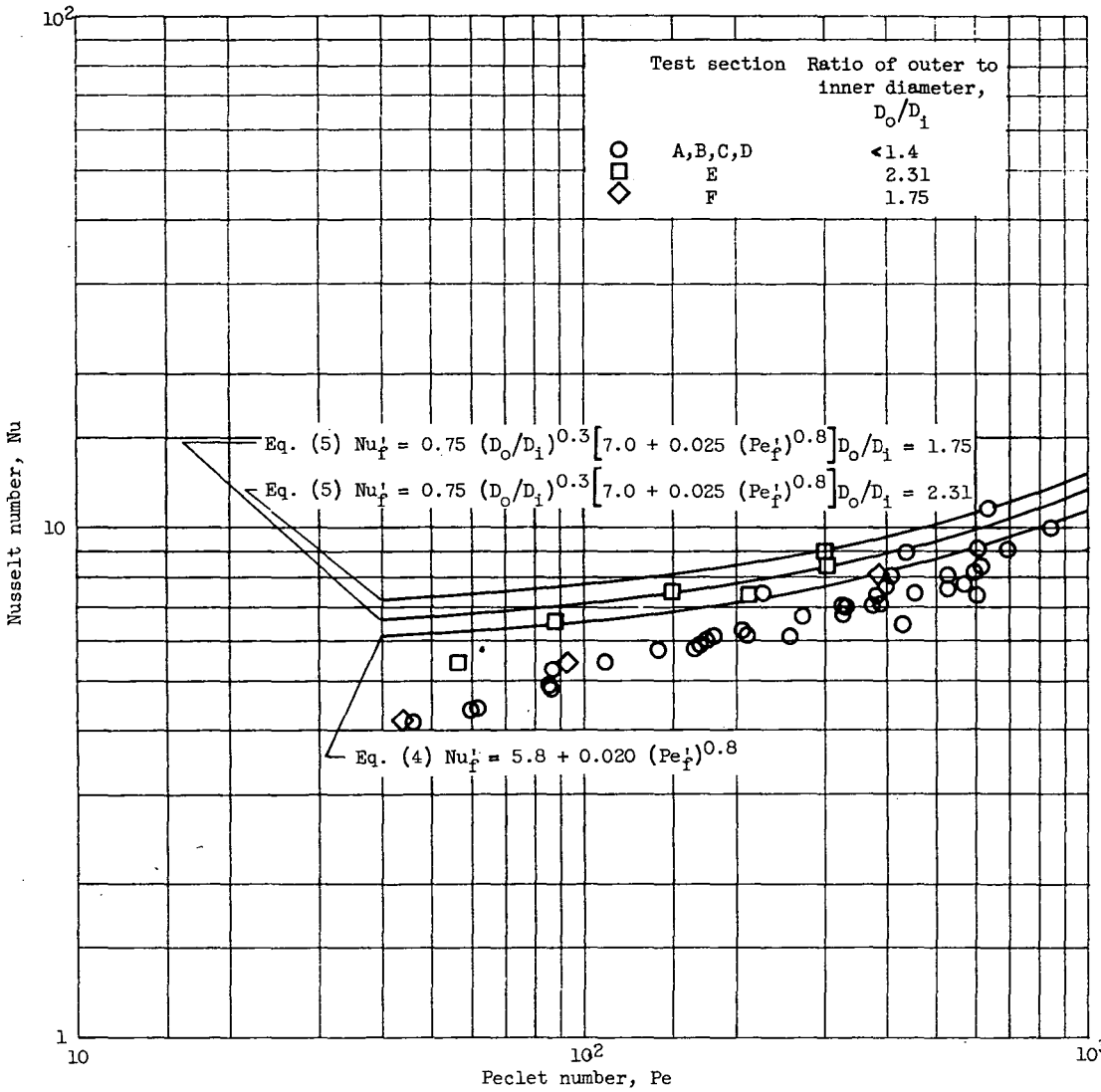

Figure 30. - Re-evaluated data of Trefethen (refs. 12 and 13) for average heat transfer to mercury in annuli. Length-diameter ratio, 79 to 334.

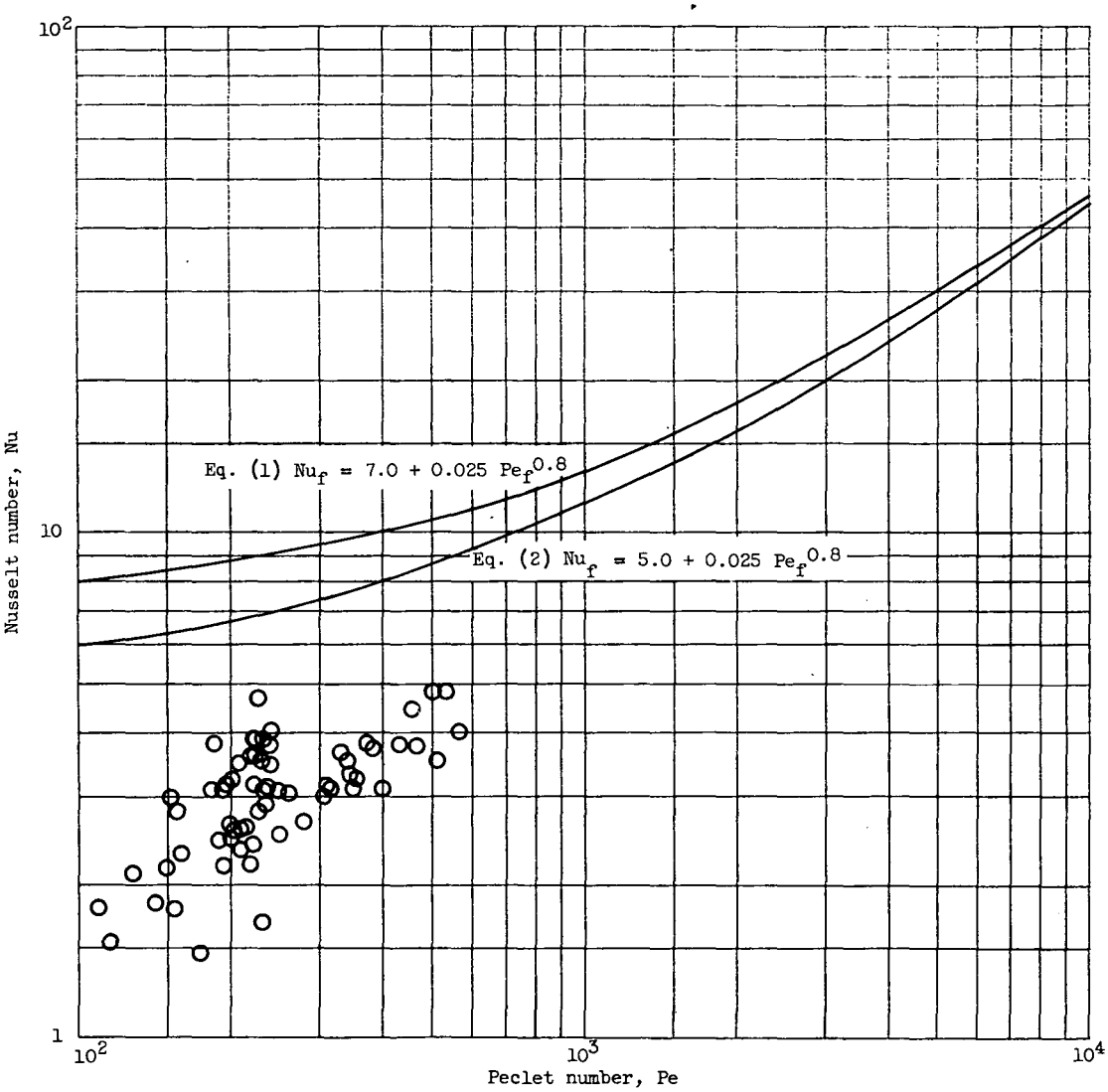

Figure 31. - Re-evaluated data of Doody and Younger (refs. 14 and 15) for heat to mercury without sodium addition in round tubes.

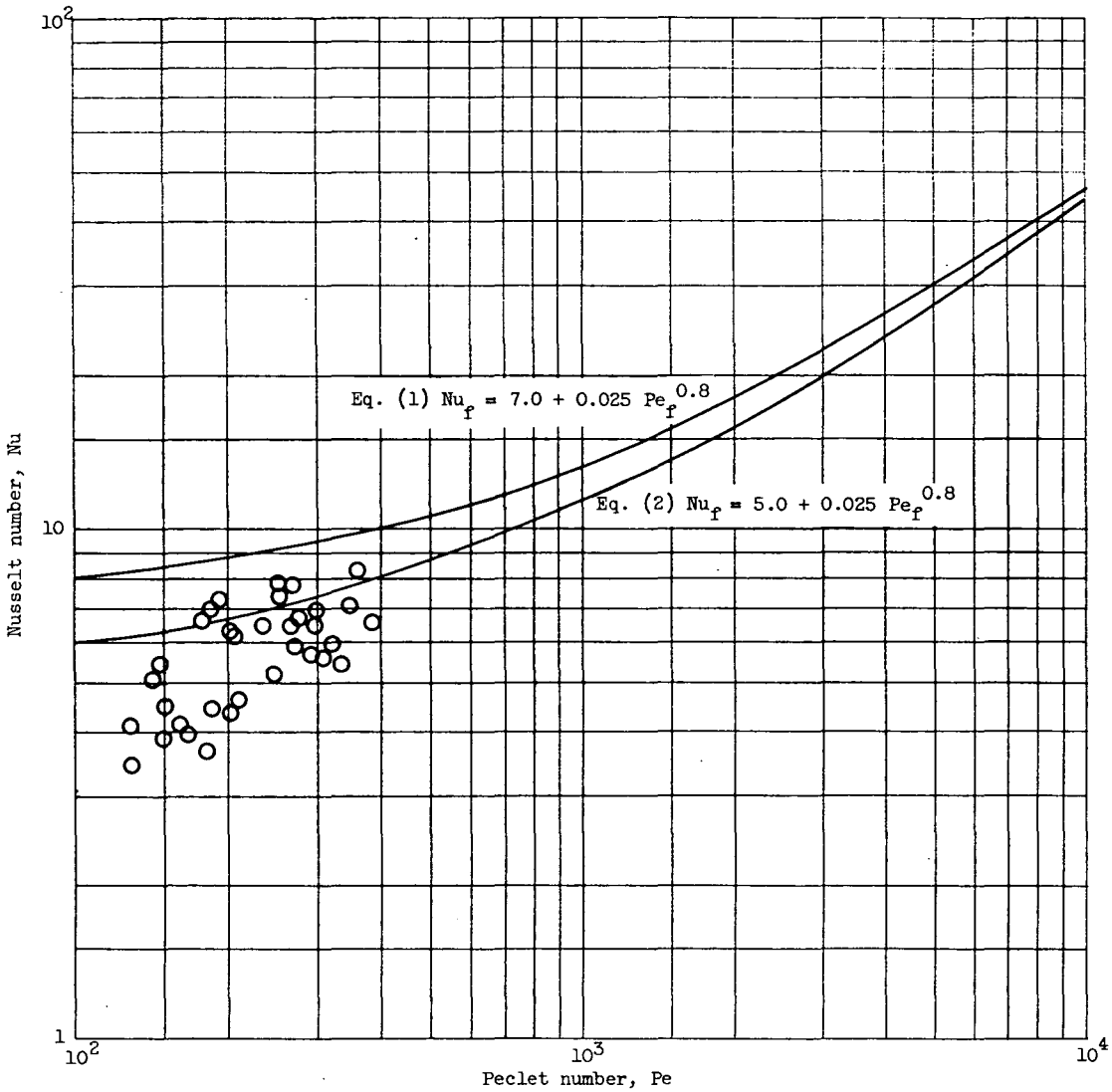

Figure 32. - Re-evaluated data of Doody and Younger (refs. 14 and 15) for heat transfer to mercury with small sodium additions in round tubes.

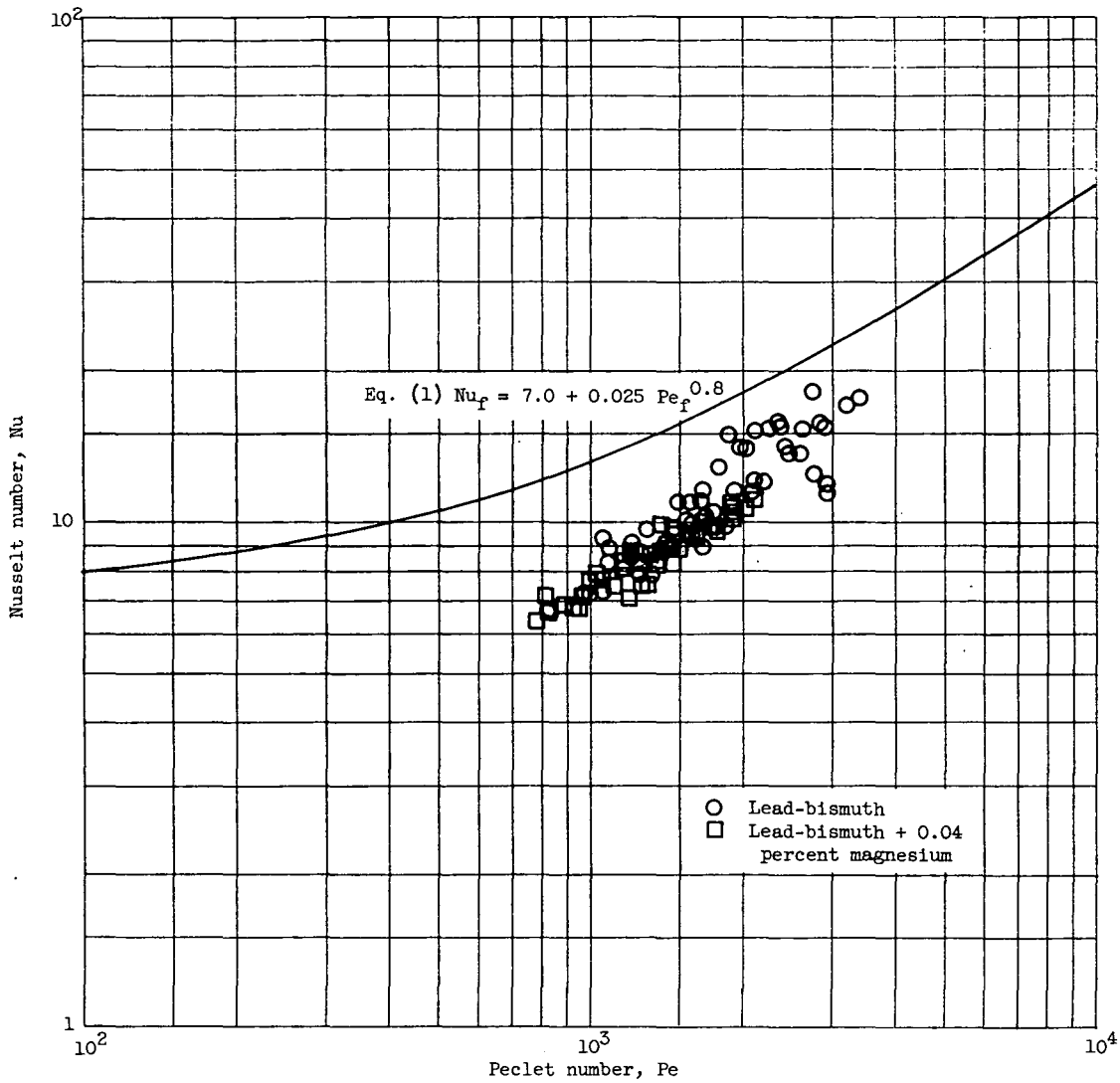

Figure 33. - Data of Lubarsky (ref. 16) for average heat transfer to lead-bismuth eutectic in round tubes. Length-diameter ratio, 100.

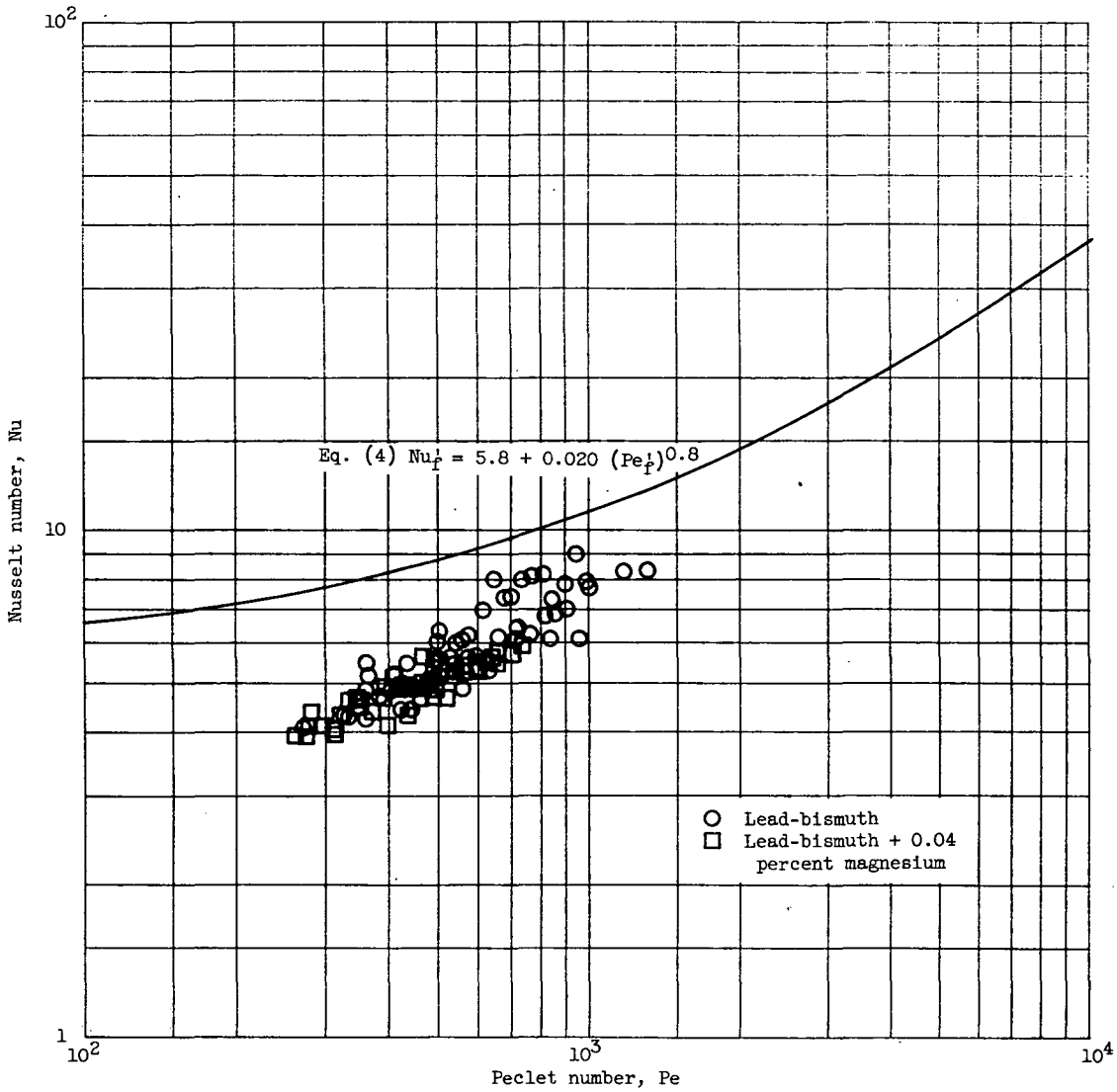

Figure 34. - Data of Lubarsky (ref. 16) for average heat transfer to lead-bismuth eutectic in annuli. Length-diameter ratio, 322.

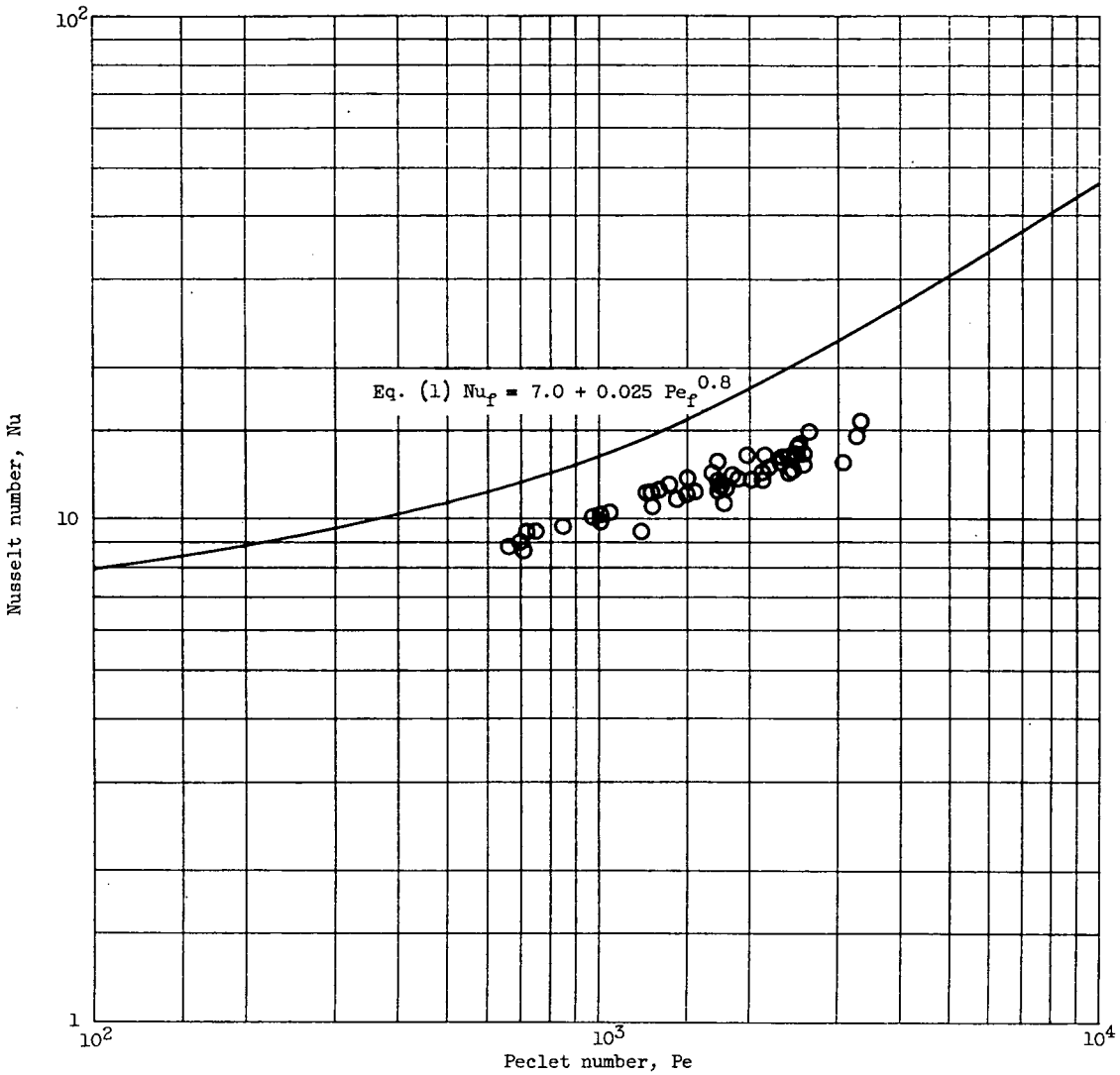

Figure 35. - Data of Johnson, Hartnett, and Clabaugh (refs. 17 and 18) for fully developed heat transfer to lead-bismuth eutectic in round tubes.

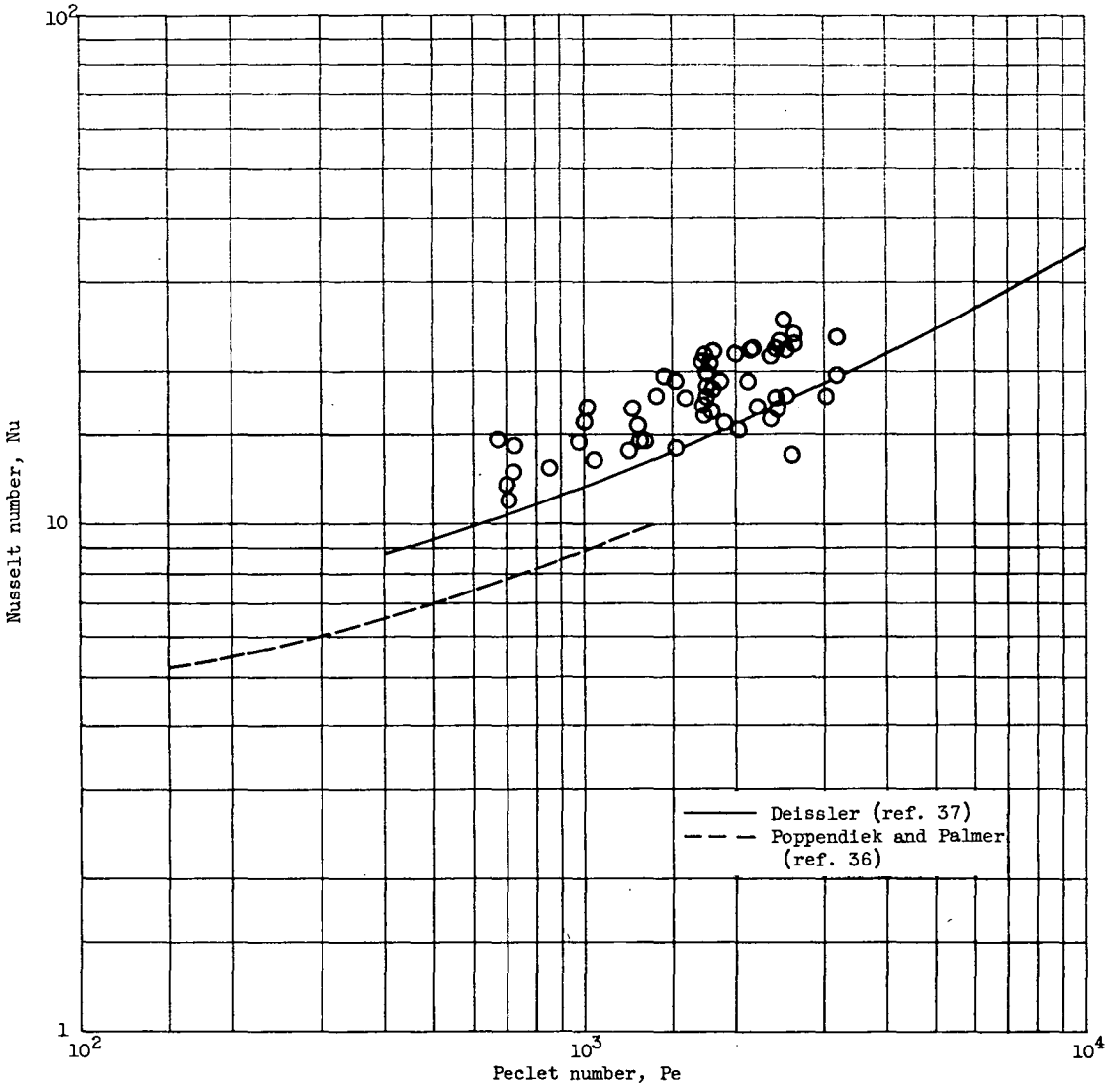

(a) x/D = 4.6.

Figure 36. - Data of Johnson, Hartnett, and Clabaugh (refs. 17 and 18) for entrance region heat transfer to lead-bismuth eutectic in round tubes.

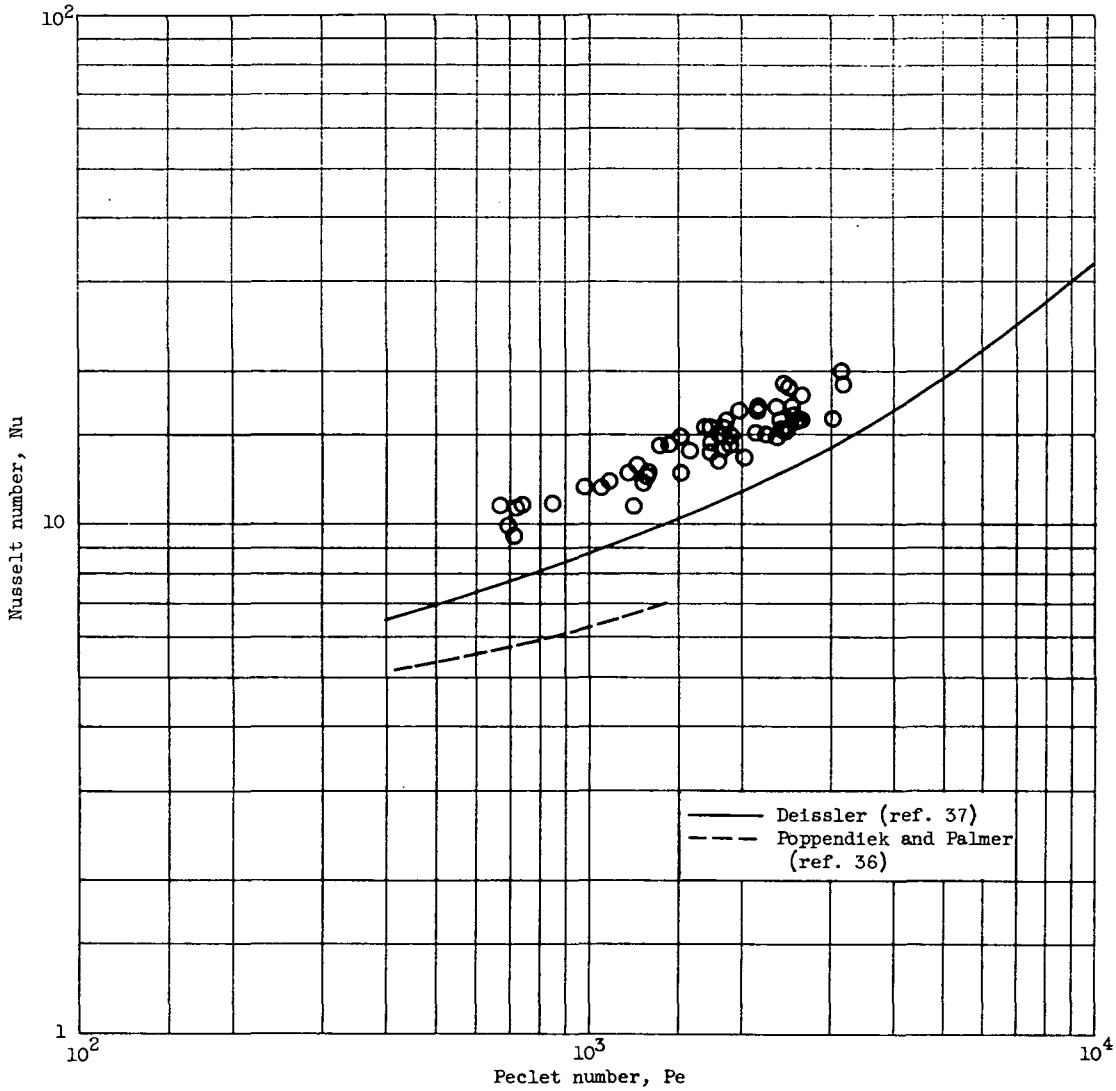

(b) x/D = 13.8.

Figure 36. - Continued. Data of Johnson, Hartnett, and Clabaugh (refs. 17 and 18) for entrance region heat transfer to lead-bismuth eutectic in round tubes.

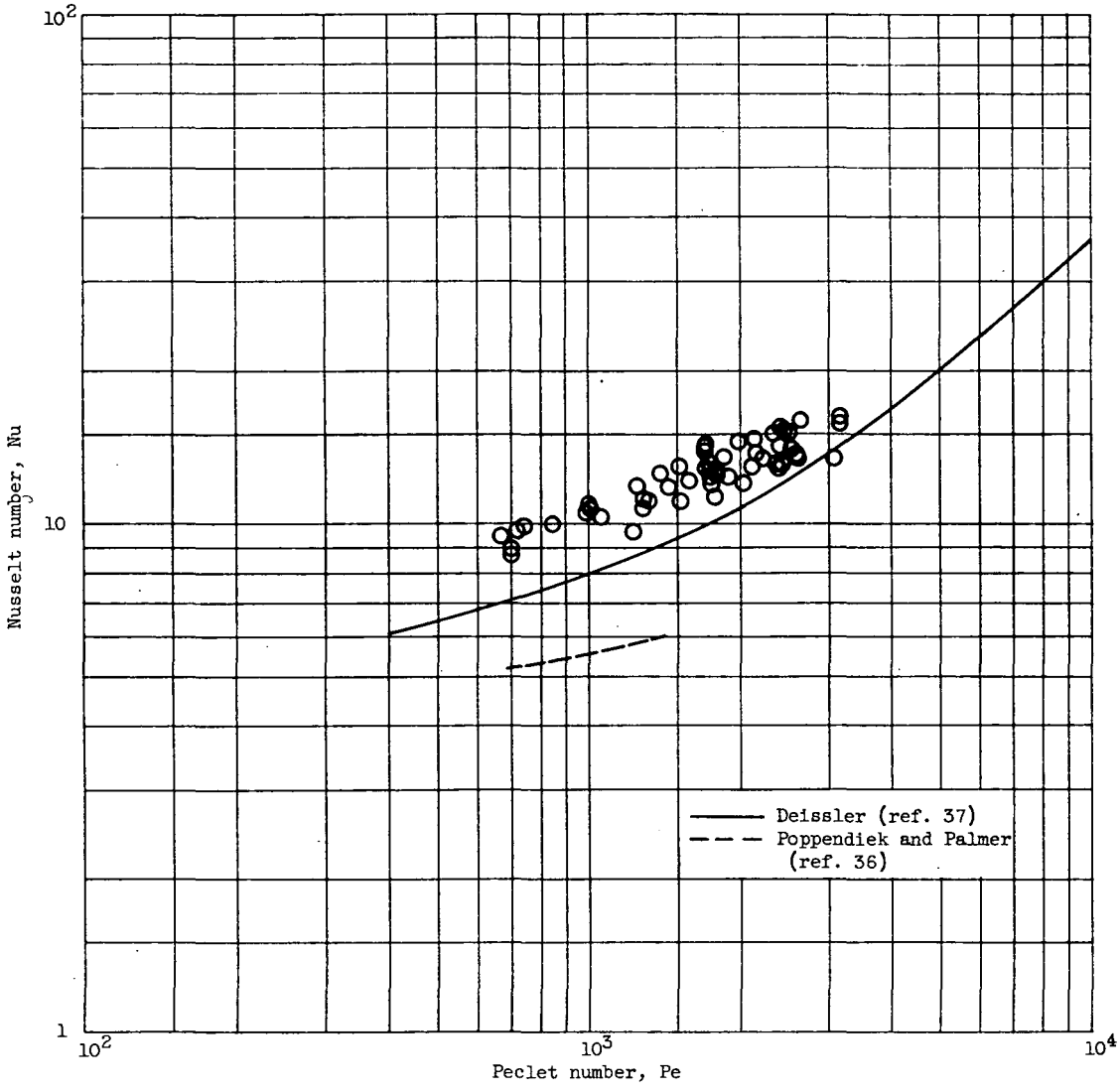

(c) x/D = 23.

Figure 36. - Concluded. Data of Johnson, Hartnett, and Clabaugh (refs. 17 and 18) for entrance region heat transfer to lead-bismuth eutectic in round tubes.

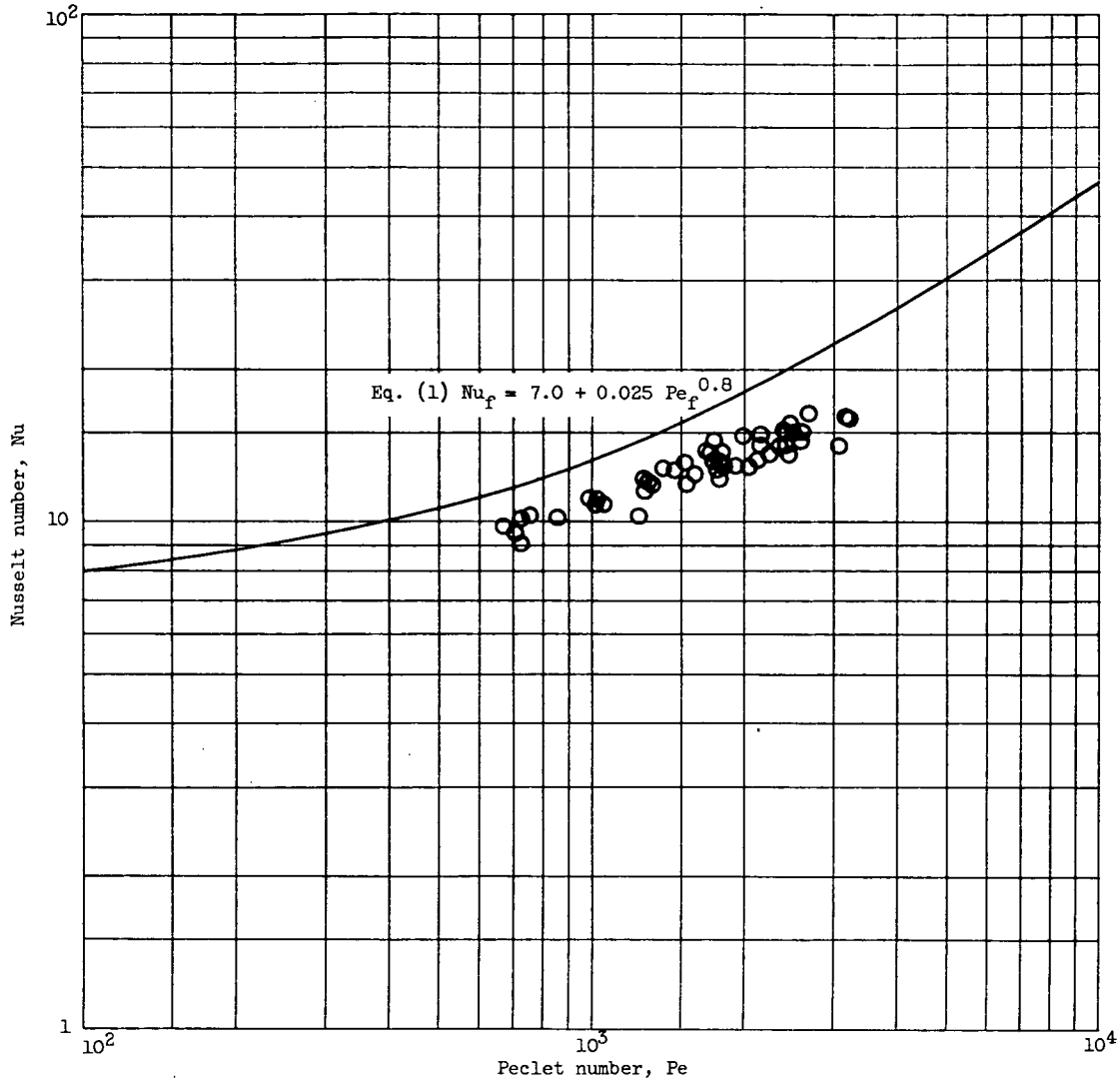

Figure 37. - Data of Johnson, Hartnett, and Clabaugh (refs. 17 and 18) for average heat transfer to lead-bismuth eutectic in round tubes. Length-diameter ratio, 74.

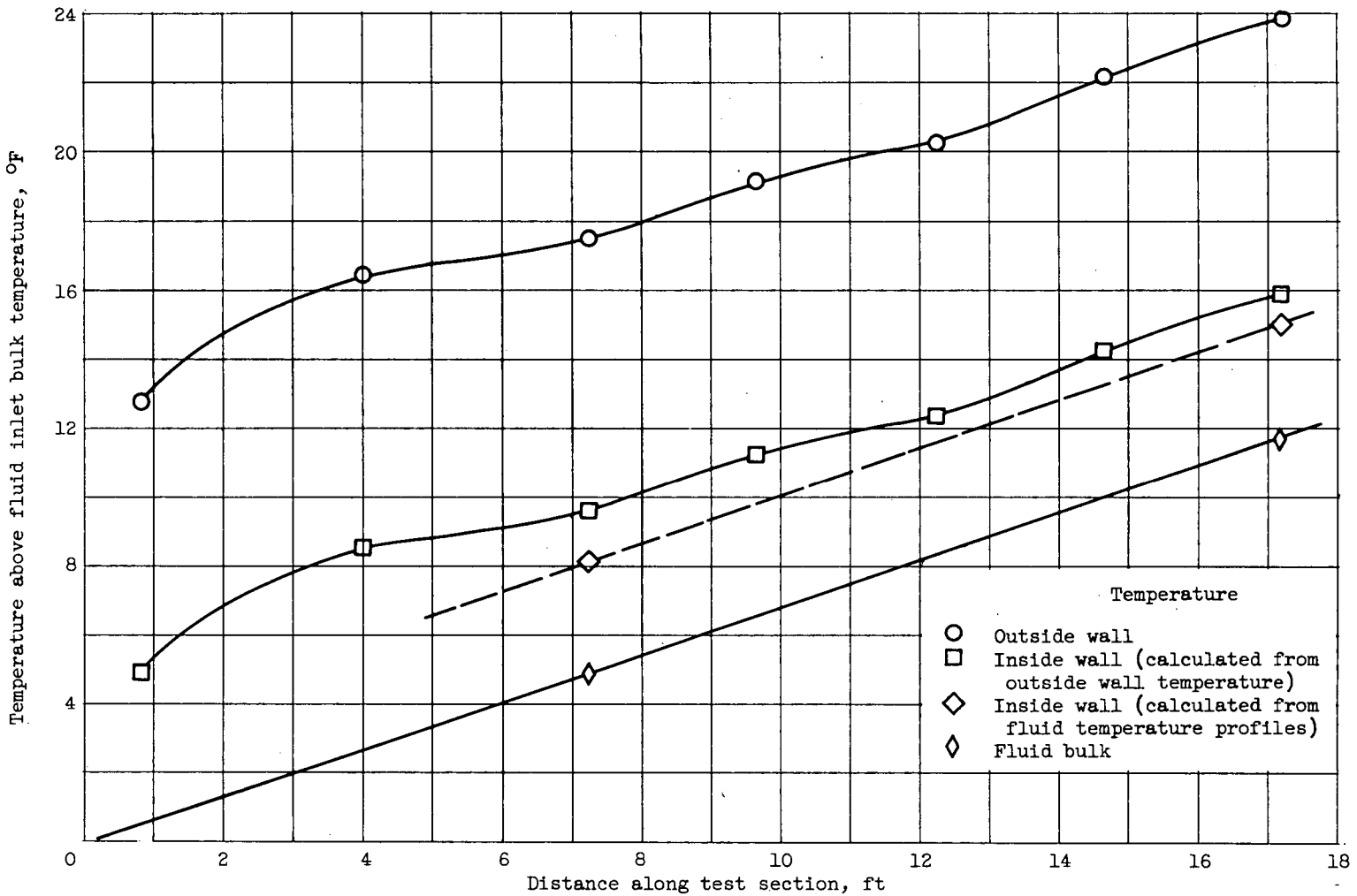

(a) Run 3.

Figure 38. - Test-section temperatures from two typical runs of Isakoff and Drew (refs. 19 and 20).

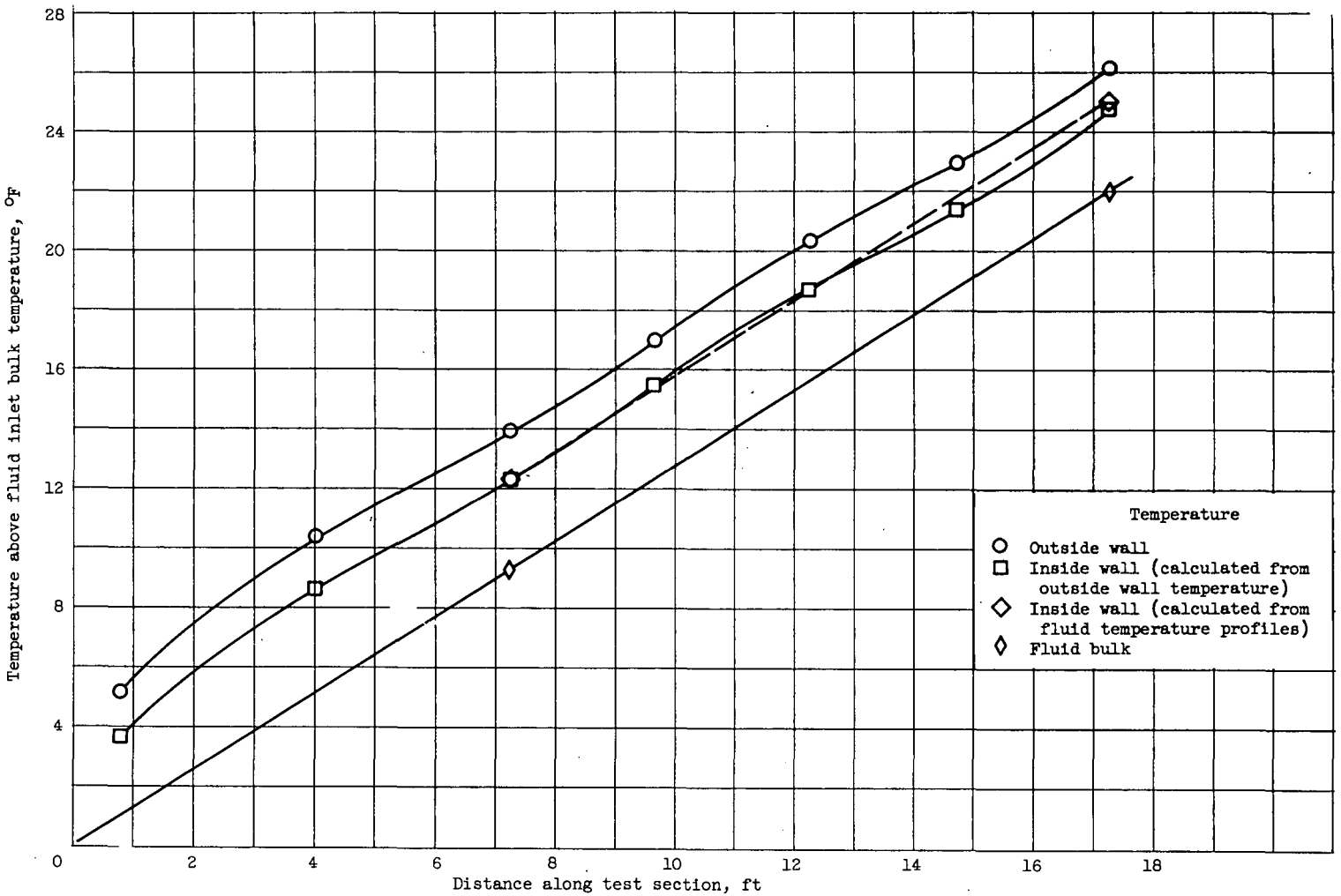

(b) Run 12.

Figure 38. - Concluded. Test-section temperatures from two typical runs of Isakoff and Drew (refs. 19 and 20).

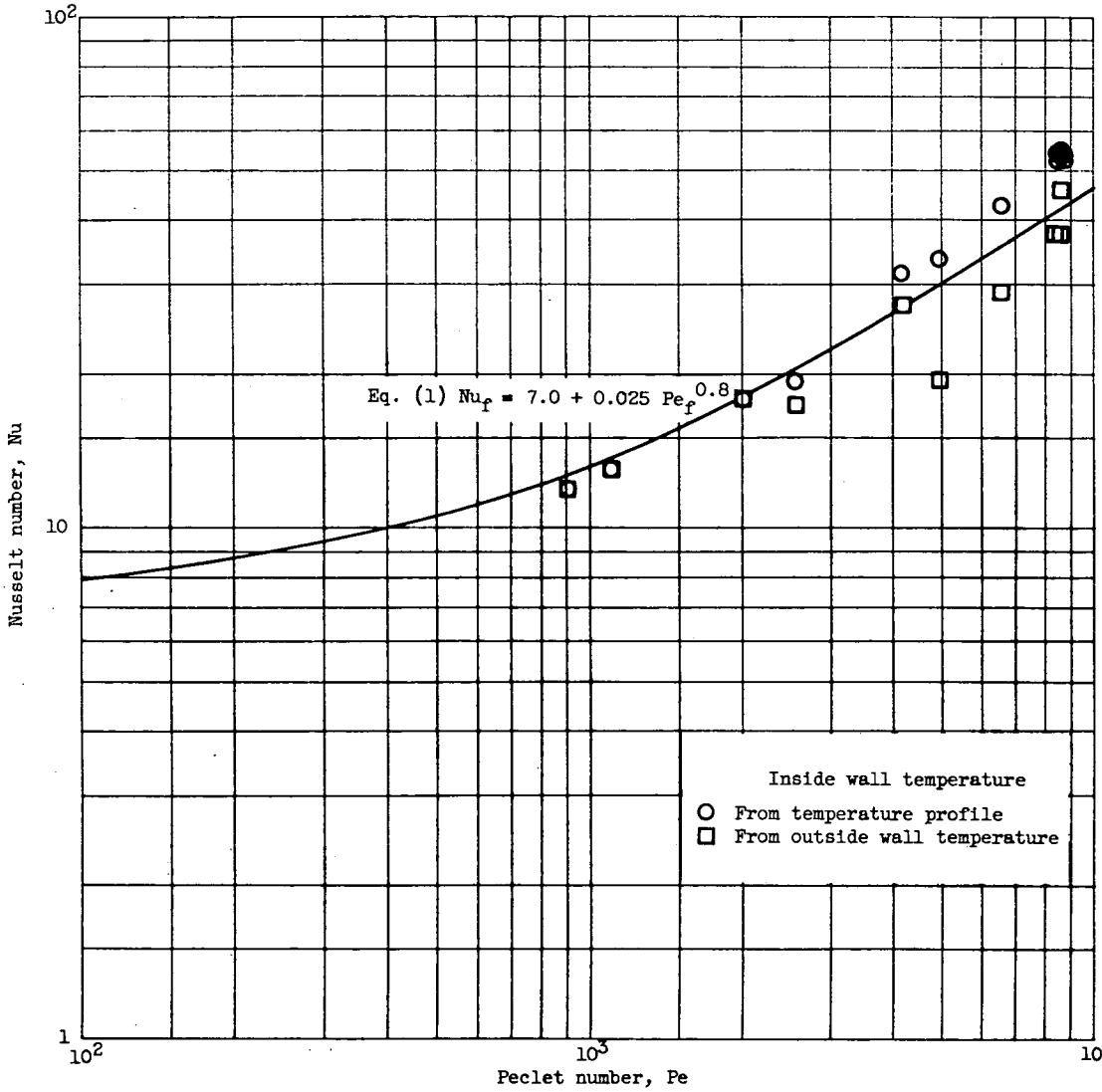

Figure 39. - Data of Isakoff and Drew (refs. 19 and 20) for fully developed heat transfer to mercury in round tubes.

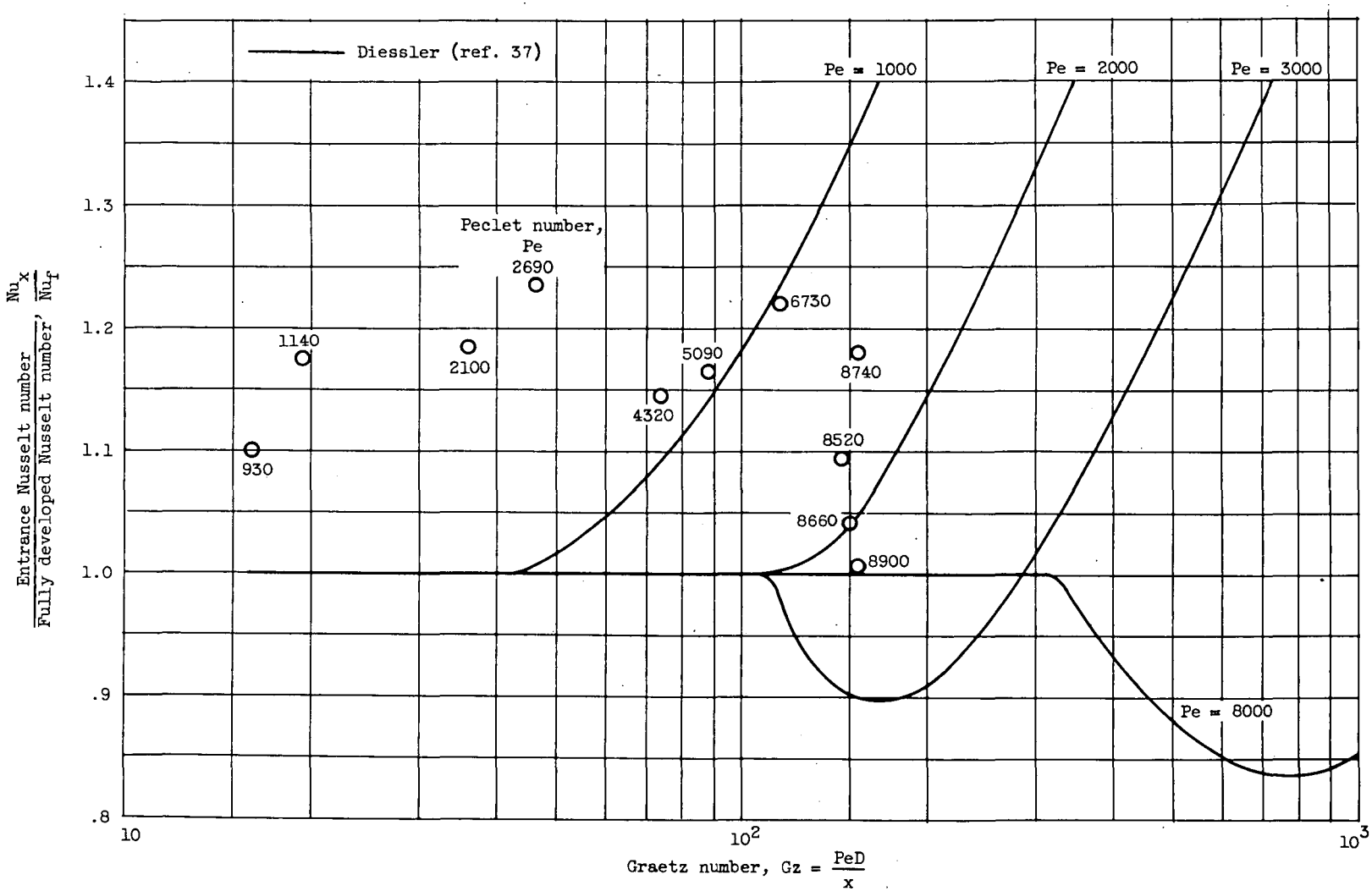

Figure 40. - Data of Isakoff and Drew (refs. 19 and 20) for entrance region heat transfer to mercury in round tubes (inside wall temperatures extrapolated from fluid temperature profile).

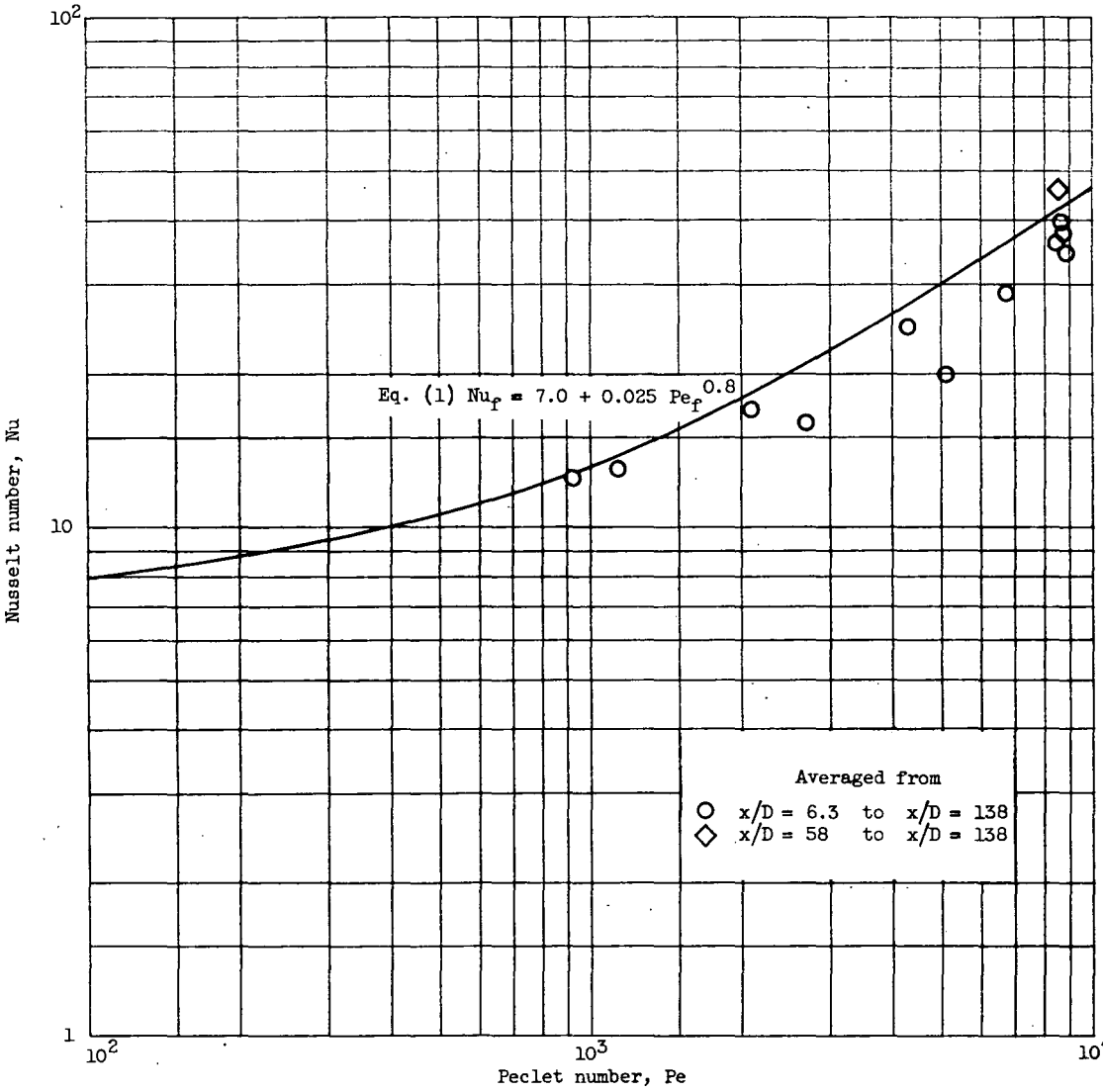

Figure 41. - Data of Isakoff and Drew (refs. 19 and 20) for average heat transfer to mercury in round tubes (inside wall temperatures calculated from outside wall temperatures).

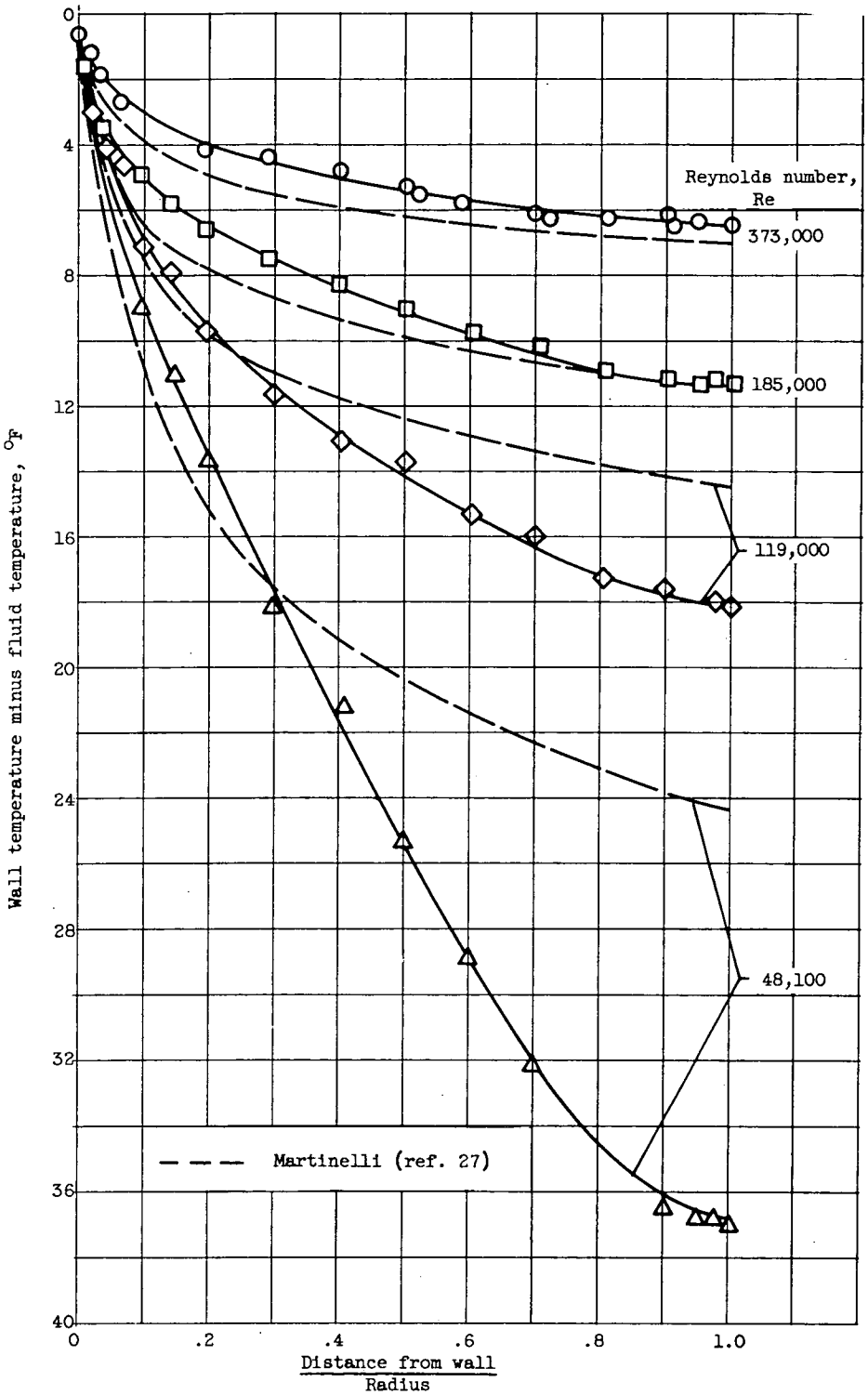

Figure 42. - Data of Isakoff and Drew (refs. 19 and 20) for fully developed temperature distribution for heat transfer to mercury in round tubes.

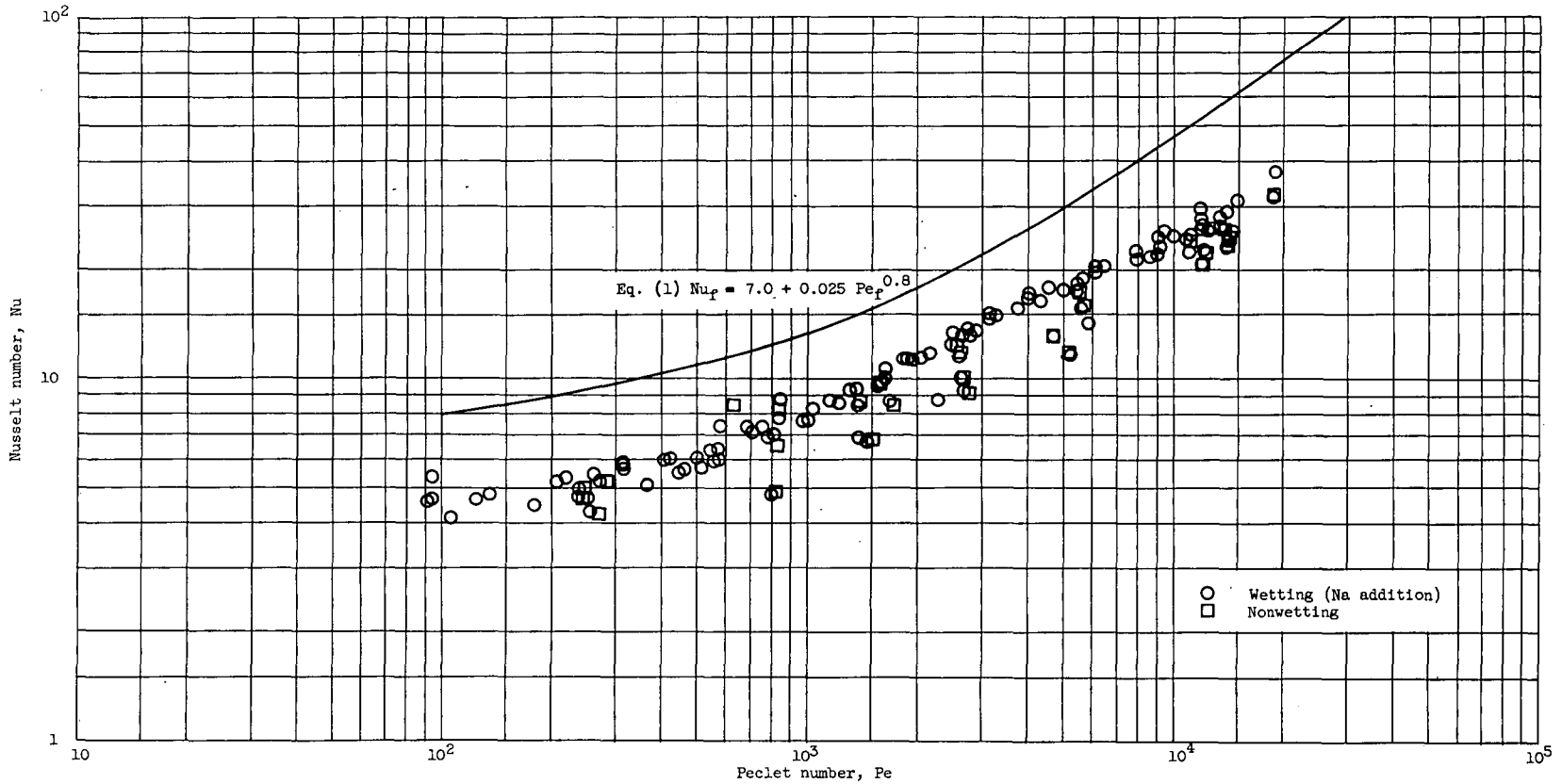

Figure 43. - Data of Stromquist (ref. 21) for fully developed heat transfer to mercury, with and without sodium additions, in round tubes.

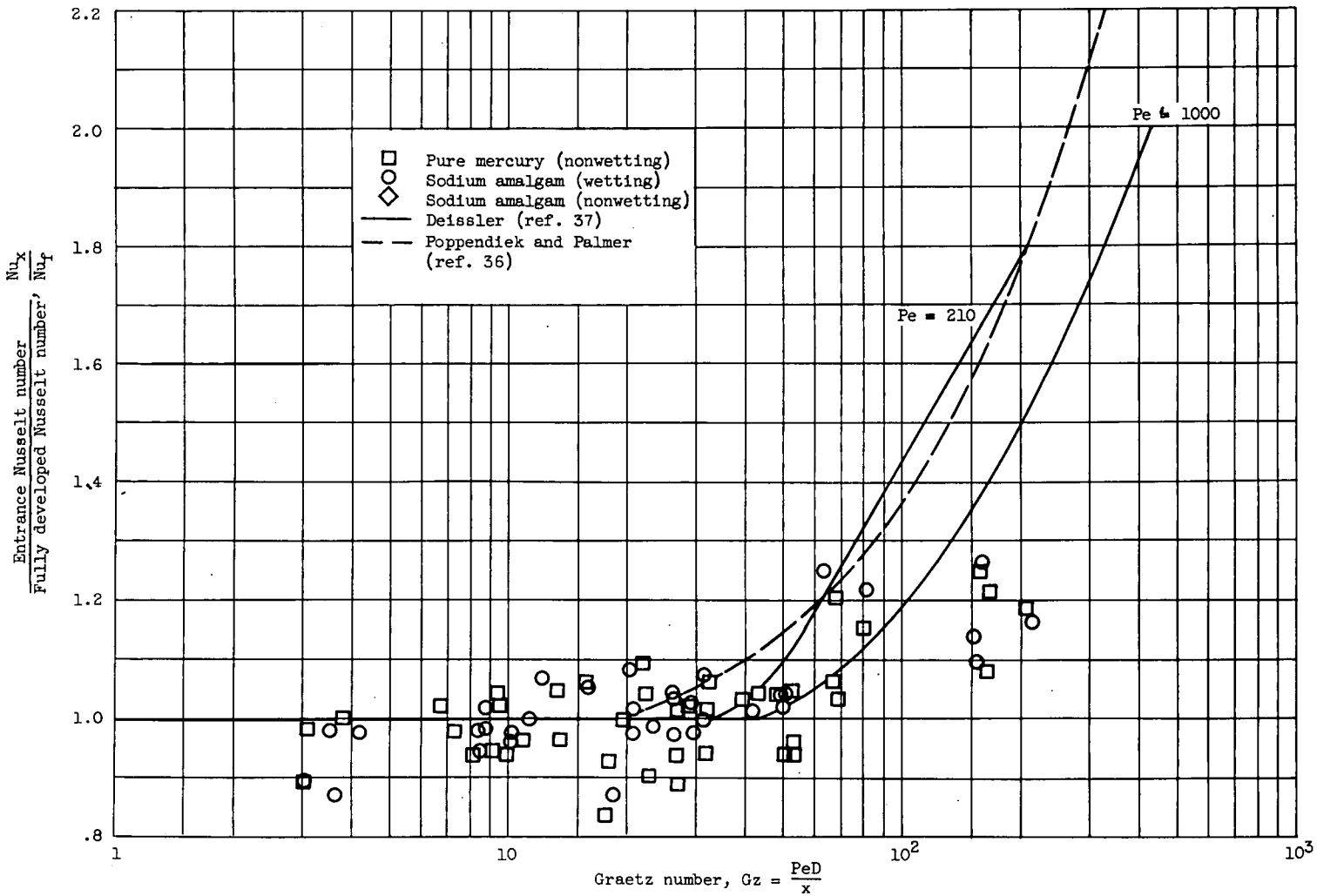

(a) 170 < Peclet number < 1000.

Figure 44. - Data of Stromquist (ref. 21) for entrance region heat transfer to mercury, with and without sodium additions, in round tubes.

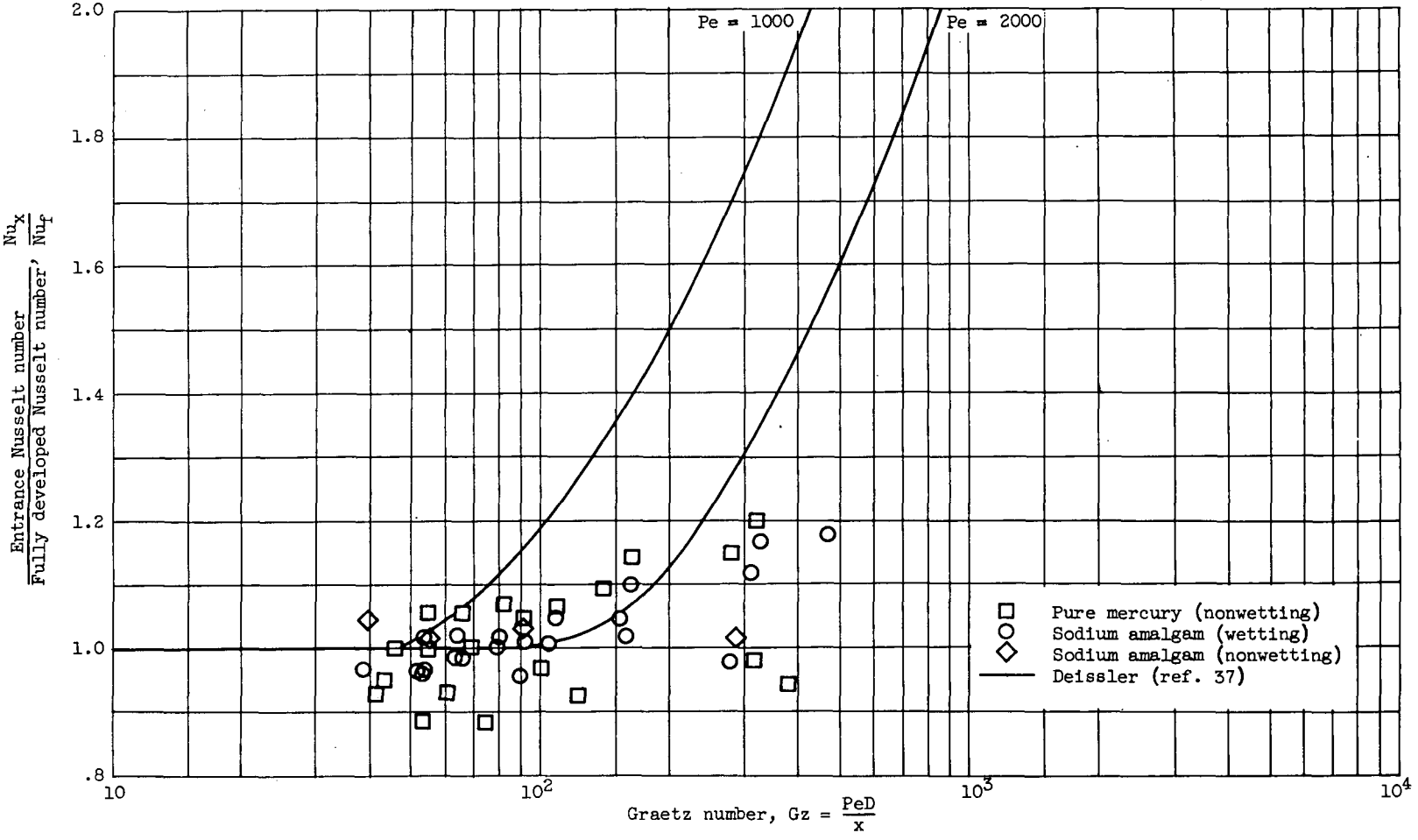

(b) 1000 < Peclet number < 2000.

Figure 44. - Continued. Data of Stromquist (ref. 21) for entrance region heat transfer to mercury, with and without sodium additions, in round tubes.

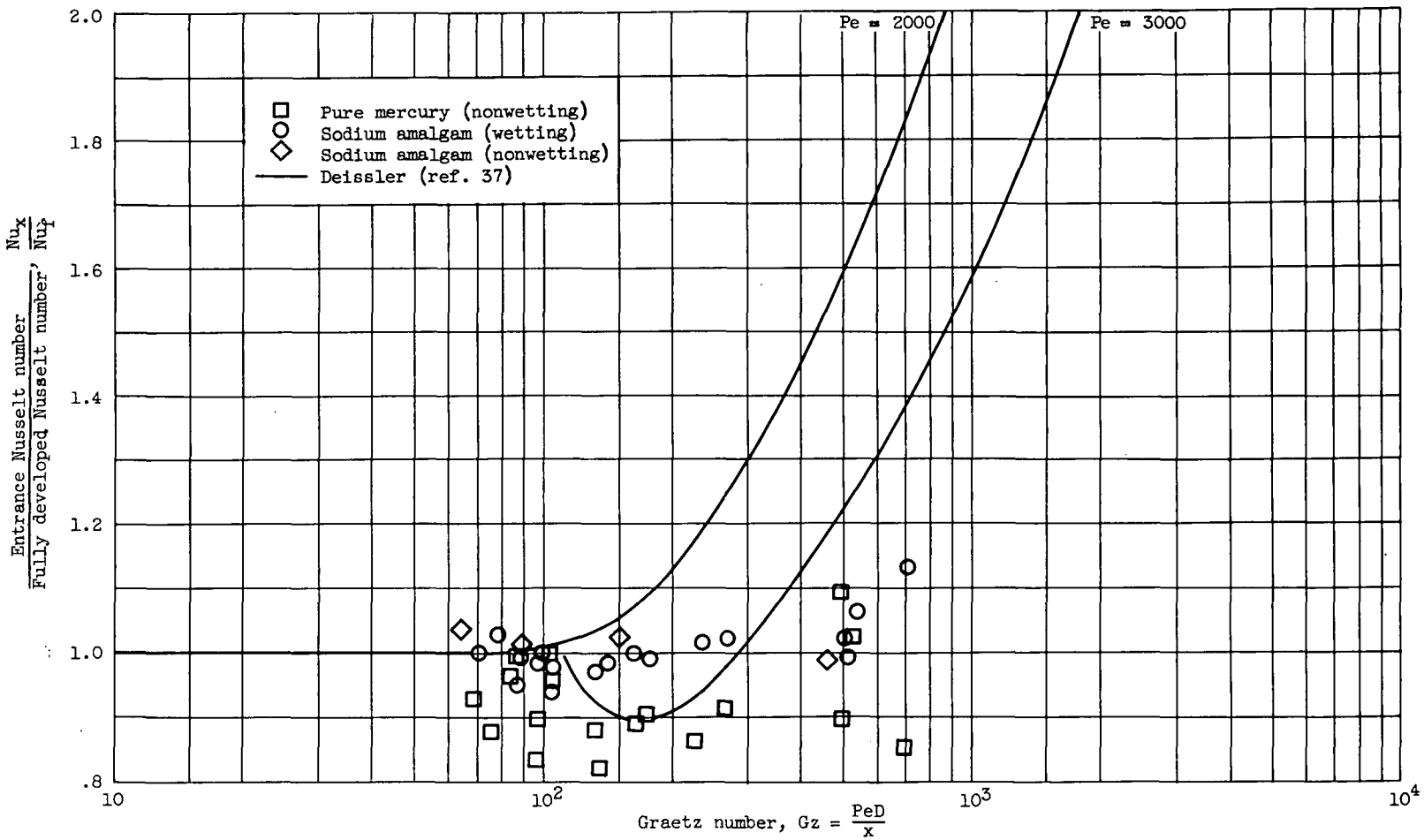

(c) 2000 < Peclet number < 3000.

Figure 44. - Continued. Data of Stromquist (ref. 21) for entrance region heat transfer to mercury, with and without sodium additions, in round tubes.

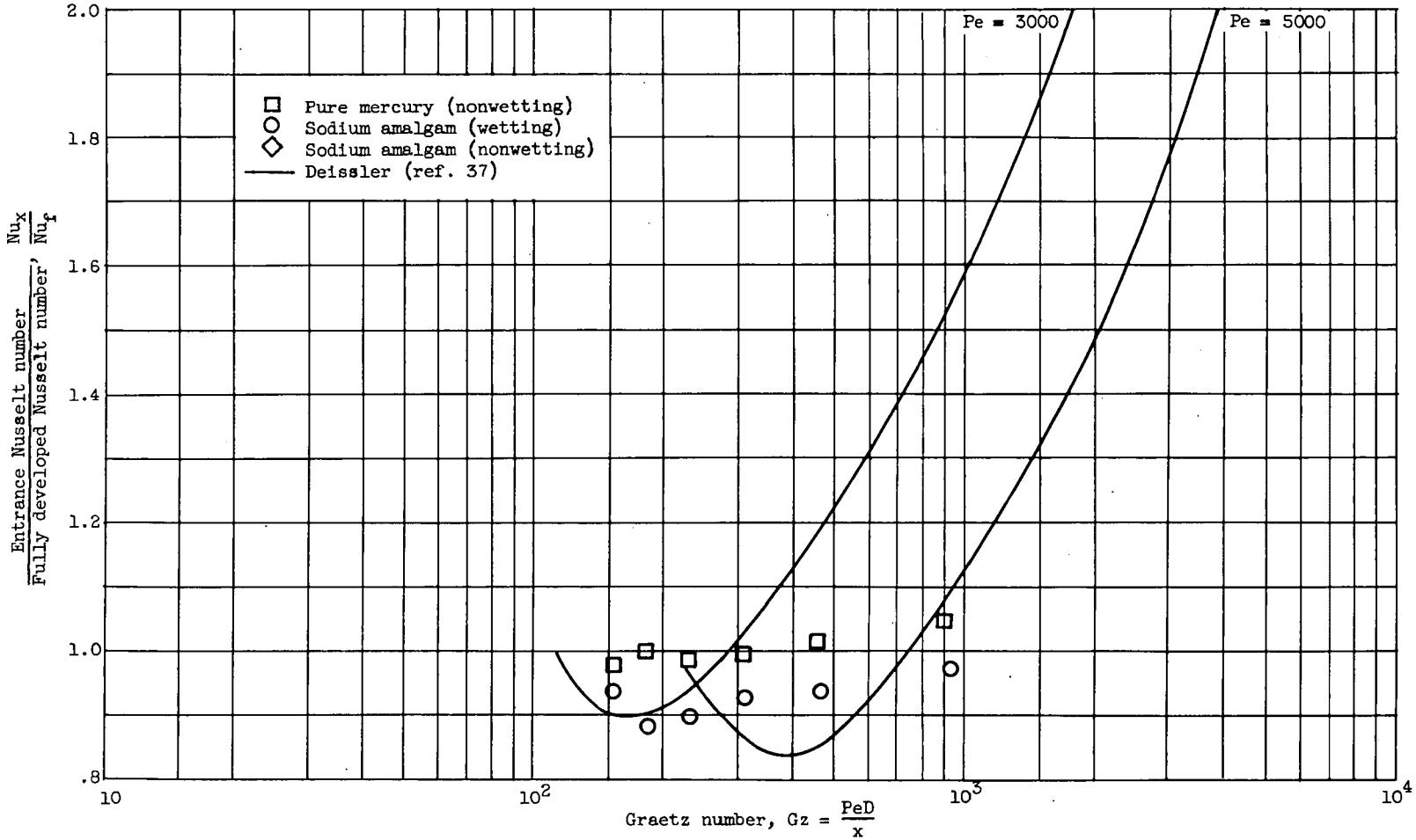

(d) 3000 < Peclet number < 5000.

Figure 44. - Continued. Data of Stromquist (ref. 21) for entrance region heat transfer to mercury, with and without sodium additions, in round tubes.

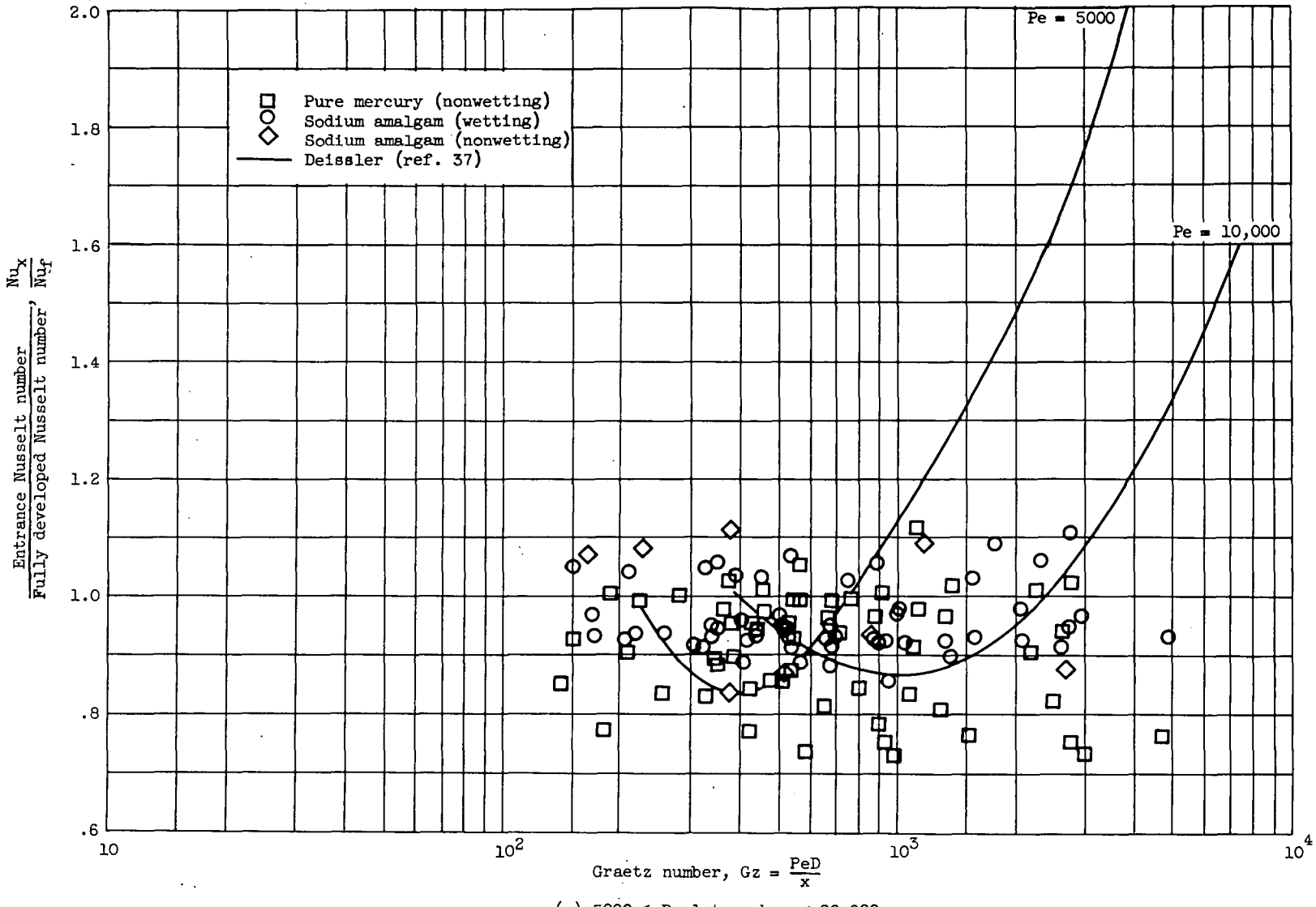

(e) 5000 < Peclet number < 20,000.

Figure 44. - Concluded. Data of Stromquist (ref. 21) for entrance region heat transfer to mercury, with and without sodium additions, in round tubes.

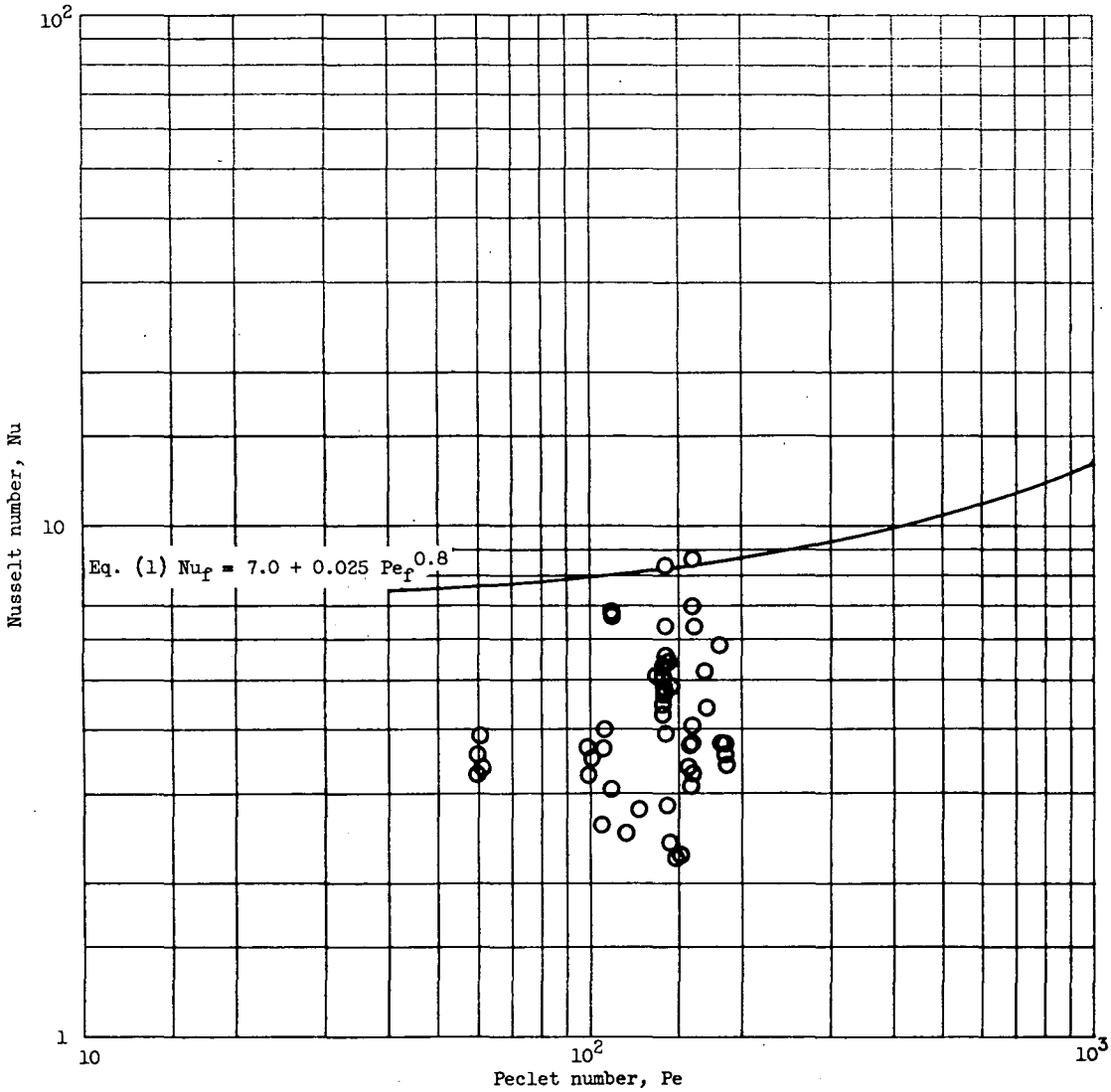

Figure 45. - Data of MacDonald and Quittenton (refs. 22 and 23) for fully developed heat transfer to sodium in round tubes.

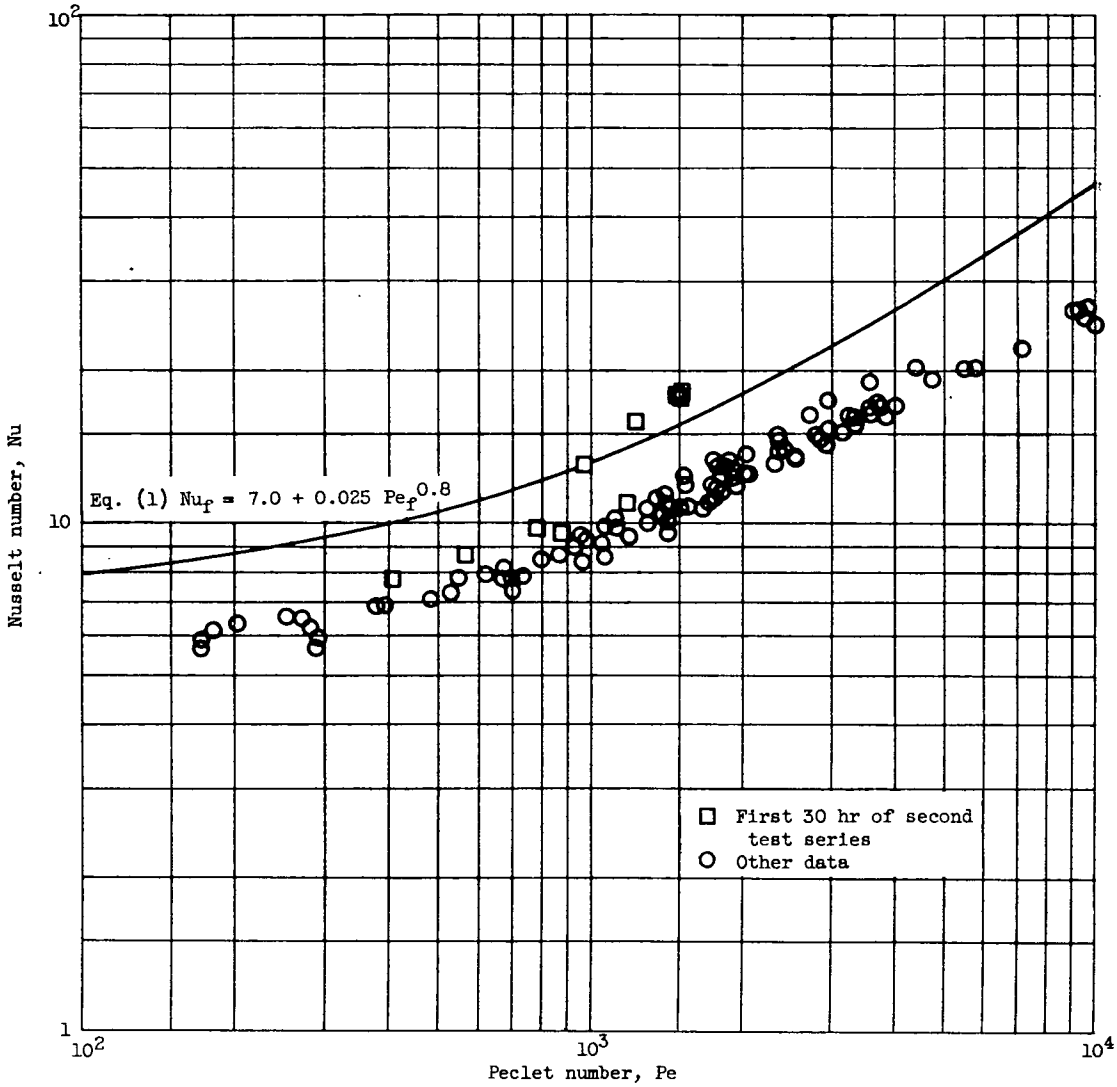

Figure 46. - Data of Johnson, Clabaugh, and Hartnett (ref. 24) for fully developed heat transfer to mercury in round tubes.

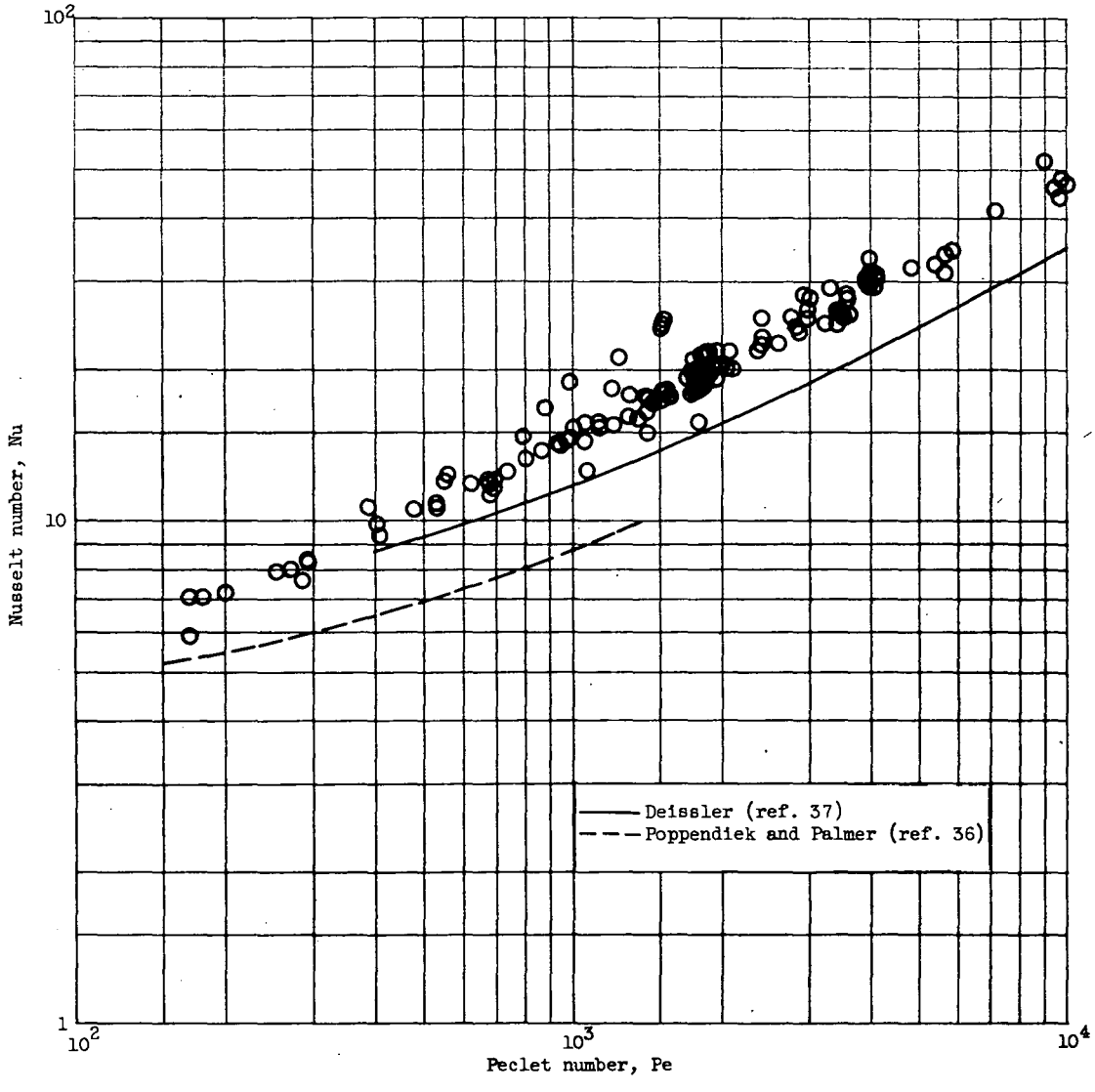

(a) x/D = 4.6.

Figure 47. - Data of Johnson, Hartnett, and Clabaugh (ref. 24) for entrance region heat transfer to mercury in round tubes.

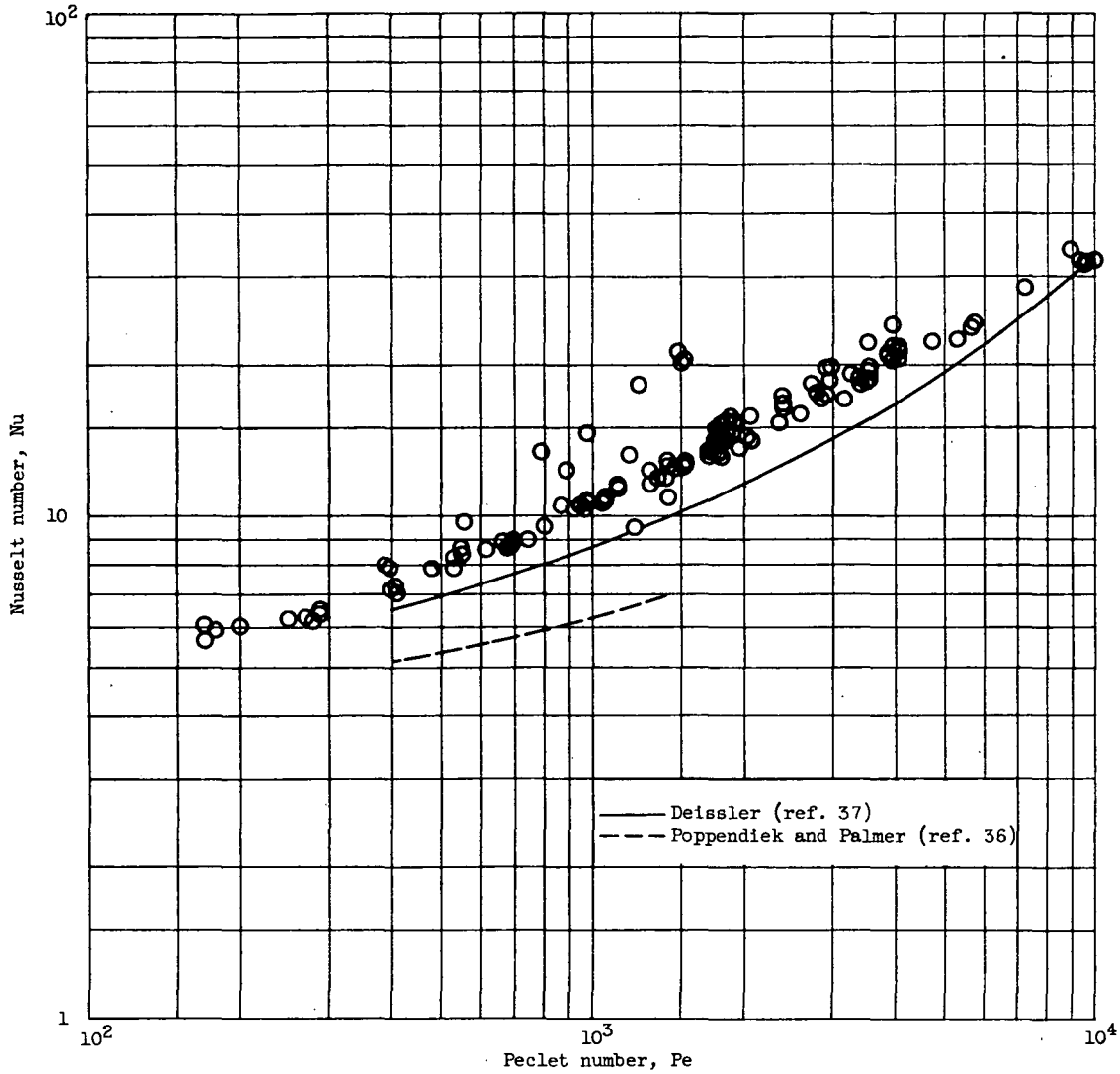

(b) x/D = 13.8.

Figure 47. - Continued. Data or Johnson, Hartnett, and Clabaugh (ref. 24) for entrance region heat transfer to mercury in round tubes.

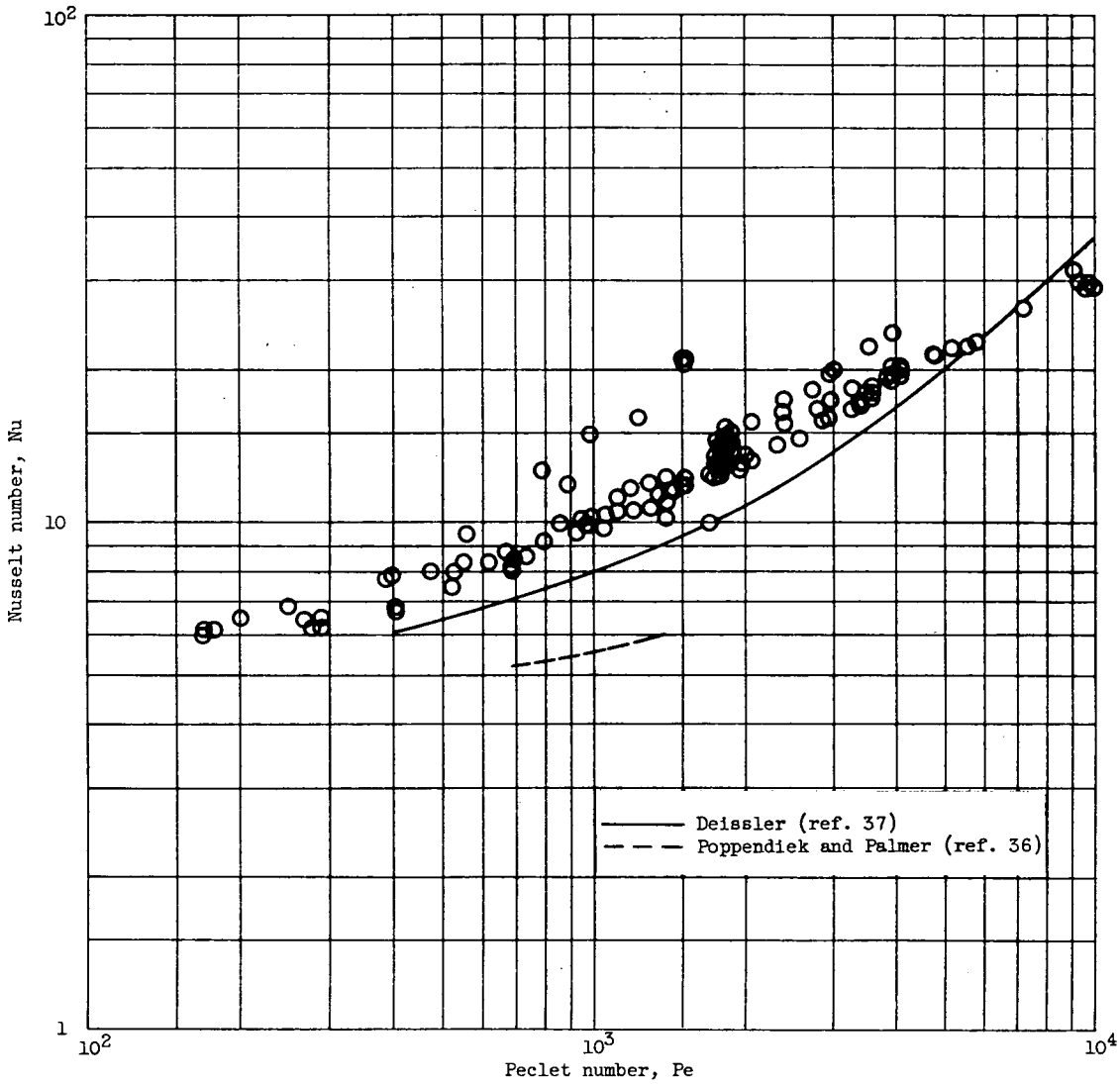

(c) x/D = 23.

Figure 47. - Concluded. Data of Johnson, Hartnett, and Clabaugh (ref. 24) for entrance region heat transfer to mercury in round tubes.

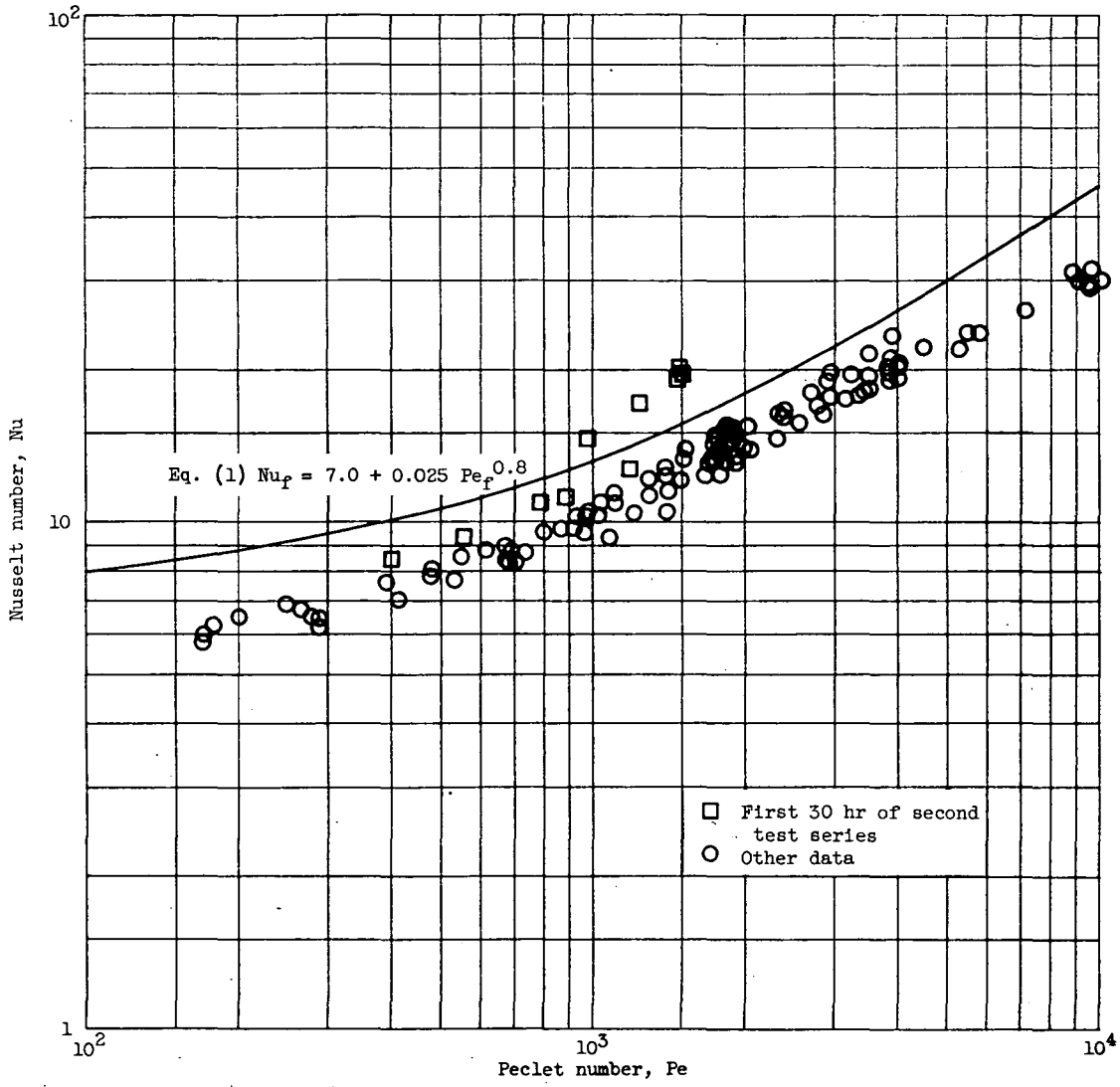

Figure 48. - Data of Johnson, Clabaugh, and Hartnett (ref. 24) for average heat transfer to mercury in round tubes. Length-diameter ratio, 74.

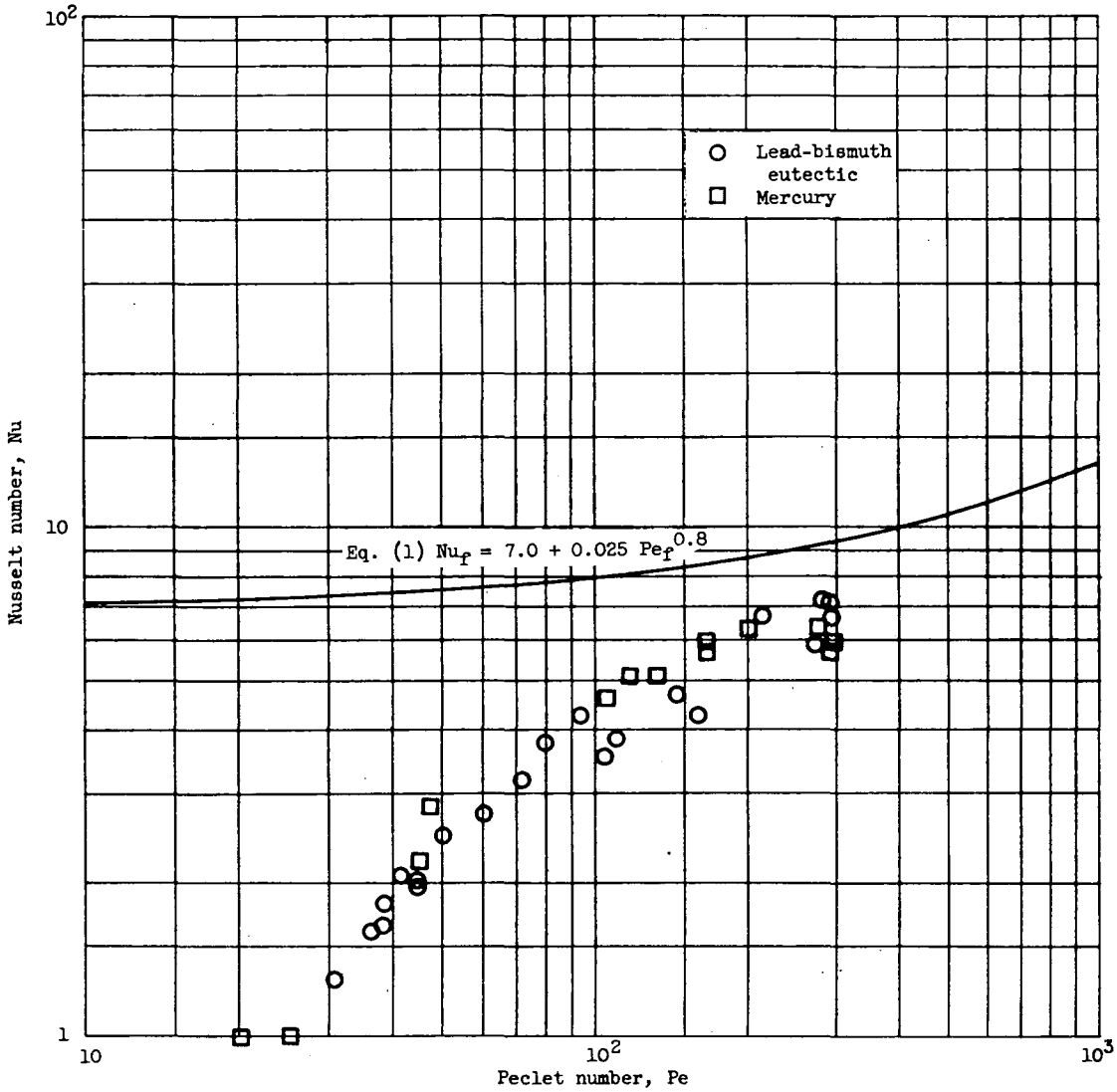

Figure 49. - Data of Johnson, Hartnett, and Clabaugh (ref. 25) for fully developed heat transfer to lead-bismuth eutectic and mercury in round tubes in laminar and transition flow regions.

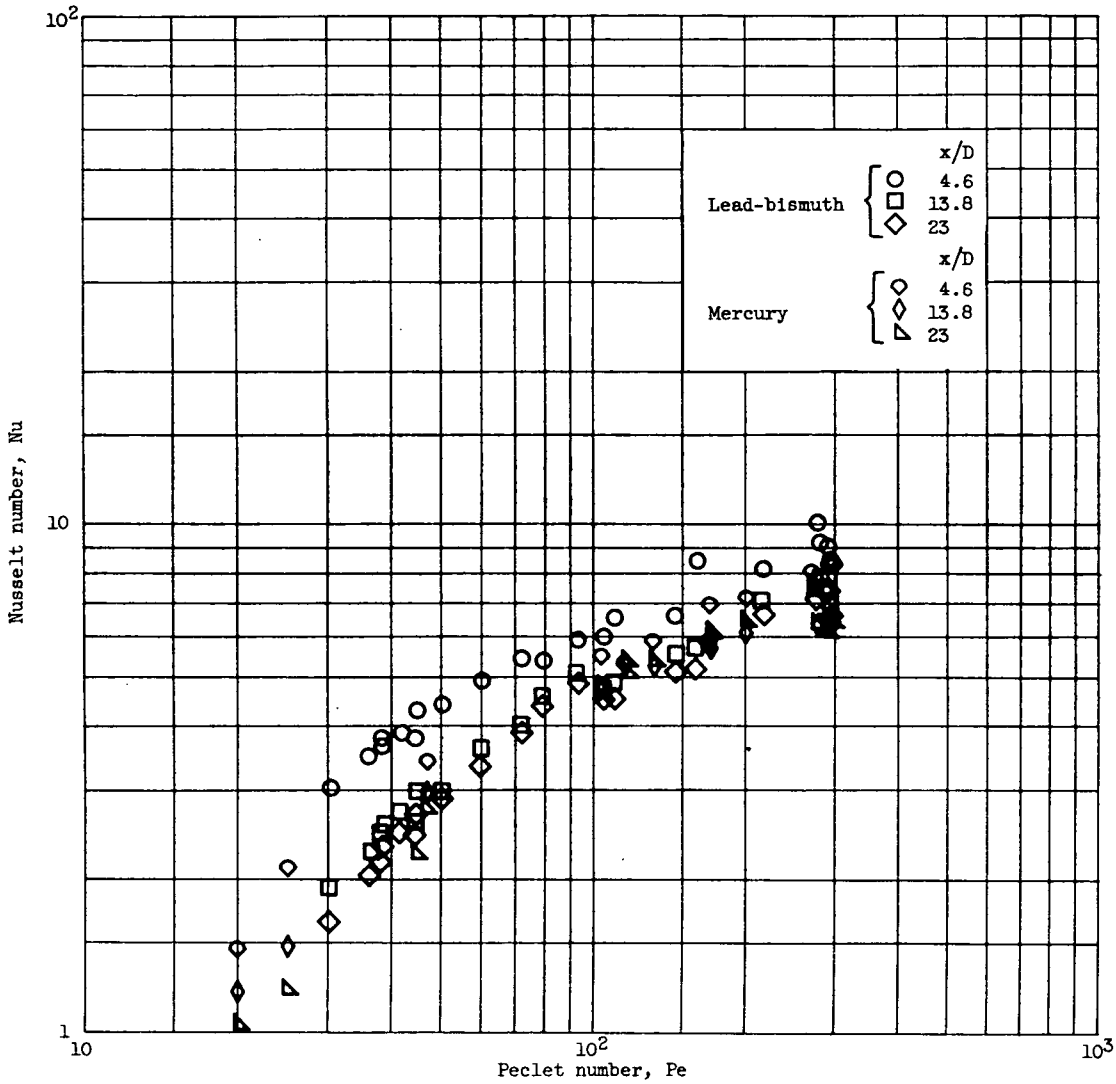

Figure 50. - Data of Johnson, Hartnett, and Clabaugh (ref. 25) for entrance region heat transfer to lead-bismuth eutectic and mercury in round tubes in laminar and transition flow regions.

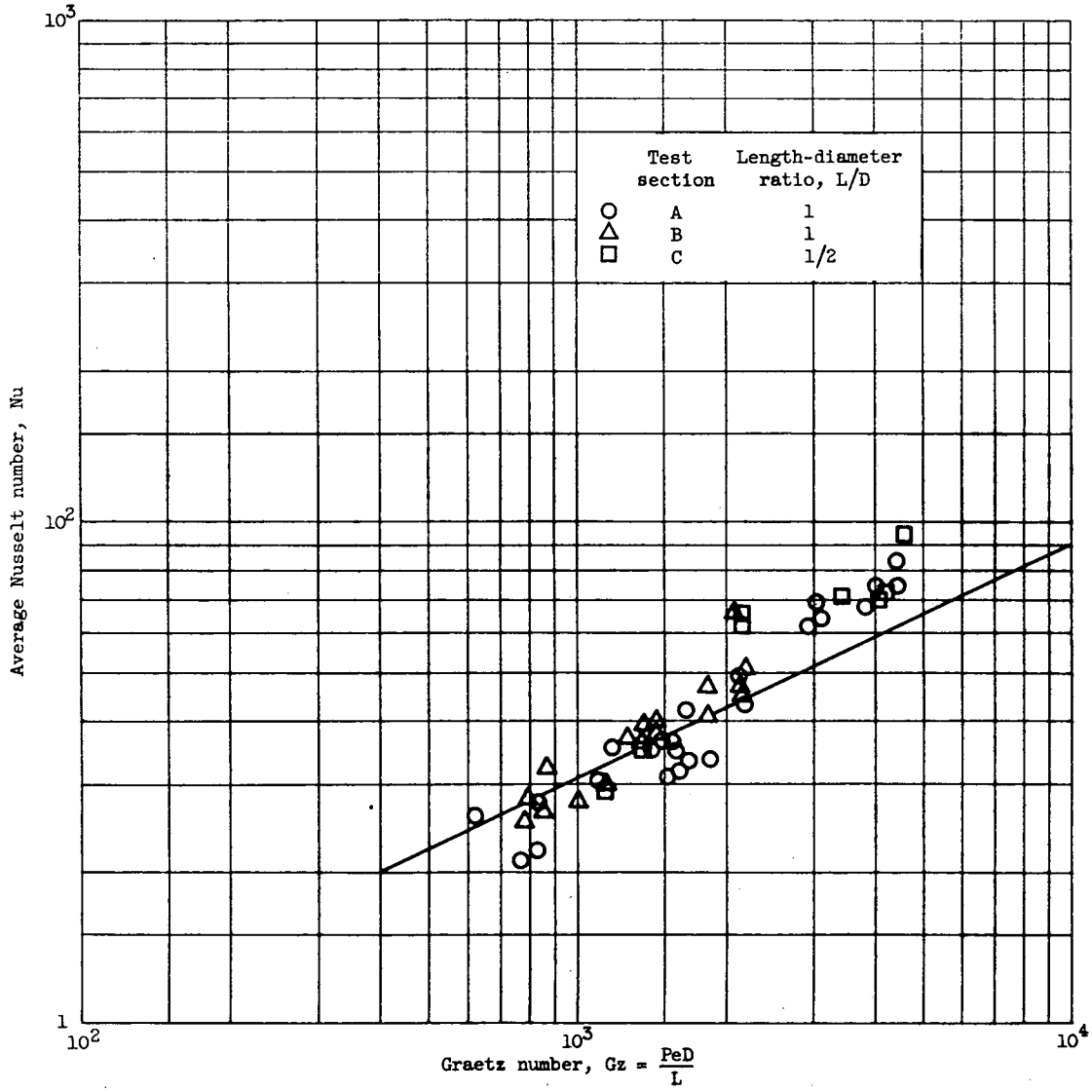

Figure 51. - Data of Poppendiek and Harrison (ref. 26) for average heat transfer to mercury in very short round tubes.

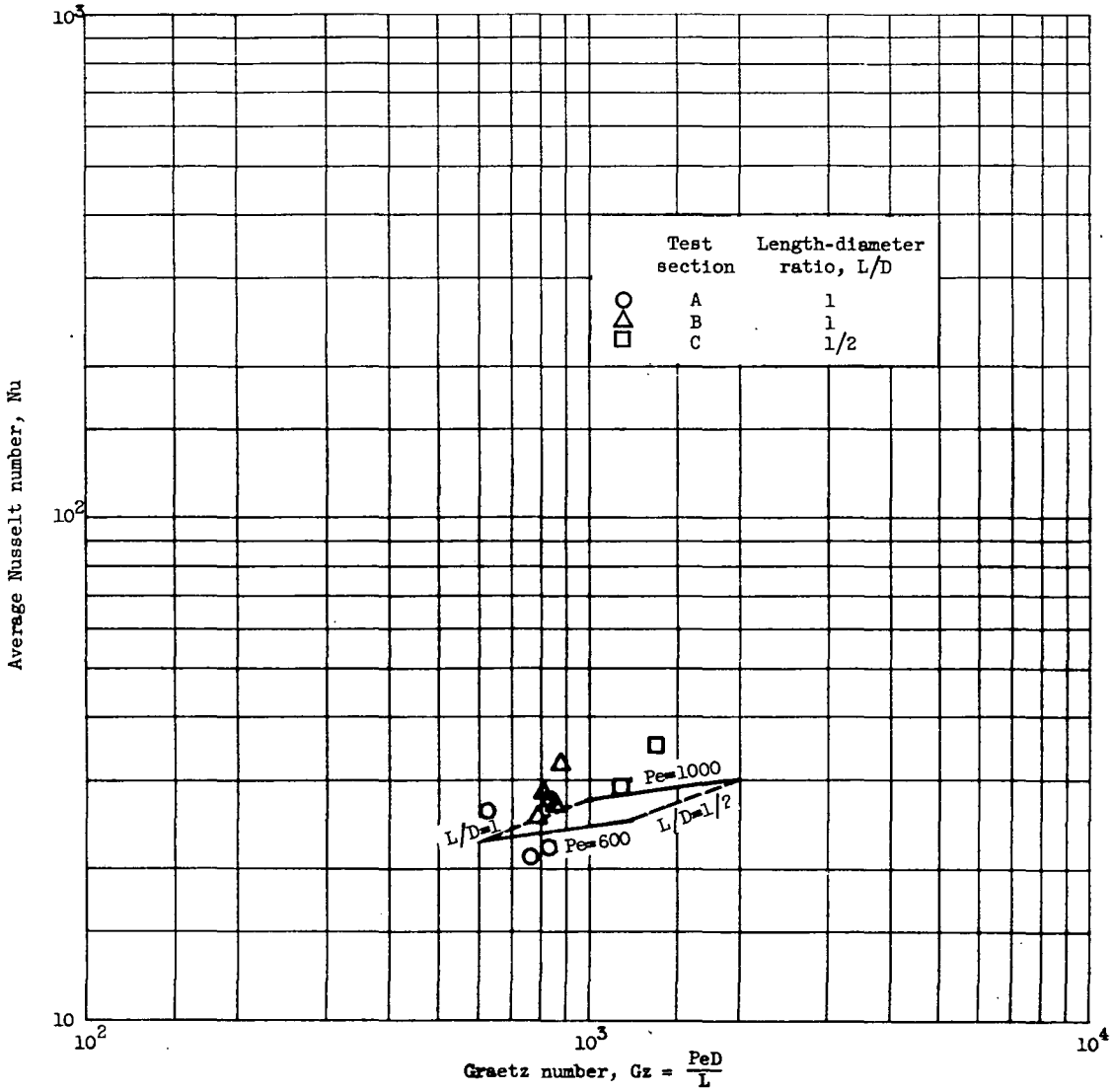

(a) 600 < Peclet number < 1000.

Figure 52. - Data of Poppendiek and Harrison (ref. 26) for average heat transfer to mercury in very short round tubes compared with prediction of Deissler (ref. 37).

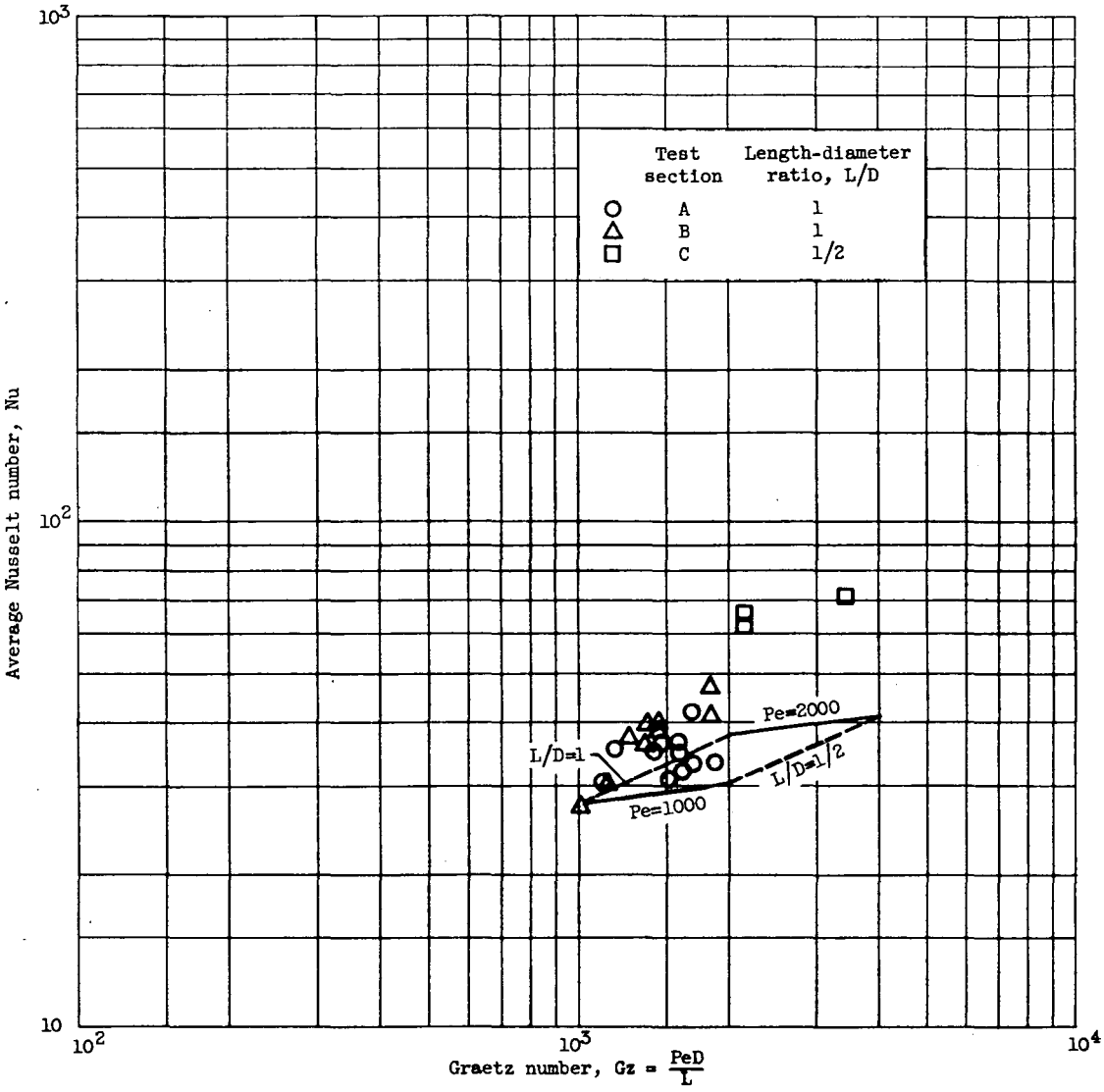

(b) 1000 < Peclet number < 2000.

Figure 52. - Continued. Data of Poppendiek and Harrison (ref. 26) for average heat transfer to mercury in very short round tubes compared with prediction of Deissler (ref. 37).

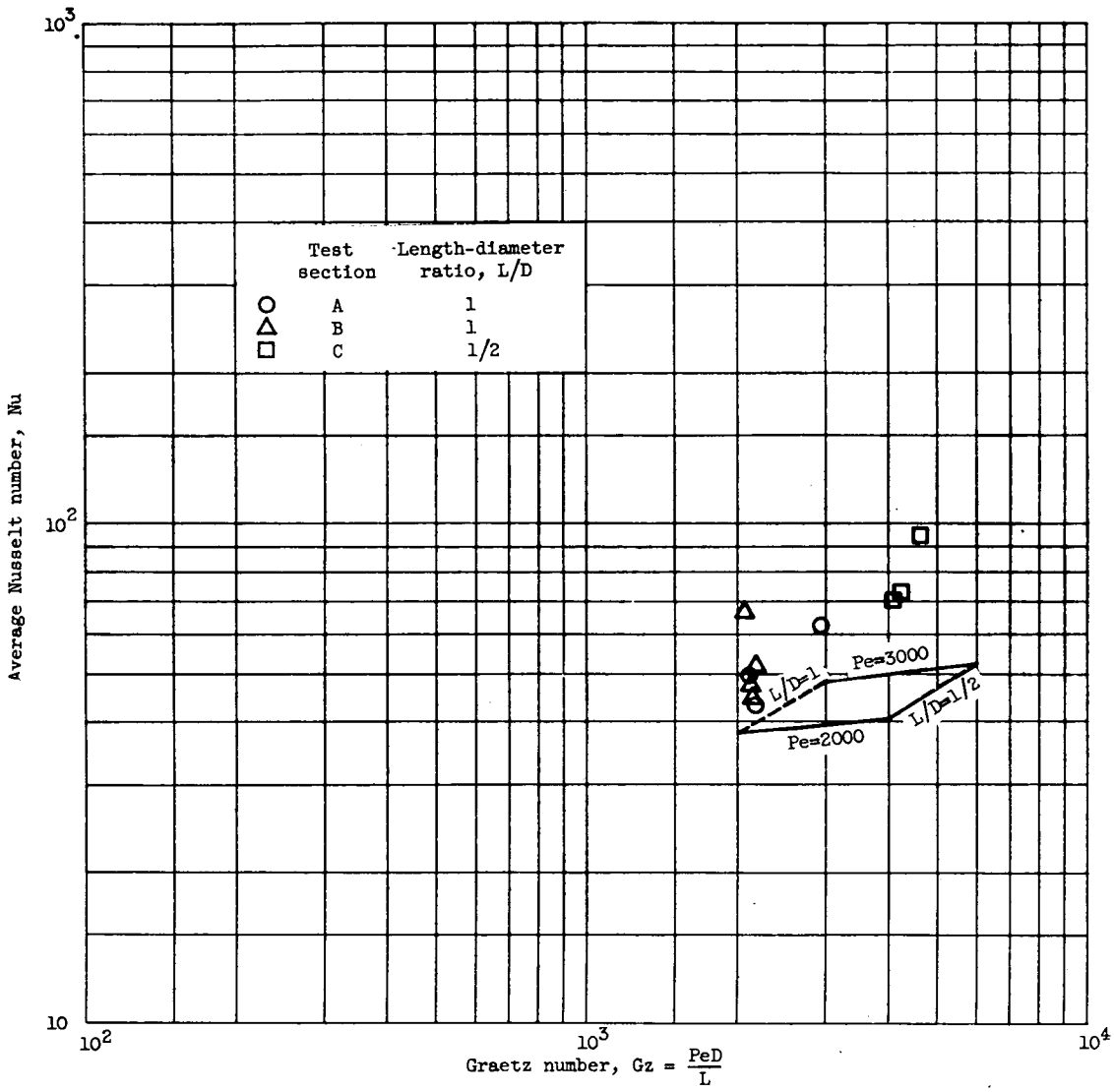

(c) 2000 < Peclet number < 3000.

Figure 52. - Continued. Data of Poppendiek and Harrison (ref. 26) for average heat transfer to mercury in very short round tubes compared with prediction of Deissler (ref. 37).

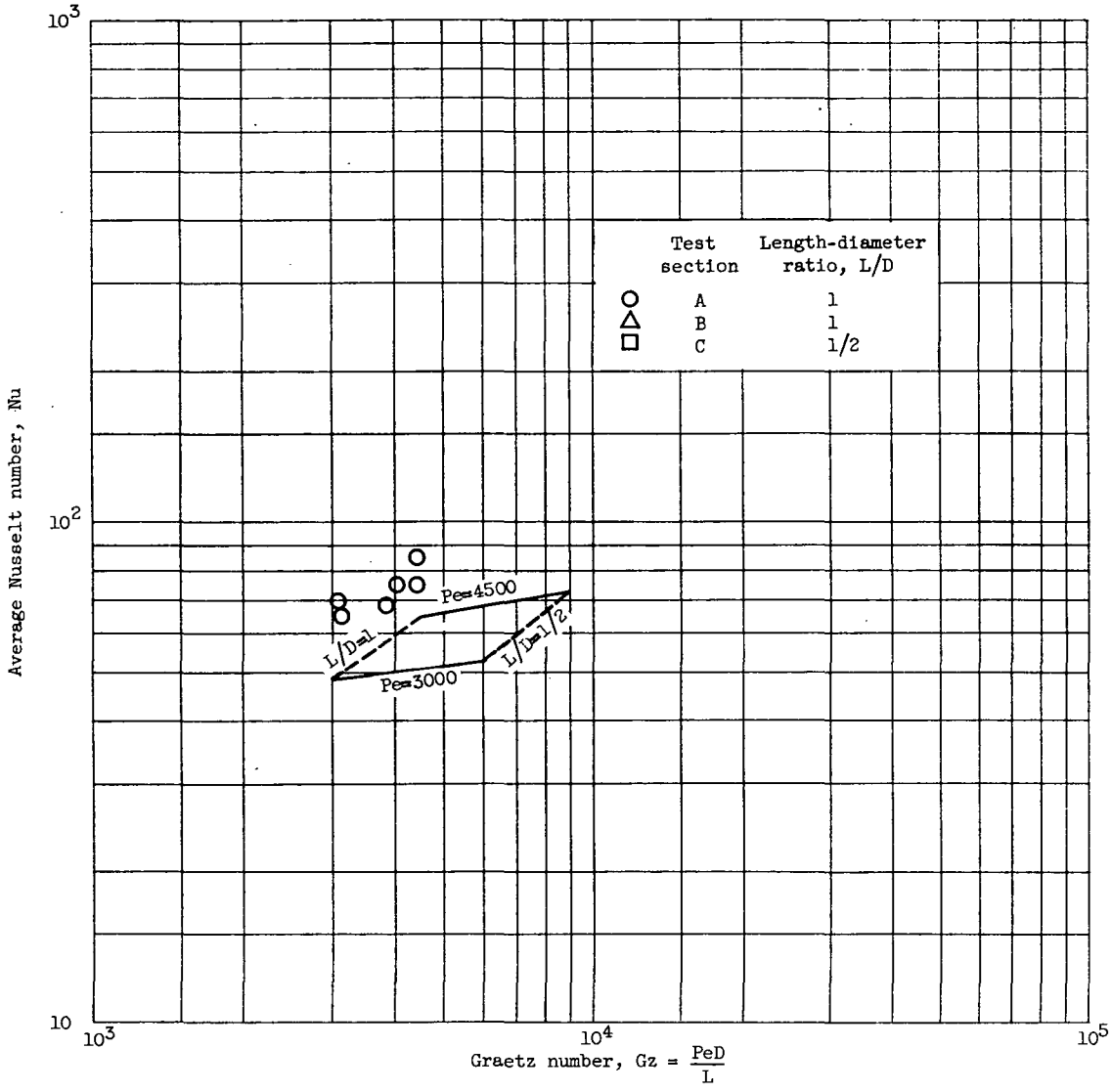

(d) 3000 < Peclet number < 4500.

Figure 52. - Concluded. Data of Poppendiek and Harrison (ref. 26) for average heat transfer to mercury in very short round tubes compared with prediction of Deissler (ref. 37).

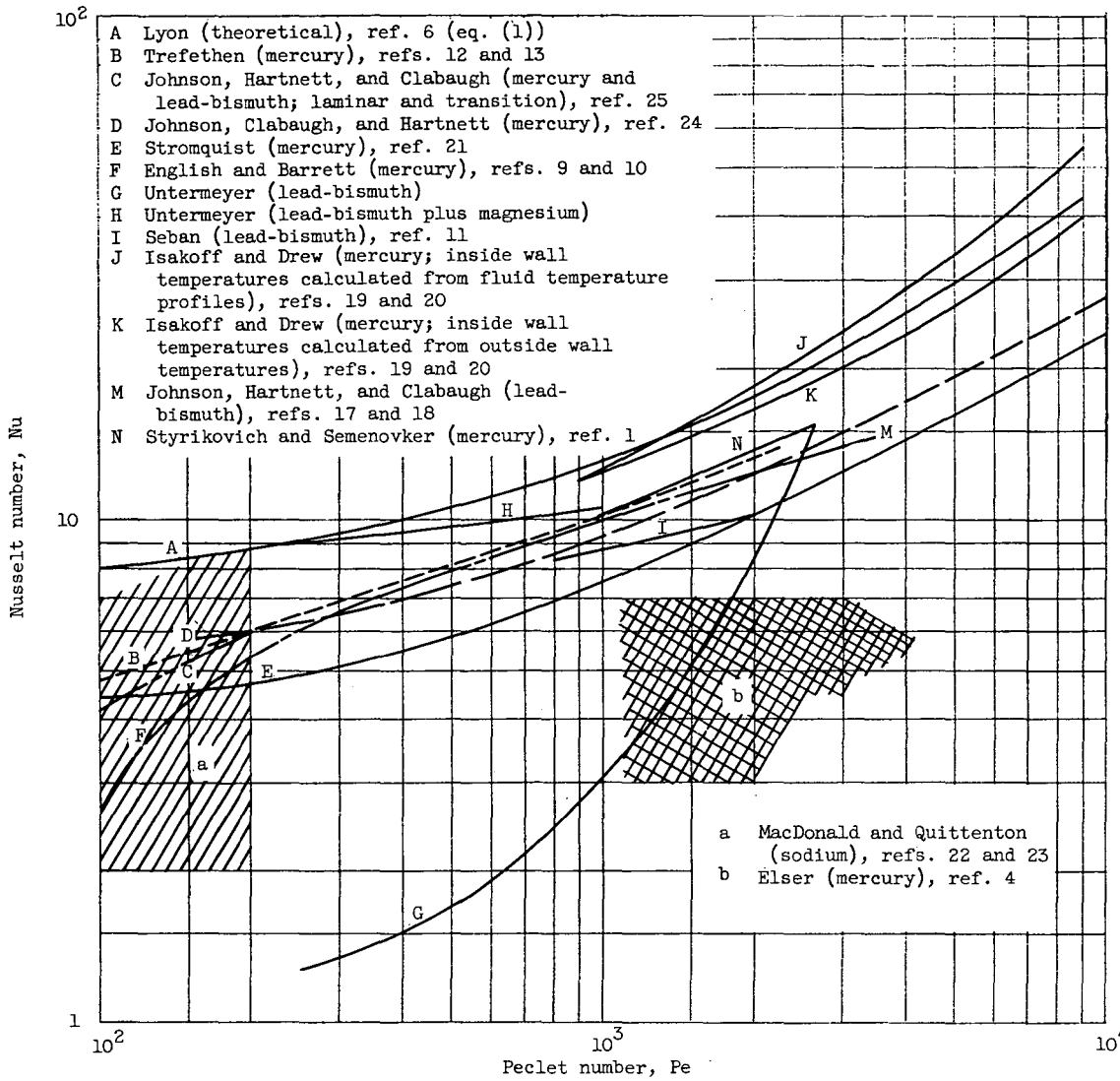

(a) Faired curves of experiments.

Figure 53. - Comparison of measured and predicted fully developed Nusselt numbers in round tubes with constant heat input to wall.

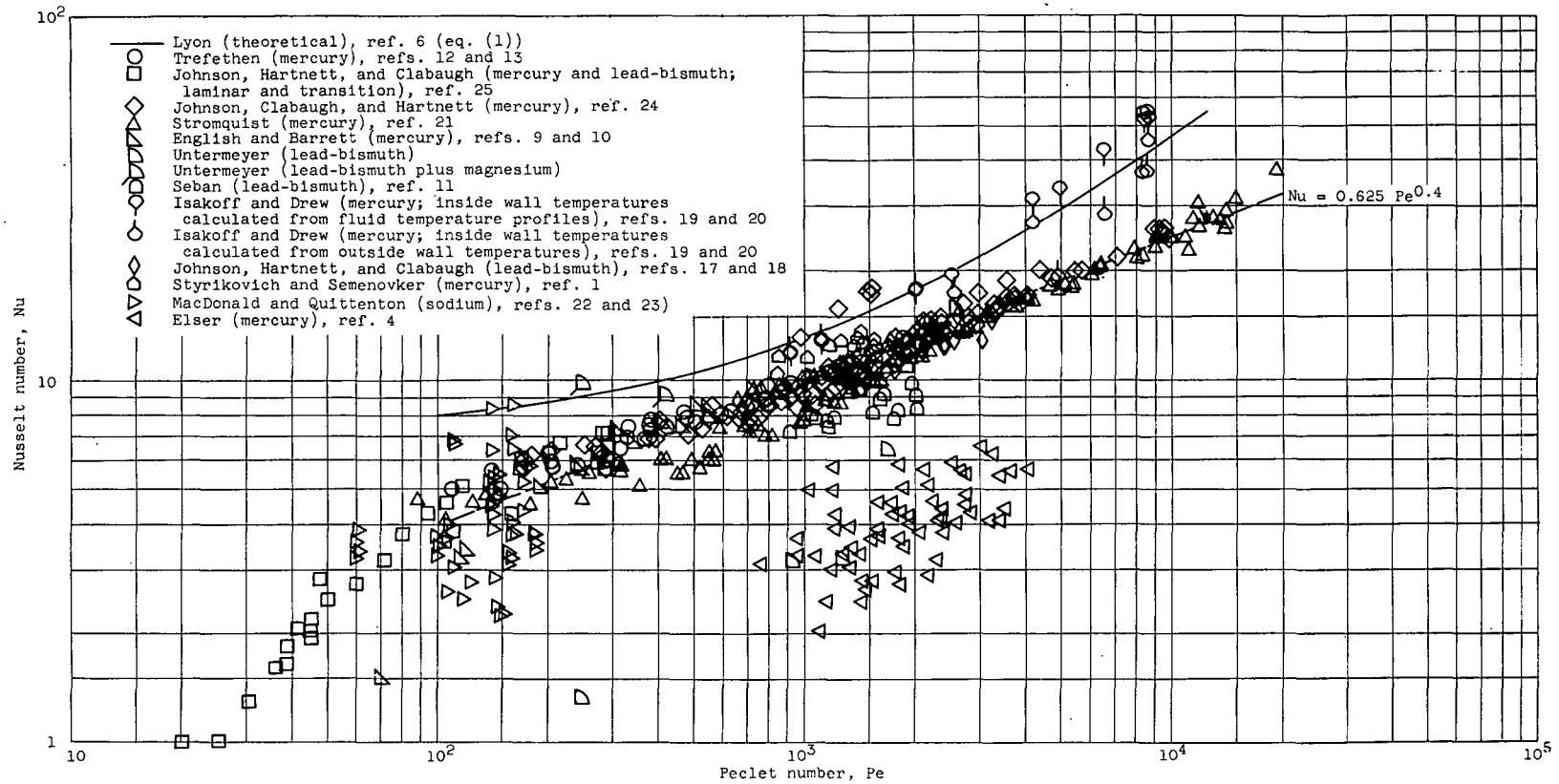

(b) Re-evaluated data points.

Figure 53. - Concluded. Comparison of measured and predicted fully developed Nusselt numbers in round tubes with constant heat input to wall.

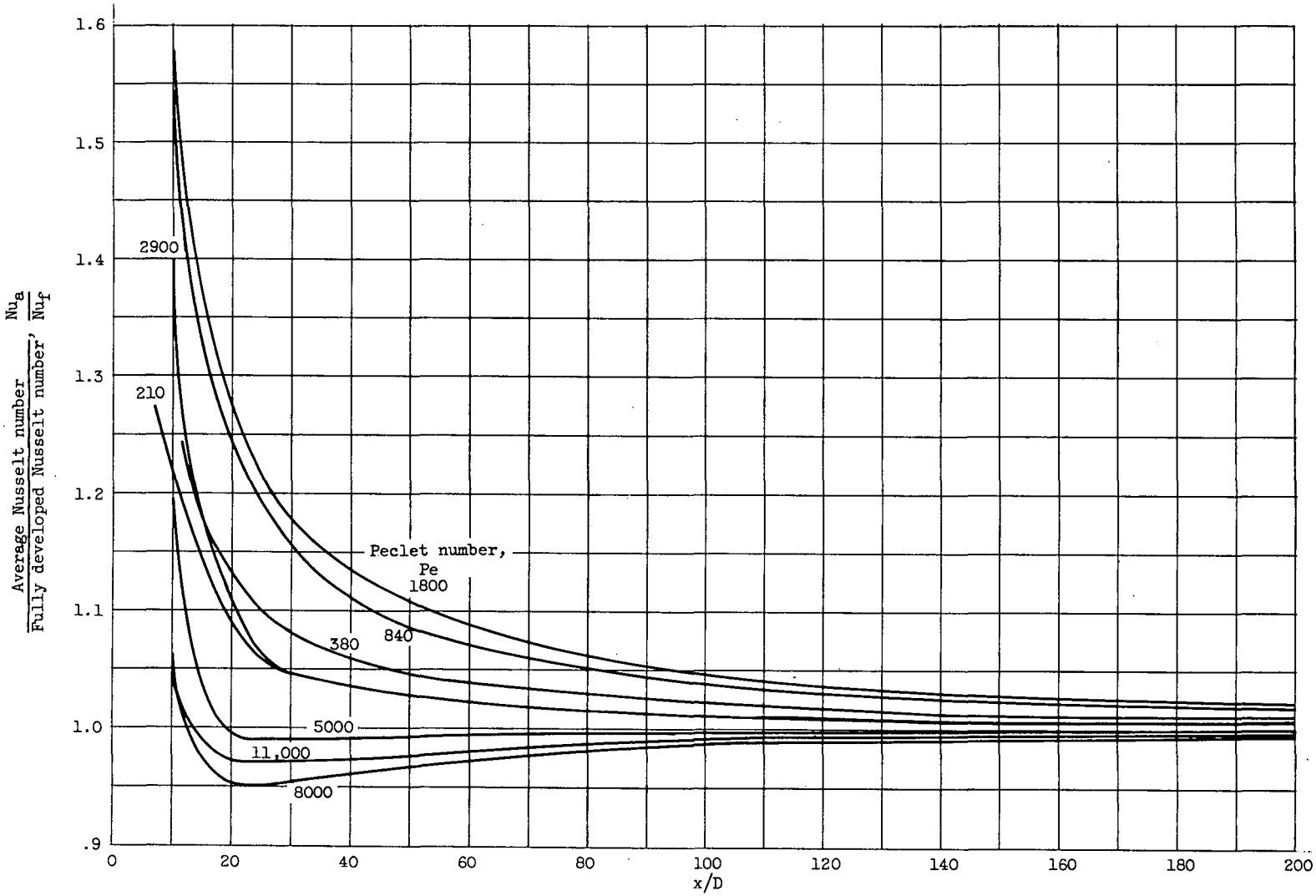

Figure 54. - Predictions of Deissler (ref. 37) for variation of ratio of average Nusselt number to fully developed Nusselt number with length-diameter ratio for various Peclet numbers (Prandtl number, 0.01).

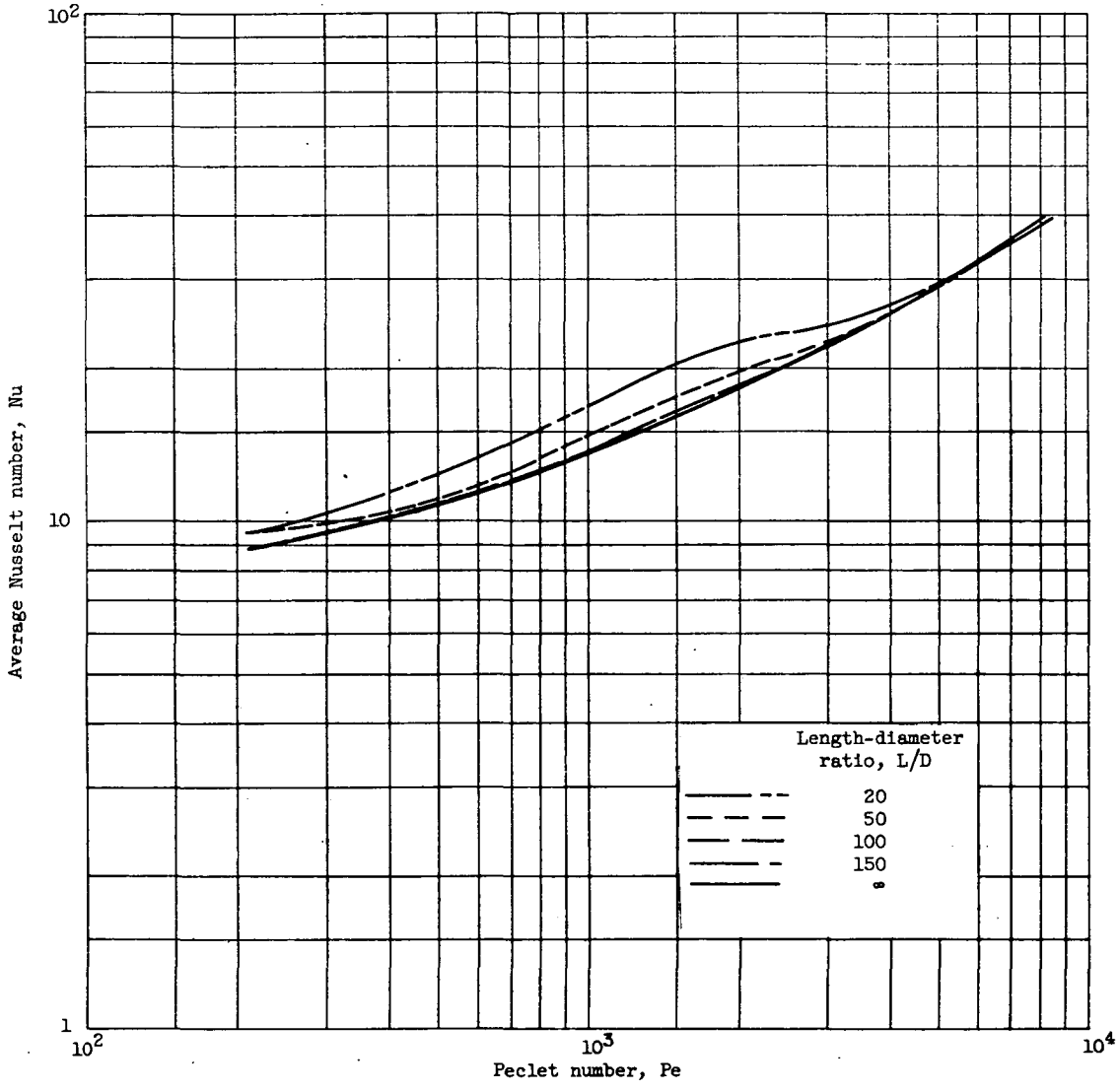

Figure 55. - Variation of average Nusselt number with Peclet number for several length-diameter ratios as determined from figure 54 and equation (1).

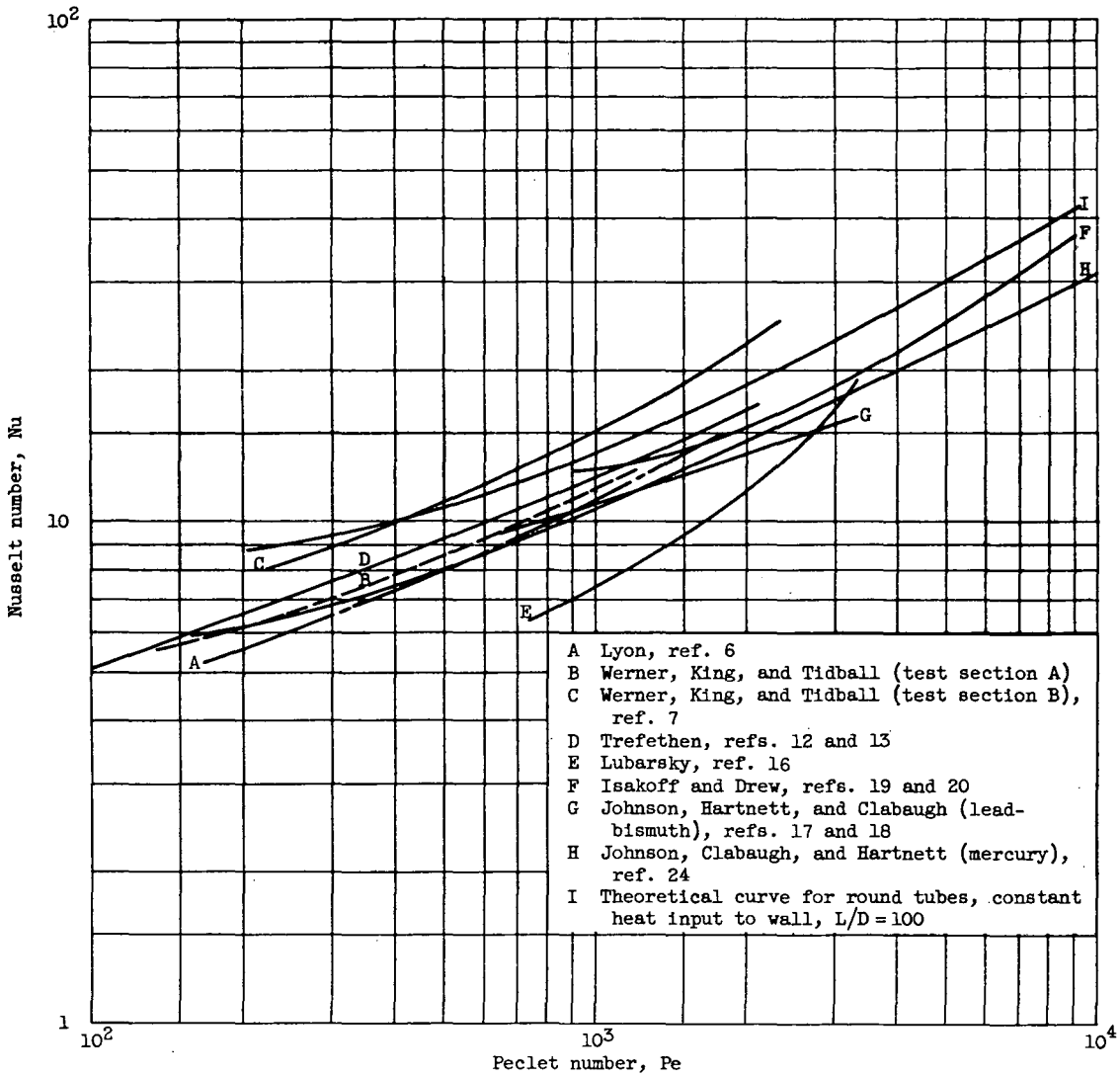

Figure 56. - Comparison of measured and predicted average Nusselt numbers in round tubes with uniform heat input to wall.

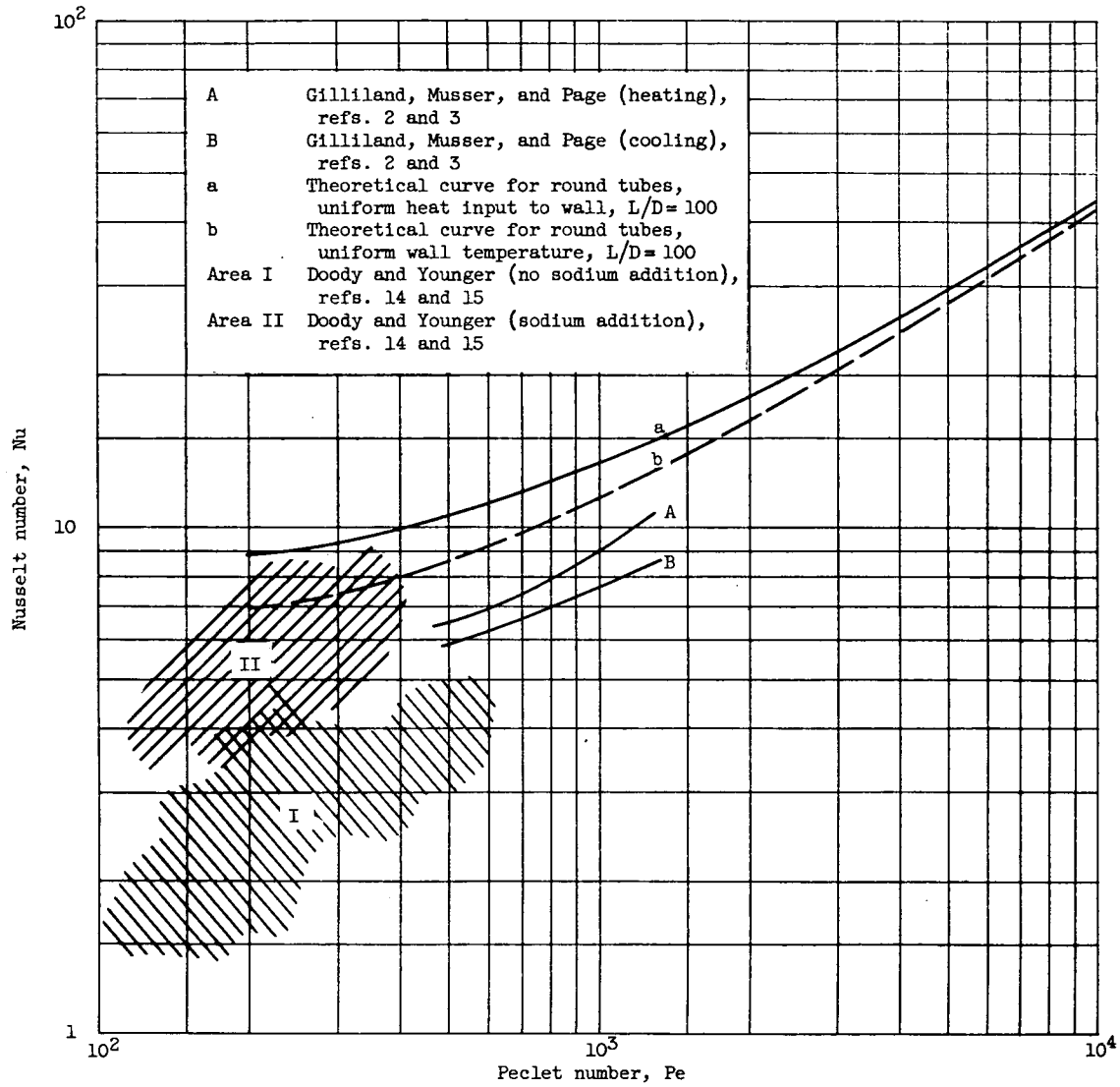

Figure 57. - Comparison of measured and predicted average Nusselt numbers in round tubes with uniform wall temperature or with a wall condition somewhere between uniform wall temperature and uniform heat input.

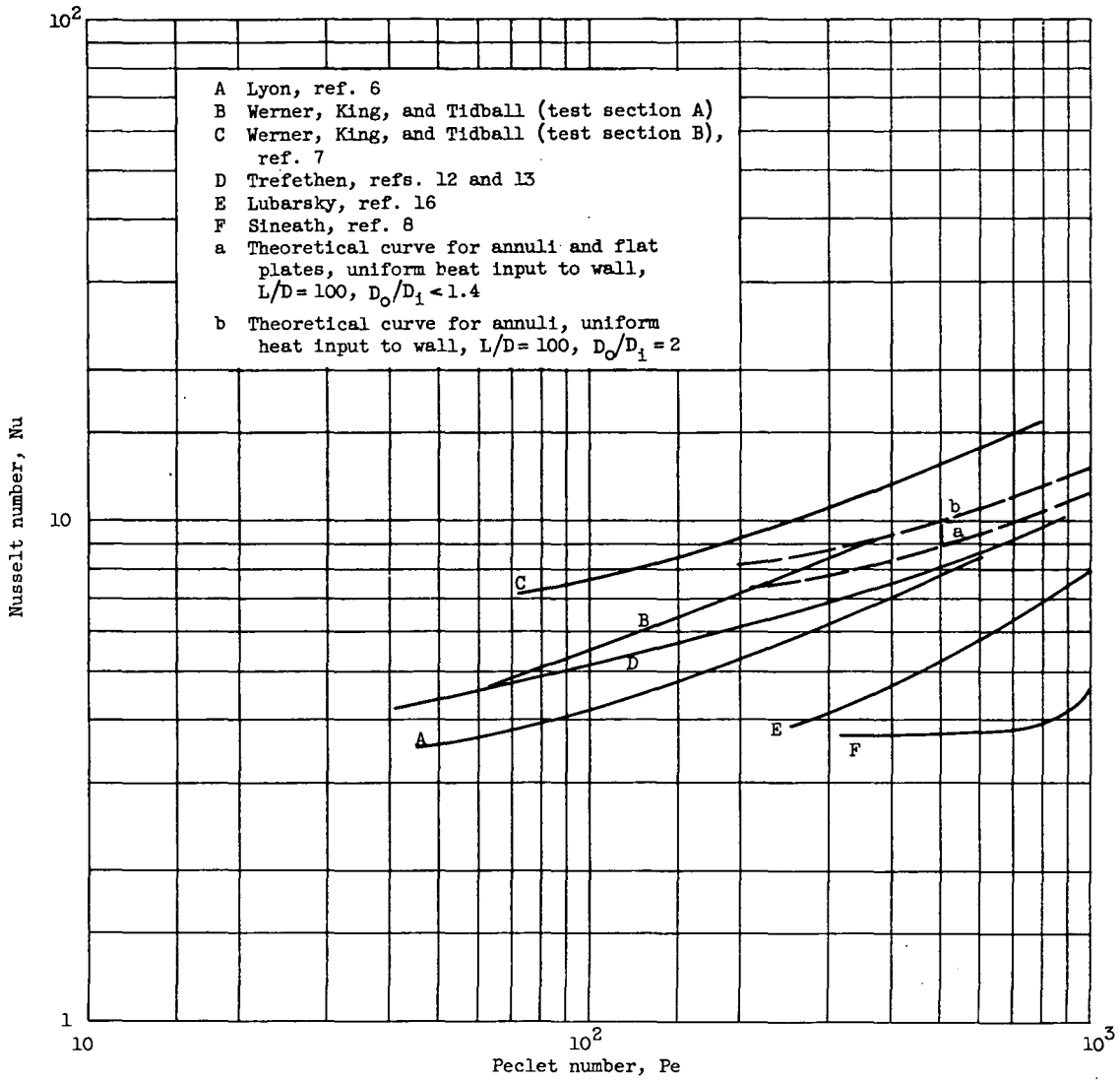

Figure 58. - Comparison of measured and predicted average Nusselt numbers in annuli and between flat plates with uniform heat input to wall.

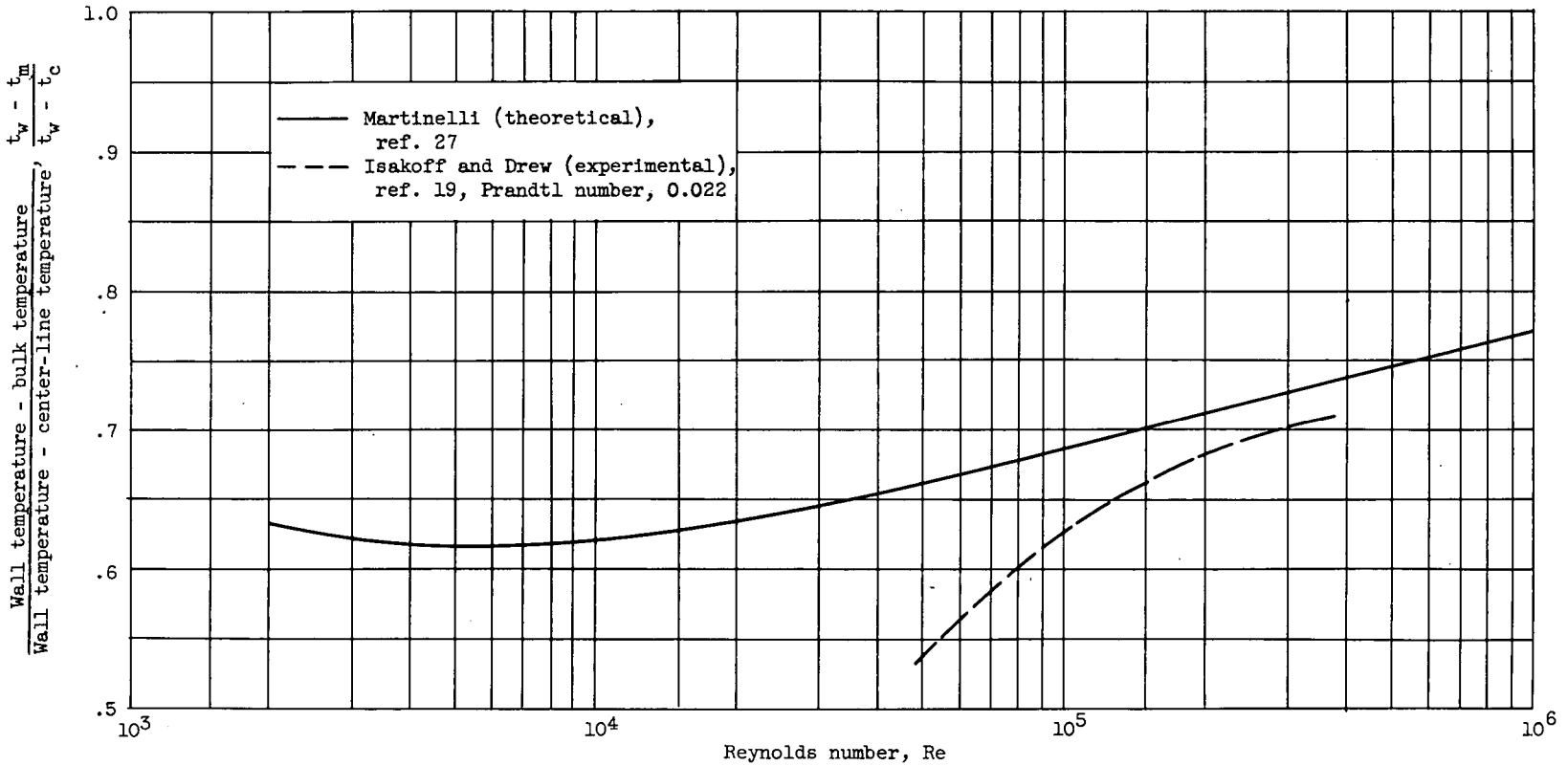

Figure 59. - Comparison of measured and predicted values of ratio $(t_w - t_m/t_w - t_c)$ in round tubes with uniform heat input to wall.

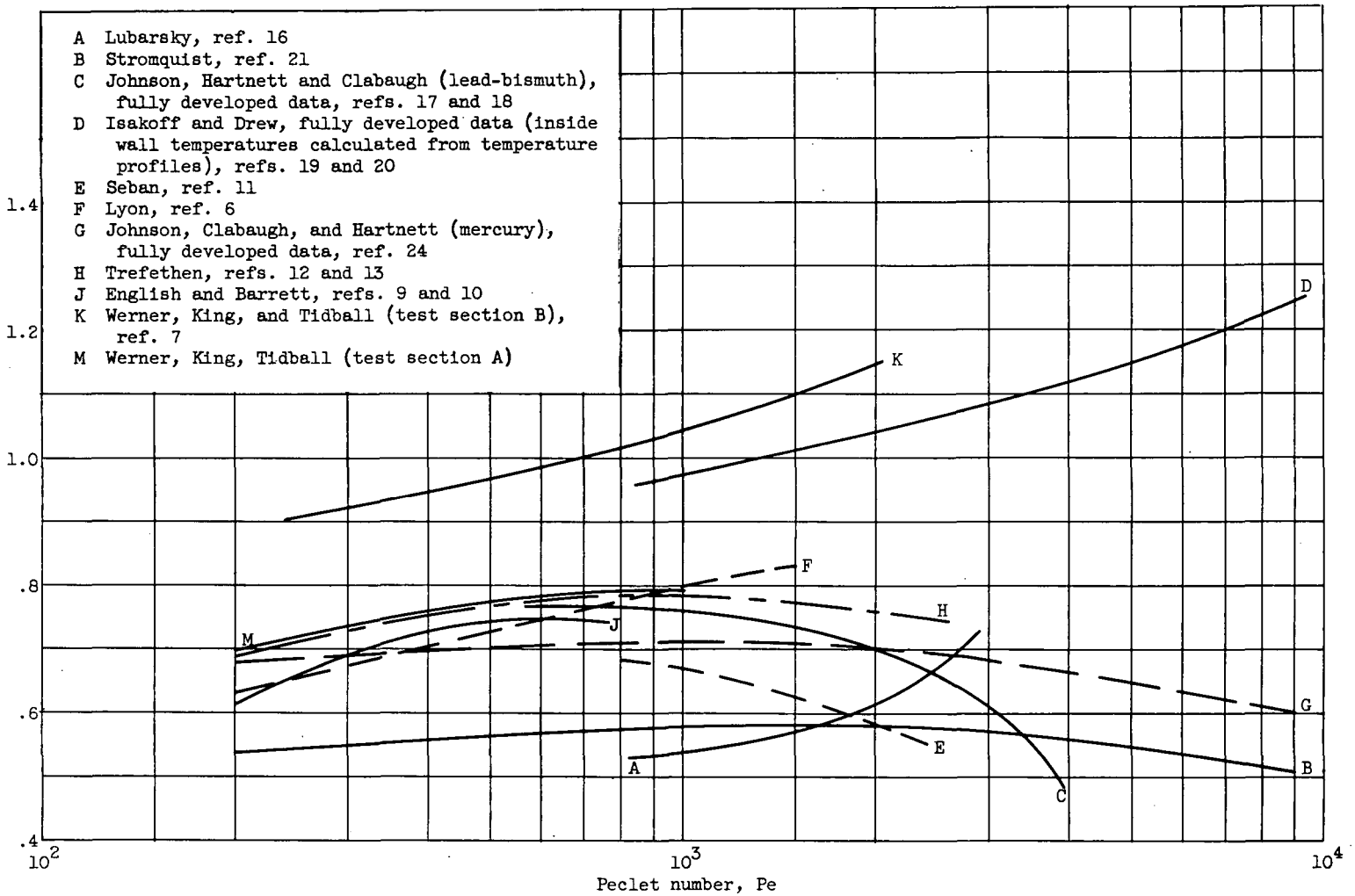

Figure 60. - Variation of ratio of measured Nusselt number to predicted Nusselt number with Peclet number.